12-11-2014 12:00 AM

The effects of dissolution on the silicon and oxygen isotope compositions of silica phytoliths

Andrea Prentice
The University of Western Ontario

Supervisor
Dr. Elizabeth Webb
The University of Western Ontario

Graduate Program in Geology
A thesis submitted in partial fulfillment of the requirements for the degree in Doctor of Philosophy

THE EFFECTS OF DISSOLUTION ON THE SILICON AND OXYGEN ISOTOPE COMPOSITIONS OF SILICA PHYTOLITHS

(Thesis format: Integrated-Article)

by

Andrea J. Prentice

Graduate Program in Geology

A thesis submitted in partial fulfillment
of the requirements for the degree of
Doctor of Philosophy

The School of Graduate and Postdoctoral Studies
The University of Western Ontario
London, Ontario, Canada

Abstract

The $\delta^{30}Si$ and $\delta^{18}O$ values of silica phytoliths have applications for reconstructing paleoenvironmental conditions. This study examines the effect of partial dissolution and burning of phytoliths on their isotopic compositions, dissolution behaviour, and physical characteristics (specific surface area, mean particle size, and visual appearance) and discusses problems with the use of phytolith $\delta^{18}O$ and $\delta^{30}Si$ values that have been modified in soils in paleoclimate reconstruction. Dissolution experiments were conducted in batch reactors under a range of pH (4-10) and temperature (4-44˚C) conditions. The $\delta^{18}O$ and $\delta^{30}Si$ values of fresh phytoliths behave similarly as dissolution progresses, with values increasing until the solution is approximately 30-40% saturated with silicic acid. During this phase of the experiment the isotopic composition of the remaining silica is dominated by dissolution preferentially removing the light isotope (^{16}O and ^{28}Si) to the solution. After ~30-40% saturation back reactions begin to affect the isotopic composition of remaining silica, despite net movement in the forward direction (i.e. dissolution). The $\delta^{18}O$ values of precipitated silica are determined by the $\delta^{18}O$ value of water in the solution and the temperature of the experiment. The $\delta^{30}Si$ values of precipitated silica are determined by the $\delta^{30}Si$ value of silicic acid. Phytoliths subjected to burning at 700˚C have $\delta^{18}O$ values that are 2.6 ‰ lower than unburned phytoliths while their $\delta^{30}Si$ values remain unchanged. This suggests that heating results in the incorporation of ^{18}O-depleted hydroxyl groups into the silica structure. Dissolution of burned phytoliths progressed more slowly than dissolution of fresh phytoliths in conditions that are less favourable for dissolution (i.e. low pH and T) and more quickly in conditions that are favourable (i.e. high pH and T). The $\delta^{18}O$ values of partially dissolved burned phytoliths follow the same general trend as those of unburned phytoliths but with less overall change in $\delta^{18}O$ values. Burning may increase silanol sites that are more susceptible to dissolution. We recommend caution in using the $\delta^{18}O$ and $\delta^{30}Si$ values of soil phytoliths in paleoclimate reconstructions. Care must be taken to identify alteration by dissolution or burning, which may not always be visually evident.

Keywords: phytoliths, oxygen isotopes, silicon isotopes, dissolution, burned phytoliths

Acknowledgments

I would like to thank my supervisor, Elizabeth Webb, for her help and guidance throughout my studies. I would also like to thank Kim Law and Iffat Jabeen for their advice and assistance in the lab. This project could not have been completed without their extensive knowledge and troubleshooting skills. Thank you to Dr. Fred Longstaffe and Dr. Desmond Moser for their guidance and insight during this project.

Thank you to my office mates in 1031 for making our office such a supportive environment. I would like to thank Rachel Schwartz-Narbonne for her advice, encouragement, and ability to turn math into pictures.

A special thanks to my family and friends for their unwavering support over the years: Patti Prentice, Michael Prentice, Kristi Ferguson, Dave Wallace, Ciara Murphy, Leslie Pizzanelli, Lily Adele Taylor, and Eduardo el Gato. I could not have come this far without you.

Table of Contents

ABSTRACT ii

ACKNOWLEDGEMENTS iii

TABLE OF CONTENTS iv

LIST OF TABLES vii

LIST OF FIGURES viii

LIST OF APPENDICES x

CHAPTER 1. INTRODUCTION 1

1.1 PHYTOLITHS 2
1.1.1 Precipitation of silica phytoliths 2
1.1.2 Phytolith preservation 3
1.2 THE SILICON CYCLE 4
1.3 SILICON AND OXYGEN ISOTOPE SYSTEMATICS IN PHYTOLITHS 6
1.3.1 Oxygen isotopes 6
1.3.2 Silicon isotopes 7
1.4 DISSOLUTION STUDIES 8
1.5 APPLICATIONS OF THE ISOTOPIC STUDY OF PHTYOLITHS 11
1.6 REFERENCES 12

CHAPTER 2. SIMULTANEOUS MEASUREMENT OF $\delta^{18}O$ AND $\delta^{30}SI$ VALUES OF SMALL SAMPLES OF OPAL-A 18

2.1 INTRODUCTION 18
2.1.1 Extraction from soil and sediments 18
2.1.2 Exchangeable hydroxyl groups on opal-A 19
2.1.2.1 Step-wise fluorination 20
2.1.2.2 Inductive High-temperature Carbon Reduction 21
2.1.2.3 Controlled isotope exchange 21
2.1.2.4 Inert gas flow dehydration 22
2.1.3 Carbon contamination affecting Si-isotopes 22
2.2 METHODS 23
2.2.1 Inert gas flow dehydration 23
2.2.2 Dual oxygen and silicon isotope analyses via vacuum extraction line 24
2.2.2.1 Reaction and extraction procedure 26
2.3 RESULTS AND DISCUSSION 28
2.3.1 Oxygen isotope analyses 29
2.3.2 Silicon isotope analyses 32
2.4 SUMMARY 35

2.5 REFERENCES 36

CHAPTER 3. THE EFFECT OF PROGRESSIVE DISSOLUTION ON THE SILICON ISOTOPE COMPOSITION OF OPAL-A 41

3.1 INTRODUCTION 41
3.2 METHODS 43
3.2.1 Source material 43
3.2.2 Characterization of phytoliths 43
3.2.3 Dissolution experiment 44
3.2.4 Measurement of δ^{30}Si values 44
3.3 RESULTS 45
3.3.1 Degree of dissolution 45
3.3.2 Changes in physical characteristics 47
3.3.3 δ^{30}Si values of phytoliths 48
3.4 DISCUSSION 50
3.4.1 Dissolution behaviour 50
3.4.2 Effect of dissolution on phytolith δ^{30}Si values 52
3.4.2.1 Initial dissolution 52
3.4.2.2 Approach to steady state dissolution 53
3.5 CONCLUDING REMARKS 56
3.6 REFERENCES 57

CHAPTER 4. THE EFFECT OF PROGRESSIVE DISSOLUTION ON THE OXYGEN ISOTOPE COMPOSITION OF OPAL-A 62

4.1 INTRODUCTION 62
4.2 METHODS 64
4.2.1 Removal of OH groups 64
4.2.2 Measurement of δ^{18}O values 65
4.3 RESULTS 65
4.3.1 Amount of dissolution 65
4.3.2 Oxygen isotope composition of opal-A 66
4.4 DISCUSSION 70
4.4.1 Adsorption of small particles 70
4.4.2 The reactive surface layer 71
4.4.3 Progressive dissolution 72
4.5 CONCLUDING REMARKS 74
4.6 REFERENCES 76

CHAPTER 5. THE EFFECT OF BURNING ON THE DISSOLUTION BEHAVIOUR AND SILICON AND OXYGEN ISOTOPE COMPOSITION OF PHYTOLITH SILICA 80

5.1 INTRODUCTION 80
5.2 METHODS 81

5.3 RESULTS 83
5.4 DISCUSSION 88
5.4.1 Differences in the rate of dissolution 88
5.4.2 Isotopic composition of burned and unburned phytoliths 89
5.5 CONCLUDING REMARKS 93
5.6 REFERENCES 93

CHAPTER 6. SUMMARY 98
Vita 114

List of tables

Table Page

2-1 Summary of modifications to the iGFD method originally developed by Chapligin et al. (2010).. 24

2-2 Comparison of accepted opal-A standard $\delta^{18}O$ values (Chapligin et al., 2011) to those determined in this study.....32

List of Figures

Figure Page

1-1 Cycle of silicon in continental and marine environments and associated $\delta^{30}Si$ values of the silicon pools. Arrows denote the direction of movement of silicon through the various pools and letters denote the manner of movement. D: dissolution; P: precipitation; T: transport; Up: uptake; De: death. Modified from Basile-Doelsch (2006) with additional data from Ziegler et al. (2005) and Ding et al. (2009) 5

2-1 iGFD apparatus depicting gas inlet (A) and outlet (B), glass tubing (C), and furnace (D) 23

2-2 Schematic and photographs of the reaction vessels and vacuum extraction line for the purification of O_2 and SiF_4 gas. 25

2-3 A plot of $\delta^{17}O$ to $\delta^{18}O$ for quartz (NBS-28) and opal-A standards (phytoliths (G95), diatoms (BFC), and precipitated amorphous silica (HT, PS)) displaying the approximate 1:2 relationship expected for terrestrial materials. 30

2-4 The calibration curve used to normalize oxygen isotope compositions to VSMOW. Standards included in the curve are: NBS-28 and ORX (quartz) and a selection of biogenic silica standards treated via iGFD and samples with known $\delta^{18}O$ values treated via controlled isotope exchange 31

2-5 Mass scans of SiF_4 gas obtained from a sample of Diatomite standard (A) and SiF_4 reference gas (B) 33

2-6 Cross-plot of $\delta^{30}Si$ and $\delta^{29}Si$ values of phytolith silica and the standards NBS-28 and Diatomite. 35

3-1 Percent of the solid dissolved plotted versus reaction time for pH 4 (A), pH 6 (B), pH 8 (C), and pH 10 (D) 46

3-2 Phytolith dissolution rate versus number of days reacted for experiments conducted at pH 8 and 10 (A), and at pH 4 and 6 (B) 47

3-3 $\delta^{30}Si$ values of partially dissolved phytoliths versus the % of the solid dissolved for each experiment conducted at pH 4 (A), pH 6 (B), pH 8 (C), and pH 10 (D). 49

3-4 $\delta^{30}Si$ values of partially dissolved phytoliths versus % saturation with respect to dissolved silica for each experiment conducted at pH 4 (A), pH 6 (B), pH 8 (C), and pH 10 (D). 50

4-1 $\delta^{18}O$ values of partially dissolved phytolith silica plotted against % dissolved for all temperatures at pH 4 (A), pH 6 (B), pH 8 (C), and pH 10 (D). The blue box shows the standard deviation on the $\delta^{18}O$ value of the untreated phytolith material. 67

4-2 $\delta^{18}O$ values of partially dissolved phytolith silica plotted with percent saturation of the solution with respect to dissolved silica for all temperatures at pH 4 (A), pH 6 (B), pH 8 (C), and pH 10 (D). Blue boxes represent the standard deviation associated with the $\delta^{18}O$ value of untreated phytolith material. 69

5-1 Dissolution rate of burned phytoliths over the course of dissolution 84

5-2 Comparison of dissolution rates between burned and unburned phytoliths over the course of dissolution. The sampling interval was the same for both burned and unburned dissolution experiments. 84

5-3 The change in $\delta^{18}O$ of partially dissolved phytoliths plotted against the percent of the solid dissolved (A) and percent saturation (B). 86

5-4 The change in $\delta^{30}Si$ of partially dissolved phytoliths plotted against the percent of the solid dissolved (A) and percent saturation (B). 87

5-5 The $\delta^{18}O$ and $\delta^{30}Si$ values of partially dissolved burned and unburned phytoliths reacted for the same length of time at pH 4 (A), pH 6 (B), and pH 8 (C). 92

List of Appendices

Page

Appendix A. SEM photographs 103

A-1 SEM images of phytoliths prior to dissolution 103

A-2 SEM images of phytoliths after dissolution for 70 days at T = 4˚C and pH = 4. 104

A-3 SEM images of phytoliths after dissolution for 10 days at T = 44˚C and pH = 10. 105

A-4 SEM images of phytoliths after dissolution for 28 days at T = 44˚C and pH = 4 106

A-5 SEM images of phytoliths after dissolution for 70 days at T = 19˚C and pH = 6 107

A-6 SEM images of phytoliths after dissolution for 10 days at T = 4˚C and pH = 10. 108

A-7 SEM images of phytoliths after dissolution for 10 days at T = 19˚C and pH = 10 109

Appendix B. Summary of experimental conditions and results of dissolution experiments conducted on fresh phytoliths 110

Appendix C. Summary of experimental conditions and results of dissolution experiments conducted on burned phytoliths 113

1. Introduction

Biogenic silica can be preserved in soils and sediments for thousands of years (Piperno, 2006). The oxygen and silicon isotope compositions of both phytolith and diatom silica can be used to examine past climate and biogeochemical cycles (Labeyrie, 1974; Juillet-Leclerc and Labeyrie, 1987; Shahack-Gross et al., 1996; Cardinal et al., 2007; Alexandre et al., 2012). Diatoms provide a useful alternative to carbonates in lakes, and silica from phytoliths provides a terrestrial climate proxy that is sensitive to short-term fluctuations in climate. Previous research has demonstrated the potential to use the $\delta^{18}O$ values of biogenic silica for paleoclimate reconstruction because these values vary with temperature and the $\delta^{18}O$ values of formation water (e.g. Juillet-Leclerc and Labeyrie, 1987; Shahack-Gross et al., 1996; Dodd and Sharp 2010). Researchers have also begun using the $\delta^{30}Si$ values of biogenic silica to glean information on the silicon cycle in both terrestrial and marine environments (e.g. De La Rocha et al., 1998; Basile-Doelsch et al., 2005).

Many studies have examined how formation processes and environments affect the final isotopic composition of biogenic silica, although most focus on diatoms rather than phytoliths (Dodd and Sharp 2010; Brandriss et al., 1998; Moschen et al., 2005; Matheney and Knauth, 1989; Labeyrie 1974). It is only more recently that phytoliths have become a focus for researchers (Shahack-Gross et al., 1996; Webb et al., 2002; 2003). However, to use fossil phytolith or diatom assemblages successfully as paleoclimatic indicators, further investigation into the stability of opal-A in soils and sediments is necessary. Post-depositional alteration of biogenic silica may change the isotopic composition of samples. The dissolution kinetics of diatoms, and those effects on their isotopic compositions, has been studied previously (e.g. Schmidt et al., 2001; Demarest et al., 2006; Wetzel et al., 2014). Studies have demonstrated that the relationship between $\delta^{18}O$ values of water, diatoms and temperature vary depending on the age of the deposit indicating that isotope exchange with pore waters may alter the $\delta^{18}O$ values of opal-A (Brandriss et al., 1998; Schmidt et al., 2001). The loss of surface hydroxyl groups from the hydrated opal-A structure during burial in the sediments may cause a shift in the $\delta^{18}O$ values of these

proxy materials (Schmidt et al., 2001). Issues such as isotope fractionation during partial (thinner parts of the particle may dissolve first) or selective dissolution of diatoms/phytoliths from different species or plant tissues must be investigated as they have the potential to alter the isotope compositions of fossil opal-A and influence paleoclimate estimates (Brandriss et al., 1998; Demarest et al., 2009). More recently phytolith dissolution behaviour has been investigated, but the effect on isotopic composition has not been a focus (Fraysse et al., 2006a/b, 2009). In addition, many phytoliths dissolution experiments were done using flow-through reactors, where the dissolved silica is immediately removed from the system, eliminating the possibility of silica re-precipitation.

Although there is potential for the $\delta^{30}Si$ and $\delta^{18}O$ values of phytoliths preserved in soils to be used as proxies for weathering rates and climate, presently there are no studies that extract phytoliths from soils for this purpose. This work is limited by difficulties in extracting purified samples from the soil and the uncertainty regarding the preservation of their isotope signatures. The present research aims to contribute to the field through the development of a technique for analysing small samples and by examining the effect of dissolution on the $\delta^{18}O$ and $\delta^{30}Si$ values of phytolith silica through dissolution experiments under a range of temperature and pH conditions. The results from this project will contribute to our understanding of silicon isotope systematics in global geochemical cycles.

1.1 Phytoliths

Phytoliths are silica bodies tens of microns in size that form in plant tissues. They are composed of a form of hydrated amorphous silica called opal-A ($SiO_2 \cdot nH_2O$). Phytolith content in plants ranges from approximately 0.5% dry weight or less in dicotyledons, 1-3% in dryland grasses, and up to 10-15% in some wetland species (Epstein 1994). Monocotyledons are the highest accumulators and *Equisetum arvense* (horsetails), in particular, can accumulate up to 25% of their dry weight as silica (Chen and Lewin 1969). Silica accumulation varies with plant species, plant part, and environmental

conditions controlling the amount of dissolved silica available to the plant (Piperno, 2006).

1.1.1 Precipitation of silica phytoliths

When plants take up water they also take up silicon in the form of aqueous silicic acid ($Si(OH)_4$) (Piperno, 2006). The silicic acid is transported throughout the plant and precipitates out of solution to form solid silica bodies (phytoliths) in intra- and intercellular spaces (Piperno, 2006; Alexandre et al., 1994; Raven, 1983). Deposition occurs where plant water becomes supersaturated with respect to silicic acid, primarily as the result of removal of water through transpiration (Piperno, 2006; Raven 1983). However, silica deposition also occurs in cells not directly related to water loss as a result of induced silica saturation (Walker and Lance 1991). An increase in the ionic activity of Na^+ or K^+, a change in pH, or reaction with ionized surfaces of some organic compounds can trigger silica precipitation (Kaufman et al., 1981; Perry and Mann, 1989). Carbohydrate polymers, namely hemicelluloses and cellulose, can also influence phytolith formation by helping to initiate silica polymerization and aggregation (Perry and Lu 1991). The distribution of silica with specific ultrastructural motifs throughout the plant (e.g. small amounts of fibrillar silica that is common in stems can be found at the base of leaves) suggests that the fundamental silica particles are nucleated within the transpiration stream and then transported throughout the plant before they ripen (Perry and Fraser 1991), but this has not been confirmed.

1.1.2 Phytolith preservation

The preservation of phytoliths in soils varies widely. Well-preserved phytoliths have been recovered from Pliocene-aged deposits, while in some tropical soils the bulk of phytolith input turns over within 6 months (Baker, 1960; Jones; 1964; Alexandre et al., 1997). Clearly, preservation is variable, and depends on phytolith morphology and the chemical characteristics of the soil (e.g. pH, temperature, Al content) (Alexandre et al., 1997; Piperno, 2006). It has been suggested that the presence of aluminum in the silica structure or adsorbed onto the surface of particles of biogenic silica can aid in preservation, but contradictory results have been reported (Bartoli and Wilding 1980;

Fraysse et al., 2009). Alexandre et al. (1994) examined phytoliths found in the litter and upper layer of a tropical soil and found that phytolith dissolution was selective, favouring the removal of cell wall phytoliths. The surfaces of those remaining in the soil were rugulose or stippled indicating partial dissolution.

Phytolith preservation can also be influenced by wildfires. Changes in morphology as a result of the loss of fine features can occur at temperatures as low as 600ºC (Runge 1998). Resistance to heat alteration appears to be somewhat species and plant part specific; phytoliths from some species of rice plants retained their diagnostic morphologies until up to 1000ºC (Wu et al., 2012). In addition, wildfires have the potential to regionally re-distribute phytoliths in smoke and ash potentially contaminating assemblages with non-local phytoliths (Fredlund and Tieszen 1994).

Methods of determining the preservation of a phytolith assemblage rely heavily on visual examination and consideration of general preservation patterns in the study area (Piperno 2006). Preservation can be assessed by examining an assemblage for the presence of weathered morphotypes (i.e. identifiable shapes that are pitted or display irregular fine features) (Fredlund and Tieszen 1997). The presence of phytolith shapes that are relatively unstable (e.g. hair and long cells or any shape that is highly decorated) is the best indicator of a well-preserved assemblage (Cabanes et al., 2011). Methods of determining if assemblages have been subjected to fire, in particular, are phytolith colouration (Parr, 2006) and refractive indices (Elbaum et al., 2003). While darker coloured phytoliths can occur without burning, darkly coloured burned phytoliths differ in appearance when observed through an optical microscope in that burned phytoliths have a dull opaque finish while pristine dark phytoliths are transparent/opalescent (Parr, 2006). The refractive index of a phytolith can also be used to detect assemblages that have been subject to burning. A shift to higher refractive indices indicates burning; an assemblage that has a large fraction of individual phytoliths with a refractive index higher than 1.440 have likely been subject to burning (Elbaum 2003).

1.2 The silicon cycle

The biogeochemical cycle of silicon is complex and links many environments, both on continents and in the oceans. The main reservoirs through which silicon cycles are soils, aquifers, lakes and rivers, oceans, and marine sediments (Fig. 1-1; Basile-Doelsch, 2006). This section will focus on the role of plants in the biogeochemical cycle of silicon.

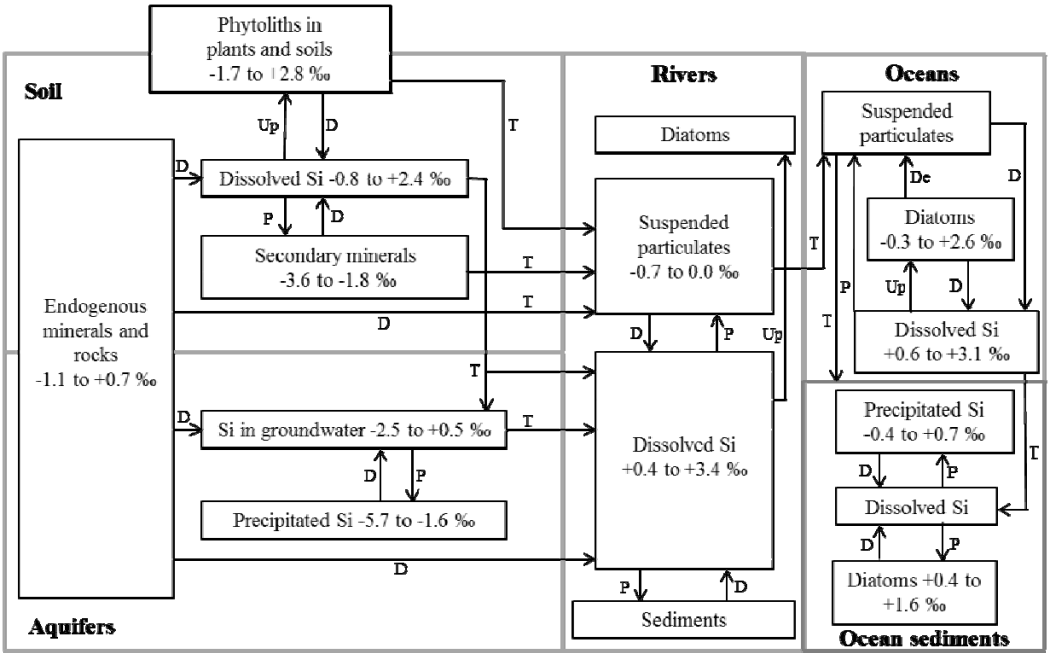

Fig.1-1. Cycle of silicon in continental and marine environments and associated $\delta^{30}Si$ values of the silicon pools. Arrows denote the direction of movement of silicon through the various pools and letters denote the manner of movement. D: dissolution; P: precipitation; T: transport; Up: uptake; De: death. Modified from Baile-Doelsch (2006) with additional data from Ziegler et al. (2005) and Ding et al. (2009).

Land plants effect the terrestrial silicon cycle through several pathways. They modify soil pH through the production of CO_2 and organic acids, they alter the physical properties of soils, and contribute to the physical breakdown of bedrock (Drever 1994). In addition, the influence of land plants on continental precipitation patterns is likely very important, although difficult to quantify (Berner, 1992; Drever, 1994).

The concentration of silicic acid in the terrestrial silicon pool is modified by mineral weathering, plant uptake, secondary clay mineral formation, adsorption onto oxides, and leaching to the hydrosphere (Sommer et al., 2006). The biogeochemical cycling of silicon in terrestrial ecosystems has been much less studied than in aquatic ecosystems, despite the fact that terrestrial plant silica contributes significantly to the marine silicon content and its related biological activity (Meunier et al., 2005). Terrestrial plants take up a large portion of the dissolved silica produced during weathering, meaning that much of the silicic acid the ultimately ends up in the oceans via rivers goes through plants first (Sommer et al., 2006; Derry et al., 2005; Conley 2002; Alexandre et al., 1997). For example, in some equatorial rainforests only about 7.5% of phytoliths formed a stable pool of biogenic silica in the soil; the rest were dissolved and taken up again by plants, deposited as new phytoliths in other soil horizons, or flushed from the system into waterways (Alexandre et al., 1997). In temperate deciduous ecosystems about 85% of the soluble silicon in soils has been released from biogenic silica, while in a temperate coniferous ecosystem only ~15% of the soluble silicon was biogenic in origin (Bartoli 1983). Turnover of biologically derived silicon in tropical rainforest ecosystems is high (up to 75 kg/ha/yr), while in temperate deciduous and pine forests it is considerably lower (~35.5 and 4.5 kg/ha/yr, respectively) (Bartoli and Souchier 1987). In general, phytolith fixation of silica ranges from 60-200 Tmol/yr among different ecosystems (Conley 2002). The land-to-ocean silicon flux contributes more than 80% of the dissolved Si input to the oceans (Tréguer et al., 1995) and much of this Si, in some environments, almost all has moved through plants (Derry et al., 2005). Decreases in species diversity of both fresh-water and marine diatoms have been linked with grassland expansion demonstrating the role of plants in the link between terrestrial and marine/aquatic silicon cycles (Kidder and Gierlowski-Kordesch 2005; Rabosky and Sorhannus 2009).

1.3 Silicon and oxygen isotope systematics in phytoliths

1.3.1 Oxygen isotopes

Phytoliths are composed of silica that precipitates directly from plant water. Their $\delta^{18}O$ values are determined by a temperature dependant fractionation between the silica and

plant water $\delta^{18}O$ values. The $\delta^{18}O$ values of plant water are dependent on the $\delta^{18}O$ value of soil water, the $\delta^{18}O$ value of atmospheric vapour, temperature, and relative humidity. The uptake of soil water by roots is not associated with any oxygen isotope fractionation and so water in the root and stem has the same isotopic composition as soil water (Allison et al., 1984). The soil water composition is essentially that of local meteoric water (i.e. precipitation and shallow groundwater) (Dawson et al., 1998; Gat 1998; Yakir et al., 1998). Prior to root uptake, soil water in the shallow soil horizons can be modified by evaporation from the soil surface (Barnes and Allison, 1983).

Relative humidity can also influence the $\delta^{18}O$ values of phytolith silica in that the isotopic composition of leaf water is modified through evapotranspiration. During transpiration leaf water becomes enriched in ^{18}O and the extent of this enrichment is inversely correlated with relative humidity (Farris and Strain, 1978). This signal, along with the temperature-related fractionation that occurs during the transition from dissolved to solid silica, influences phytolith $\delta^{18}O$ values (Shahack-Gross et al., 1996; Webb and Longstaffe, 2002). Temperature influences the degree of fractionation between amorphous silica and the water from which it forms, and this has been applied to the study of phytoliths (Shahack-Gross et al., 1996). In the stem, where ^{18}O-enrichment of plant water through transpiration is not a factor, the primary influence on the $\delta^{18}O$ value of phytoliths is the temperature-dependent fractionation factor (Webb and Longstaffe, 2002). Shahack-Gross et al. (1996) developed a paleo-thermometer equation for silica phytoliths:

$$t\,(°C) = 5.8 - 2.8\,(\,\delta^{18}O_{silica} - \delta^{18}O_{plant\ water} - 40\,) \qquad (1\text{-}1)$$

However, when phytoliths with high $\delta^{18}O$ values from transpiring tissues that carry a relative humidity signal are combined with those from non-transpiring tissues in a soil-phytolith assemblage this relationship can be confounded (Webb and Longstaffe 2002). This can be corrected for provided the soil water oxygen isotope composition can be estimated with relative confidence (Webb and Longstaffe 2002).

1.3.2 Silicon isotopes

The silicon source for plants is in the form of dissolved silica in soil water. During mineral weathering, the lighter silicon isotope (^{28}Si) is preferentially released to the dissolved phase, and this process has a strong control on the $\delta^{30}Si$ value of soil water (Ziegler et al., 2005; Basile-Doelsch 2006). Dissolved silica in soils has a $\delta^{30}Si$ value between ~ -0.8 to +2.4 ‰ (Ziegler et al., 2005; Ding et al., 2009). It has been shown for bamboo that there is a biochemical fractionation of silicon isotopes ($\alpha_{plant\text{-}water} = 0.9988$) during root uptake of dissolved silica, which means that ^{28}Si is preferentially taken up by the plant (Ding et al., 2009). Similar $\delta^{30}Si$ values have been observed for rice and banana plants (Ding et al., 2005; Opfergelt et al., 2006). The $\delta^{30}Si$ values of phytoliths increase from the plant stem through branches and leaves (Ding et al., 2005; 2009; Opfergelt et al, 2006). A Rayleigh fractionation model has been proposed to explain the ^{30}Si enrichment in both phytoliths and the plant water dissolved silicon pool along this gradient (Ding et al., 2005; 2008). In this model ^{28}Si is taken up during phytolith formation and the remaining plant water is enriched in ^{30}Si. Phytoliths formed subsequently will have higher $\delta^{30}Si$ values. Phytolith $\delta^{30}Si$ values ranging from -2.3 to +2.8 ‰ have been reported (Douthitt 1982; Ziegler et al., 2005; Ding et al., 2009). Although phytolith formation preferentially uses the lighter Si isotope, when the silica supply is limited more of the heavy isotope is incorporated into the phytoliths. As a result, the lower the concentration of silicic acid inside the plant the higher the $\delta^{30}Si$ values of the phytoliths (Ding et al., 2009). The $\delta^{30}Si$ values of phytoliths carry information on the $\delta^{30}Si$ values of soil water, which can potentially be related to local agricultural history and climate conditions (Opfergelt et al., 2008; Ding et al., 2009).

1.4 Dissolution studies

It is important to understand how phytoliths dissolve and to what degree this alters their oxygen and silicon isotope compositions. The dissolution of silica involves hydrolysis in an excess of water:

$$SiO_2 + 2\ H_2O \leftrightarrow Si(OH)_4 \qquad (1\text{-}2)$$

so the majority of silica released to natural waters is in the form of monosilicic acid (Langmuir, 1997). Because silica is comprised of Si-O-Si linkages it is Si-O bonds that

must be broken for dissolution to occur. Silica solubility increases dramatically above pH of approximately 9 as a result of the dissociation of silicic acid, which drives the reaction in (1-2) to the right.

Phytolith solubility is close to that of inorganic amorphous silica, and their dissolution rates fall between that of quartz and vitreous silica (Fraysse et al., 2006b; 2009). Based on an examination of the aqueous reactivity of horsetail and pine phytoliths Fraysse et al. (2006a) suggest that the rate of phytolith dissolution is independent of topology and the geometry of local structures, and that there are no preferential dissolution sites on the surface of phytoliths. Phytoliths of some species are more soluble than others; for example, pine phytoliths are more resistant to dissolution than those of other plants such as horsetails and beech (Bartoli and Wilding, 1980; Fraysse et al., 2006a). There are conflicting results on the effect of structural aluminum in protecting phytolith silica against dissolution (Bartoli and Wilding, 1980; Fraysse et al., 2009). It has been suggested that the protection against dissolution provided by aluminum is the result of both chemisorption of Al to the silica surface, and a coagulative effect during silica synthesis that results in reduced surface area (Bartoli and Wilding, 1980; Bartoli, 1985). However, other studies saw no relationship between phytolith dissolution rate and aluminum content (Fraysse et al., 2009). There are no studies that examine the effect of dissolution on the isotopic composition of phytolith silica, although this has been studied for diatoms.

Diatom frustules and phytoliths are both composed of hydrated amorphous silica, and the surface chemistry and reactivity of diatom silica has been extensively studied. There is a notable difference in the dissolution rates and surface properties of fresh versus sedimentary diatoms (Dixit and VanCappellen 2002; VanCappellen et al., 2002; Hurd et al., 1981; Barker et al., 1994). The discrepancy in dissolution rates estimated for surface (fresh) versus sedimentary diatoms has been attributed to differences in Al content, specific surface area, temperature, and degree of undersaturation (VanCappellen et al., 2002). In marine sediments, the decrease in the specific surface area of diatom silica with depth and the Al content of pore waters act to reduce silica solubility while diatoms age

in the sediment (Dixit et al., 2001; VanCappellen 1996; VanCappellen et al., 2002; Dixit and VanCappellen 2002).

Fresh diatoms have oxygen-isotope values that are fractionated relative to water 3 to 10 ‰ lower than fossil diatoms formed in the same environment (Schmidt et al., 1997; Brandriss et al., 1998). It has been suggested that preferential dissolution of ^{16}O-enriched Si-OH groups could alter the δ^{18}Osilica values of fossil diatoms (Schmidt et al., 1997; Brandriss et al., 1998). Schmidt et al. (2001) found no evidence of dissolution of isotopically light Si-OH groups but did find that the ratio of integrated peak intensities for Si-O-Si/SiOH infrared vibrational modes correlate with increases in $\delta^{18}O_{silica}$. This suggests that internal condensation reactions are responsible for the enrichment of sedimentary diatoms in ^{18}O. Silica condensation involves the combination of two Si-OH groups to form Si-O-Si bonds. It is suggested that this process selectively releases ^{16}O resulting in higher δ^{18}O values of biogenic opal after deposition in sediments (Schmidt et al., 2001).

Studies of the silicon isotope effects during biogenic silica dissolution have focussed on the δ^{30}Si value of silicon in solution or the offset in δ^{30}Si values between solid and dissolved diatom silica (Demarest et al., 2009; Geilert et al., 2014; Wetzel et al., 2014). There are currently no studies examining the effect of dissolution on the silicon isotope composition of phytolith silica. For diatoms, the dissolved phase generally has lower δ^{30}Si values than its source solid (Demarest et al., 2009; Geilert et al., 2014; Wetzel et al., 2014). A similar trend was reported for the δ^{30}Si value of dissolved silicon sourced from phytoliths (Ziegler et al., 2005). Dissolution of diatom silica was found to discriminate against ^{30}Si with an enrichment factor of $\varepsilon_{\text{dissolved Si-biogenic Si}}$ of -0.55 ‰, and this enrichment factor did not vary with source material or temperature between 3 and 20°C (Demarest et al., 2009). However, a similar study by Wetzel et al. (2014) found no significant silicon isotope fractionation accompanying the dissolution of diatom frustules. The difference between these studies was attributed to differences in the aluminum content of the frustules used, but more work is needed to understand the mechanisms responsible for the fractionation, of lack thereof, of silicon isotopes during the dissolution of biogenic silica (Demarest et al., 2009; Wetzel et al., 2014). All studies were consistent

in that after nearly 50% of the original mass of biogenic silica had dissolved no changes in the initial $\delta^{30}Si$ values of the solid diatoms were observed (Demarest et al., 2009; Geilert et al., 2014; Wetzel et al., 2014).

1.5 Applications of the isotopic study of phytoliths

The isotopic composition of paleo-plant material such as cellulose, pollen, and, more recently *n*-alkanes from leaf wax, has been used extensively in the reconstruction of past environments (e.g. Liu and Huang, 2005; Lichtfouse et al., 1994; Nelson et al., 2008; Richter et al., 2008). Archaeological and sedimentary phytoliths also have the potential to provide information about terrestrial climate as their oxygen isotope composition is influenced by environmental factors. The temperature models developed and further investigated by Shahack-Gross et al. (1996) and Webb and Longstaffe (2002, 2003) have not yet been used in reconstructions of past environments. However, the use of modern soil phytolith $\delta^{18}O$ values to examine relative changes in soil water/precipitation $\delta^{18}O$ values and annual temperature was successful (Alexandre et al., 2012). Work has been done examining the various factors that determine the $\delta^{18}O$ values of phytolith silica from different plant parts but there are still some inconsistencies and further study of modern plants is needed before phytolith $\delta^{18}O$ values can be used reliably as a proxy of environmental conditions during plant growth (Shahack-Gross et al., 1996; Webb and Longstaffe, 2002, 2003; Hodson et al., 2008). The silicon isotope composition of diatom frustules has been applied as a means of tracking the flux of silicon through the oceans over long timescales (e.g. Cardinal et al., 2007). A similar approach to tracking Si-fluxes may be possible for terrestrial environments via the $\delta^{30}Si$ values of phytoliths.

The yet unstudied issue of the effect of post-deposition alteration of phytolith silica on its isotopic composition will be explored in this thesis. Changes in the isotopic composition of biogenic silica can effect interpretations of paleoenvironmental conditions. An increase in $\delta^{18}O$ values by 2 ‰ would result in an underestimation of temperature by more than 5˚C. Post depositional modification of $\delta^{18}O_{silica}$ values will also impact studies concerned only with relative changes in $\delta^{18}O$ values if the degree of alteration is not the same through the entire chronology (sediment core or soil profile). Changes in $\delta^{30}Si$ to

higher values would result in underestimations the availability of silicic acid (Ding et al., 2008). These effects must be taken into account when examining changes in the isotopic composition of biogenic silica. This type of study lays the groundwork for improving our understanding of the role of terrestrial biogenic silica in global geochemical cycles.

This thesis is divided into four main chapters written as independent research articles. Chapter 2 outlines the development of a microsilicate vacuum line for the extraction, purification, and analysis of oxygen and silicon isotopes from a single 1mg sample. Chapter 3 discusses the silicon isotope results of a series of dissolution experiments conducted on phytolith silica and implications relating to the role of phytoliths in modifying the $\delta^{30}Si$ values of waters leaving the soil. Chapter 4 reports the oxygen isotope results from the same dissolution experiments outlined in chapter 3 and discusses the ways in which phytolith $\delta^{18}O$ values can be modified once in the soil. Chapter 5 investigates the effect of burning on the $\delta^{18}O$ and $\delta^{30}Si$ values of phytoliths. Also discussed are changes in specific surface area and dissolution characteristics of burned phytoliths. Chapter 6 provides a summary of the results from preceding chapters and comments on the utility of phytolith isotopic compositions in investigating paleoclimate and the silicon cycle.

1.6 References

Alexandre, A., Colin, F., Meunier, J.D. (1994) Phytoliths as indicators of the biogeochemical turnover of silicon in equatorial rainforest. Comptes Rendus de l'Académie des Sciences: Série Geoscience 319(2), 453-458.

Alexandre, A., Meunier, J.D., Colin, F., Koud, J.M. (1997) Plant impact on the biogeochemical cycle of silicon and related weathering. Geochimica et Cosmochimica Acta 61(3), 677-682.

Alexandre, A., Crespin, J., Sylvestre, F., Sonzogni, C., Hilbert, D.W. (2012) The oxygen isotopic composition of phytolith assemblages from tropical rainforest soil tops (Queensland, Australia): validation of a new palaeoenvironmental tool. Climate of the Past 8, 307-324.

Allison G. B., Barnes C. J., Hughes M. W., and Leaney F. W. J. (1984) Effect of climate and vegetation on oxygen-18 and deuterium profiles in soils. In *Isotope Hydrology* (IAEA SM 270/20), Vienna, pp. 105–124.

Baker, G. (1960) Fossil opal-phytoliths. Micropaleontology 6(1), 79-85.

Barnes C.J. and Allison G.B. (1983) The distribution of deuterium and ^{18}O in dry soils. Journal of Hydrology 60, 141-156.

Bartoli, F. (1983) The biogeochemical cycle of silicon in two temperate forests. Environmental Geochemistry Ecological Bullentins 35, 469-476.

Bartoli, F. (1985) Crystallochemistry and surface properties of biogenic opal. Journal of Soil Science 36, 335-350.

Bartoli, F. and Souchier, B. (1978) Cycle et rôle du silicium d'origine végétale dans les écosystèmes forestiers tempérés. Annaels des Sciences Forestières 35, 187-202.

Bartoli, F., Wilding, L.P. (1980) Dissolution of biogenic opal as a function of its physical and chemical properties. Soil Science Society of America Proceedings 44, 873-878.

Basile-Doelsch, I., Meunier, J.D., Parron, C. (2005) Another continental pool in the terrestrial silicon cycle. Nature 433, 399-402.

Basile-Doelsch, I. (2006) Si stable isotope in the Earth's surface: A review. Journal of Geochemical Exploration 88, 252-256.

Berner, R.A. (1992) Weathering, plants, and the logs term carbon cycle. Geochimica et Cosmochimica Act 56, 3225-3231.

Brandriss, M.E., O'Neil, J.R., Edlund, M.B., Stoermer, E.F. (1998) Oxygen isotope fractionation between diatomaceous silica and water. Geochimica et Cosmochimica Acta 62(7), 1119-125.

Chen, C. and Lewin, J. (1969) Silicon as a nutrient for *Equisetum arvense*. Annals of Botany 47, 125-131.

Cabanes, D., Weiner, S., Shahack-Gross, R. (2011) Stability of phytoliths in the archaeological record: a dissolution study of modern and fossil phytoliths. Journal of Archaeological Science 38, 2480-2490.

Conley, D.J. (2002) Terrestrial ecosystems and the global biogeochemical silica cycle. Global Biogeochemical Cycles 16, 68-1 – 68-8.

Demarest, M.S., Brzezinski, M.A., Beucher, C.P. (2009) Fractionation of silicon isotopes during biogenic silica dissolution. Geochimica et Cosmochimica Acta 73, 5572-5583.

Derry, L.A., Kurtz, A.C., Ziegler, K., Chadwick, O.A. (2005) Biological control of terrestrial silica cycling and export fluxes to watersheds. Nature 433, 728-731

De La Rocha, C.L., Brzezinski, M.A., DeNiro, M.J., Shemesh, A. (1998) Silicon-isotope composition of diatoms as an indicator of past oceanic change. Nature 395, 680-683.

Ding, T.P., Ma, G.R., Shui, M.X., Wan, D.F., Li, R.H. (2005) Silicon isotope study on rice plants from the Zhejiang province, China. Chemical Geology 218, 41-50.

Ding, T.P., Zhou, J.X., Wan, D.F., Chen, Z.Y., Wan, C.Y., Zhang, F. (2008) Silicon isotope fractionation in bamboo and its significance to the biogeochmical cycle of silicon. Geochimica et Cosmochimica Acta 72, 1381-1395.

Dixit, S. and Van Cappellen, P. (2002) Surface chemistry and reactivity of biogenic silica. Geochimica et Cosmochimica Acta 66, 2559-2568.

Dixit, S., Van Cappellen, P., van Bennekom, A.J. (2001) Processes controlling solubility of biogenic silica and pore water build-up of silicic acid in marine sediments. Marine Chemistry 73, 333-352.

Drever, J.I. (1994) The effect of land plants on weathering rates of silicate minerals. Geochimica et Cosmochimica Acta 58, 2325-2332.

Elbaum, M. (2003) Detection of burning of plant materials in the archaeological record by changes in the refractive indices of siliceous phytoliths. Journal of Archaeological Science 30, 217-226.

Epstein, E. (1994) The anomaly of silicon in plant biology. Proceedings of the National Academy of Sciences USA 91, 11-17.

Farris, F. And Strain, B.R. (1978) The effect of water-stress on leaf $H_2{}^{18}O$ enrichments. Radiation and Environmental Biophysics 15(2), 167-202.

Fraysse, F., Cantais, F., Pokrovsky, O.S., Schott, J., Meunier, J.D. (2006a) Aqueous reactivity of phytoliths and plant litter: Physico-chemical constraints on terrestrial biogeochemical cycle of silicon. Journal of Geochemical Exploration 88, 202-205.

Fraysse, F., Pokrovsky, O.S., Schott, J., Meunier, J.D. (2006b) Surface properties, solubility, and dissolution kinetics of bamboo phytoliths. Geochimica et Cosmochimica Acta 70, 1939-1951.

Fraysse, F., Pokrovsky, O.S., Schott, J., Meunier, J.D. (2009) Surface chemistry and reactivity of plant phytoliths in aqueous solutions. Chemical Geology 258, 197-206.

Fredlund, G.G. and Tieszen, L.T. (1994) Modern phytolith assemblages from the North American Great Plains. Journal of Biogeography 21, 321-335.

Fredlund, G.G. and Tieszen, L.L. (1997) Phytolith and carbon isotope evidence for late Quaternary vegetation and climate change in the southern Black Hills, South Dakota. Quaternary Research 47, 206-217.

Kaufman, P.B., Dayanandan, P., Takeoka, Y., Bigelow, W.C., Jones, J.D., Iler, R. (1981) Silica in the shoots of higher plants. In Silicon and Siliceous Structures in Biological Systems (eds. T.L. Simpson and B.E. Volcani), Chap. 15, pp. 409-450. Springer-Verlag.

Kidder, D.L. and Gierlowski-Kordesch, E.H. (2005) Impact of grassland radiation on the nonmarine silica cycle and Miocene diatomite. Palaios 20, 198-206.

Jones, R.L. (1964) Note on occurrence of opal phytoliths in some Cenozoic sedimentary rocks. Journal of Paleontology 38, 773-775.

Juillet-Leclerc, A. and Labeyrie, L. (1987) Temperature dependence of the oxygen isotopic fractionation between diatom silica and water. Earth and Planetary Science Letters 84, 69-74.

Labeyrie, L.D. (1974) New approach to surface seawater paleotemperatures using $^{18}O/^{16}O$ ratio in silica of diatom frustules. Nature 248, 40-42.

Lichtfouse, É., Elbisser, B., Balesdent, J., Mariotti, A., Bardoux, G. (1994) Isotope and molecular evidence for indirect input of maize leaf wax *n*-alkanes into crop soils. Organic Geochemistry 22(2), 349-351.

Liu, W., Huang, Y. (2005) Compound specific *D/H* ratios and molecular distributions of higher plant leaf waxes as novel paleoenvironmental indicators in the Chinese Loess Plateau. Organic Geochemistry 36(6), 851-860.

Matheney, R.K. and Knauth, P. (1989) Oxygen-isotope fractionation between marine biogenic silica and seawater. Geochimica et Cosmochimica Acta 53, 3207-3214.

Moschen, R., Lücke, A., Schleser, G.H. (2005) Sensitivity of biogenic silica oxygen isotopes to changes in surface water temperature and palaeoclimatology. Geophysical Research Letters 32, doi:10.1029/2004GL022167.

Nelson, D.M., Hu, F.S., Scholes, D.R., Joshi, N., Pearson, A. (2008) Using SPIRAL (Single Pollen Isotope Ratio AnaLysis) to estimate C_3- and C_4-grass abundance in the paleorecord. Earth and Planetary Science Letters 269, 11-16.

Opfergelt, S., Cardinal, D., Henriet, C., Andre, L., Delvaux, B. (2006) Silicon isotopic fractionation by banana (Musa spp.) grown in a continuous nutrient flow device. Plant and Soil 285, 333-345.

Opfergelt, S., Delvaux, B., André, L., Cardinal, D. (2009) Plant silicon isotopic signature might reflect soil weathering degree. Biogeochemistry 91, 163-175.

Parr, J.F. (2006) Effect of fire on phytolith coloration. Geoarchaeology 21, 171-185.

Perry, C.C. and Mann, S. (1989) Aspects of biological silicification. In Origin, Evolution, and Modern Aspects of Biomineralization in plants and animals (ed. R.E. Crick), pp. 419-431. Plenum Press.

Piperno, D.R. (2006) Phytoliths: A Comprehensive Guide for Archaeologists and Paleoecologists. AltaMira Press.

Rabosky, D.L. and Sorhannus, U. (2009) Diversity dynamics of marine planktonic diatoms across the Cenozoic. Nature 457, 183-187.

Raven, J.A. (1983) The transport and function of silicon in plants. Biological Reviews Cambridge Philosophical Society 58, 179-207.

Richter, S.L., Johnson, A.H., Dranoff, M.M., LePage, B.A., Williams, C.J. (2008) Oxygen isotope ratios in fossil wood cellulose: Isotopic composition of Eocene- to Holocene-aged cellulose. Geochimica et Cosmochimica Acta 72(12), 2744-2753.

Schmidt, M., Botz, R., Rickert, D., Bohrmann, G., Hall, S.R., Mann, S. (2001) Oxygen isotopes of marine diatoms and relations to opal-A maturation. Geochimica et Cosmochimica Acta 65(2), 201-211.

Schmidt, M., Botz, R., Stoffers, P., Anders, T., Bohmann, G. (1997) Oxygen isotopes in marine diatoms: A comparative study of analytical techniques and new results on the isotope composition of recent marine diatoms. Geochimica et Cosmochimica Acta 61, 2275-2280.

Shahack-Gross, R., Shemesh, A., Yakir, D., Weiner, S. (1996) Oxygen isotopic composition of opaline phytoliths: Potential for terrestrial climatic reconstruction. Geochimica et Cosmochimica Acta 60(20), 3949-3953.

Sommer, M., Kaczorek, D., Kuzyakov, Y., Breuer, J. (2006) Silicon pools and fluxes in soils and landscapes – a review. Journal of Plant Nutrition and Soil Science 169, 310-329.

Treguer, P., Nelson, D.M., Van Bennekom, A.J., DeMaster, D.J., Leynaert, A., Queguiner, B. (1995) The silica balance in the world ocean: A reestimate. Science 268, 375-379.

Walker, C.D., Lance, R.C.M. (1991) Silicon accumulation and ^{13}C composition as indices of water-use efficiency in barley cultivars. Australian Journal of Plant Physiology 18, 427-434.

Webb, E.A. and Longstaffe, F.J. (2002) Climatic influences on the isotopic composition of biogenic silica in prairie grass. Geochimica et Cosmochimica Acta 66(11), 1891-1904.

Webb, E.A. and Longstaffe, F.J. (2003) The relationship between phytolith- and plant-water $\delta^{18}O$ values in grasses. Geochimica et Cosmochimica Acta 67(8), 1437-1449.

Wetzel, F., de Souza, G.F., Reynolds, B.C. (2014) What controls silicon isotope fractionation during dissolution of diatom opal? Geochimica et Cosmochimica Acta 131, 128-137.

Van Cappellen, P. (1996) Reactive surface area control of the dissolution kinetics of biogenic silica in deep-sea sediments. Chemical Geology 132, 125-130.

Van Cappellen, P., Dixit, S., van Beusekom, J. (2002) Biogenic silica in the oceans: Reconciling experimental and field-based dissolution rates. Global Geochemical Cycles 16, 1-10.

2 Simultaneous measurement of $\delta^{18}O$ and $\delta^{30}Si$ values of small samples of opal-A

2.1 Introduction

Isotopic analysis of biogenic opal-A can be applied to studies of paleoclimate and biogeochemical cycles. The $\delta^{18}O$ values of biogenic silica can provide information about growing season temperatures in terrestrial ecosystems (phytoliths; e.g. Shahack-Gross et al., 1996; Webb and Longstaffe 2000) and sea surface/ lake water temperature (diatoms; e.g. Shemesh et al., 1992; Moschen et al., 2005; Dodd and Sharp 2010). The silicon isotope composition of biogenic opal-A yields information regarding both terrestrial and marine silicon cycles, and the role organisms play in moving silicon through this system (De La Rocha and Bickle 2005; Ding et al., 2009). However, accurate measurement of the isotopic composition of phytoliths or diatoms requires special considerations for sample purity and size, exchangeable hydroxyl groups on the surface of opal-A and traces of carbon occluded within the silica structure. This study presents the development of apparatus and techniques that allow for the simultaneous measurement of $\delta^{18}O$ and $\delta^{30}Si$ values from mg-sized samples of silica.

2.1.1 Extraction from soil and sediments

Prior to analysis, a pure sample of phytoliths or diatoms must be isolated from the soil or sediment. For oxygen isotope analysis a diatom sample must be almost completely pure; more than ~3% sediment contamination will result in low $\delta^{18}O$ values (Leng and Barker 2006). Methods of removing contamination from diatom samples involve chemical treatments for the removal of organic matter and carbonates, sieving for the removal of clays and fine silts, and differential settling techniques as well as heavy liquid flotation for the separation of diatoms from coarser silts (Shemesh et al., 1995; Morley et al., 2004; Leng and Barker 2006). A SPLITT (split-flow thin cell fractionation) device has

also been successfully used for the isolation of diatoms from sediments (Schleser et al., 2001; Rings et al., 2004). The sample travels through a thin channel (371μm) carried by water in laminar flow. The liquid in the upper and lower portions of the channel have different velocities, which separates the sample into two streams, with the finer and less dense particles forming the upper stream. The process can replace heavy liquid flotation but a similar series of pretreatment steps are required prior to the introduction of the sample to the SPLITT device (detailed in Rings et al., 2004).

Phytoliths are routinely extracted from soils for morphological studies leading to species identification and ecosystem reconstruction (Piperno 2006). However, this application does not require the same sample purity needed for isotope analyses as phytoliths can still be identified if the overall sample contains some soil particles. Various procedures for isolating the phytolith component of soils are compared and summarized in Lentfer and Boyd (1998), Zhao and Pearsall (1998), and Piperno (2006). Similar to diatoms, heavy-liquid flotation is the process used for collecting the phytoliths, but there are several steps (chemical attack and physical separation via sieving) that must be carried out first to ensure the phytoliths are free of organic matter, clays, and carbonate cements. Both heavy-liquid flotation and the SPLITT device are time consuming and, for phytoliths especially, large quantities of material must be processed to retrieve enough biogenic silica for isotope analysis. Both methods, if implemented correctly, provide high-purity fractions of biogenic silica. However, samples must be processed by the SPLITT device several times to obtain a pure sample and the channel must be thoroughly cleaned between batches (Leng and Barker 2006). Heavy-liquid flotation is equally effective but care must be taken to thoroughly rinse the sample of the heavy liquid prior to analysis as contamination results in low $\delta^{18}O$ values (Morley et al., 2004). Given these challenges, it is advantageous to be able to obtain accurate isotope analysis on very small sample sizes.

2.1.2 Solving the problem of exchangeable hydroxyl groups on opal-A

An early investigation into the suitability of radiolarian silica for oxygen isotope investigations found that sample $\delta^{18}O$ values were difficult to reproduce because of

loosely bound water within the silica samples that underwent oxygen-isotope exchange with environmental water (Mopper and Garlick, 1971). Labeyrie (1972) attempted to solve this problem by using vacuum dehydration, in which samples were heated under vacuum to 1000°C and remained at that temperature for a few hours. Oxygen isotope analyses of these samples produced results that were reproducible within ±0.1 ‰ (Labeyrie 1972). However, it was later suggested that this method reorganizes the silica structure and may allow the incorporation of ^{18}O-depleted hydroxyl groups into the structure through the formation of new Si-O-Si bonds (Labeyrie and Juillet 1982):

$$Si\text{-}OH + HO\text{-}Si \leftrightarrow Si\text{-}O\text{-}Si + H_2O \qquad (2\text{-}1)$$

This reaction is reversible until approximately 400°C (Alexandre, 1996). Therefore, any analysis of opal-A for stable oxygen isotope analyses must either eliminate the hydroxyl groups while preventing back-exchange or account for the $\delta^{18}O$ values of the hydroxyl groups that are incorporated in to the structural oxygen of the sample during dehydration. Four different methods are currently used for this purpose: step-wise fluorination, inductive high-temperature carbon reduction (iHTC), controlled isotope exchange, and inert gas flow dehydration (iGFD). Comparisons of the $\delta^{18}O$ values produced for opal-A using each of these can be found in Brandiss et al. (1998) and Chapligin et al. (2011) and generally produce $\delta^{18}O$ values that are the same within 0.3 to 0.9 ‰ depending on the material analysed.

2.1.2.1 Step-wise fluorination

In step-wise fluorination, oxygen from hydrous samples is recovered in a series of steps. Silica is reacted several times with a fluorinating agent at a high sample to reagent ratio to limit the extent of the reaction (Haimson and Knauth 1983). The water and exchangeable oxygen component reacts first, leaving the more stable Si-bound oxygen to react in later steps (Haimson and Knauth 1983). This produces a series of 2 to 7 oxygen fractions that tend to increase sequentially in ^{18}O, eventually reaching a plateau that represents the $\delta^{18}O$ value of tetrahedral oxygen (Haimson and Knauth 1983; Matheney

and Knauth 1989). At each step, the sample is reacted at 450-550°C for 20 minutes to 12 hours depending on the type of sample (Haimson and Knauth 1983; Matheney and Knauth 1989). Higher temperature (550˚C) and shorter reaction time (~20 min) is required to achieve reliable results for biogenic amorphous silica (Matheney and Knauth 1989). Leng and Sloane (2008) successfully use this method on 5-10mg size samples.

2.1.2.2 Inductive High-temperature Carbon Reduction

The iHTC device is a system designed to remove adsorbed water and exchangeable oxygen from hydrated samples, and conduct silica decomposition via carbon reduction all in the same chamber (Lucke et al., 2005). This method requires only ~1.5 mg of sample and can achieve reproducibility of 0.15 ‰ (Lucke et al., 2005). Before each sample is converted to CO any exchangeable oxygen is removed by heating under vacuum at room temperature, 850, and 1050°C. The high vacuum system removes volatilised gases before they can exchange isotopically with the sample. This method is touted as being faster and less involved than other methods used to remove exchangeable oxygen from hydrated silica samples.

2.1.2.3 Controlled isotope exchange

Controlled isotope exchange isotopically labels the exchangeable oxygen in the opal-A so that they can be accounted for and the true $\delta^{18}O$ values of the structural silica can be calculated. The method is described in detail in Labeyrie and Juillet (1982) and Leclerc and Labeyrie (1987). Briefly, a sample of biogenic silica is divided in two and each sample is allowed to exchange with a water vapour of known isotopic composition at a fixed temperature for 6 hours. After exchange the sample tube is isolated from the water reservoir, opened to the vacuum, and heated to 1000°C for at least eight hours to initiate silica reorganization. Using this method, the proportion of exchangeable oxygen and the oxygen isotope composition of only the non-exchangeable oxygen can be calculated (Labeyrie and Juillet 1982).

2.1.2.4 Inert gas flow dehydration

Inert gas flow dehydration (iGFD) removes the exchangeable components of hydrated silica through ramp degassing under a flow of inert gas. Reliable results have been obtained on samples ranging from 0.3 to 1.5 mg, with reproducibility better than 0.25 ‰ (Chapligin et al., 2010). In the procedure used by Chapligin et al. (2010), samples are weighed into holders and loaded into a horizontal ceramic tube furnace, the end caps of which are sealed with o-rings. There is a gas inlet on one end and a small outlet on the other to ensure that the atmosphere inside the ceramic tube is free of oxygen. The constant flow of inert gas, in this case helium, results in any removed exchangeable oxygen being immediately removed from the sample impeding the re-integration of oxygen (Chapligin et al., 2010). The dehydration begins with heating from room temperature to 1100°C over 2 hours under continuous helium flow at a rate of 5L/min. Once reaching 1100°C the temperature is held constant for 3 hours. The temperature is then ramped down to 400°C over 3.5 hours, and the helium flow rate decreased to 2L/min. Tests were conducted to ensure that different samples placed near each other in the furnace do not interact during the dehydration (Chapligin et al., 2010). With this method, samples should be analyzed shortly after the dehydration procedure is complete (Chapligin et al., 2010).

2.1.3 Carbon contamination affecting Si-isotopes

Fluorination of impure samples can produce an aliquot of SiF_4 gas that is contaminated by volatile fluorides and oxyfluorides of carbon, sulfur, phosphorus, and hydrogen (Douthitt 1982). These components are difficult to separate from SiF_4. Biogenic silica often contains small amounts of carbon; phytoliths can contain up to ~5% carbon in the form of inclusions, although most contain less than 1% (Jones and Milne 1963; Kelly et al., 1991; Carter 2009). As a result, some researchers dissolve and reprecipitate samples for silicon isotope analysis (Douthitt 1982; Ziegler et al., 2005; Demarest et al., 2009).

During the precipitation step only pure SiO_2 precipitates from the solution (Douthitt 1982). While this is an effective means of eliminating sources of contamination, the process completely resets the oxygen isotope composition of the sample, making the determinations of silicon and oxygen isotope compositions from the same sample impossible.

2.2 Methods

2.2.1 Inert Gas Flow Dehydration

The inert gas flow dehydration technique was adapted for this study to remove the exchangeable oxygen from opal-A prior to oxygen gas extraction. The apparatus and methods are based on those described by Chapligin et al. (2010) with some modifications. The apparatus consists of a tube furnace fitted with a quartz tube (Fig 2-1). The quartz tube is connected to a tank of ultra-high purity nitrogen gas at one end with an outlet at the other. Each sample of opal-A was weighed into a quartz boat and loaded, at room temperature into the furnace which was then ramped to 1100°C over one hour under a constant flow of 4L/min of nitrogen gas. The sample remains at 1100°C for 1.5 hours after which the temperature is lowered to 400°C over 3.5 hours. Then the gas flow was turned off and the sample was left to cool to room temperature. The differences between this procedure and that of Chapligin et al. (2010) include the inert gas used, the quartz tube, the gas flow rate, and the temperature ramp-up time (Table 2-1). This method uses ultra-high purity nitrogen gas in place of helium, as nitrogen gas is less expensive. The use of a quartz tube instead of ceramic allows us to cool the sample faster at the end of the procedure without breaking the tubing.

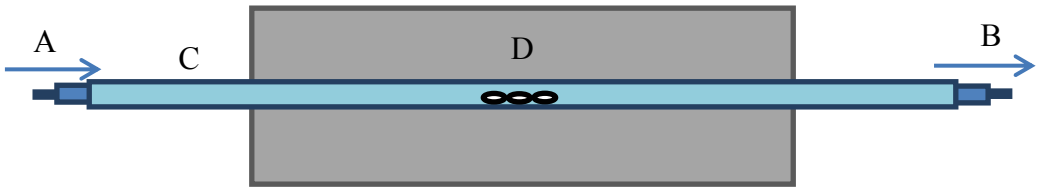

Figure 2-1. iGFD apparatus depicting gas inlet (A) and outlet (B), glass tubing (C), and furnace (D).

Table 2-1. Summary of modifications to the iGFD method originally developed by Chapligin et al. (2010).

	This study	**Chapligin et al., 2010**
Inert gas	N_2	He
Flow rate	4L/min	5L/min, 2L/min
Ramp-up time	1 hr	2 hrs
Max T	1100ºC	1100ºC hrs
Time at max T	1.5 hrs	1.5 hrs
Ramp-down time	3.5 hrs	3.5 hrs
Tube material	quartz	ceramic

2.2.2 Dual oxygen and silicon isotope analyses via vacuum extraction line

Oxygen and silicon isotope analysis of phytoliths requires that the material first be converted into oxygen (O_2) and silicon tetrafluoride (SiF_4) gas. Laser fluorination techniques have been used for oxygen and silicon isotope analysis of silicates (including biogenic silica) and oxides (Sharp 1990; Mattey and Macpherson 1993; De La Rocha et al., 1997; Crespin et al., 2008; Dodd and Sharp 2010). SIMS has been used for the determination of both oxygen and silicon isotope compositions of single mineral grains, but reproducibility can be a problem (Basile-Doelsch et al., 2005; Kita et al., 2009). In this study a vacuum extraction line was constructed to produce, purify, and collect these gases from silica and silicate minerals. The design is based largely on that of Leng and Sloane (2008) and Ding (2004). This method requires that pure silica or silicate minerals be used; samples containing C, S, or B impurities must be treated prior to fluorination to remove these elements (Ding, 2004). Minerals are reacted with BrF_5 to produce O_2 and SiF_4 and the gases purified in a vacuum extraction line. BrF_5 is used as the fluorinating agent rather than F_2 or ClF_3 because of its lower vapour pressure, making it easier to transfer by evaporation and condensation within the vacuum system.

The apparatus is made of stainless steel and copper tubing, with the exception of one glass trap and a glass collection tube for the determination of yields (one for O_2, one for SiF_4). A schematic of the extraction line is shown in Figure 2-2. Sample reaction (O_2 and SiF_4 formation) and gas extraction occurs on the right side of the line. This section

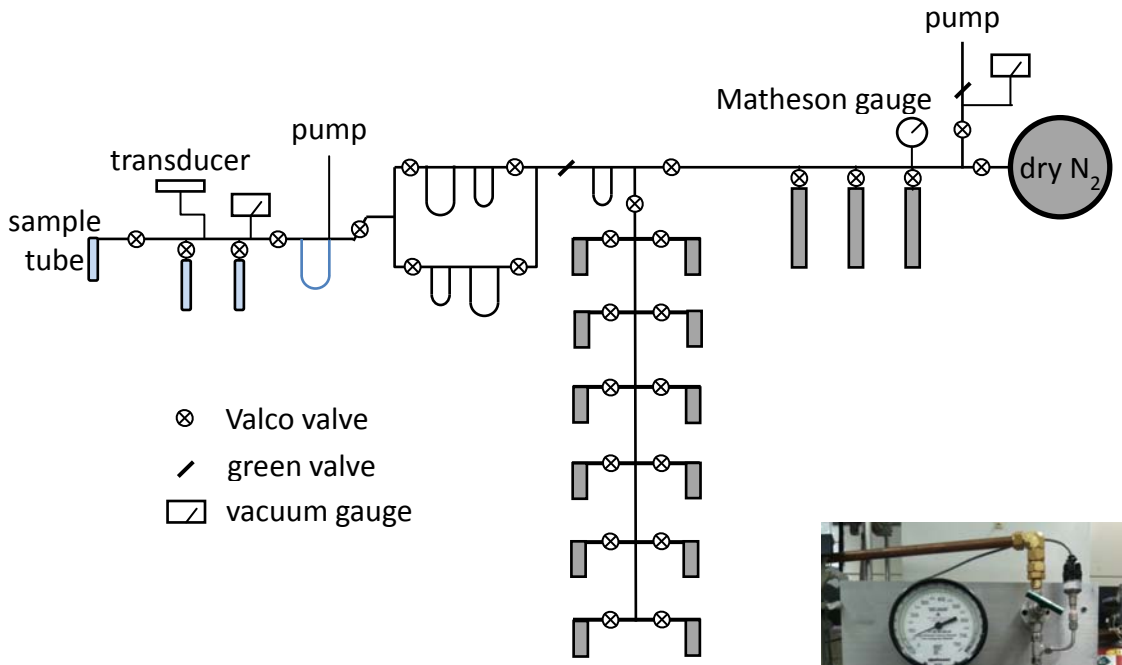

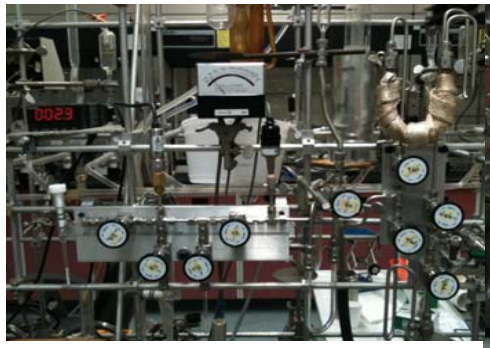

O_2 and SiF_4 purification

sample reaction

reagent storage

Figure 2-2. Schematic and photographs of the reaction vessels and vacuum extraction line for the purification of O_2 and SiF_4 gas.

contains Kel-F storage tubes for reagent and waste storage, two pressure gauges, a dry nitrogen inlet, Swagelok® valves, stainless steel tubing, and twelve nickel reaction vessels (volume = 5.2 cm^3). The left side of the line is for O_2 and SiF_4 purification and collection. This section consists of three cold traps, a KBr (lower) trap heated to 120˚C, a CuZn (upper) trap heated to 60˚C, yield fingers, and a sample collection tube. The entire system is kept under vacuum.

The line is designed for the purification of both O_2 (for $\delta^{18}O$ and $\delta^{17}O$ analyses) and SiF_4 gas produced from the same sample. This was accomplished by building two distinct routes through which to move the gases (Figure 2-2). Oxygen gas is drawn from the reaction vessel through the KBr trap by freezing the molecular sieve in the yield finger with liquid nitrogen. To ensure sample purity and reliable $\delta^{17}O$ results, transfer from the yield finger to the sample collection tube is conducted at -100˚C. The SiF_4 gas is drawn through the Zn trap by freezing on a yield finger with liquid nitrogen. The dimensions of the Zn trap have been modified from the original design of Ding (2004). Because this line processes a much smaller volume of gas than other lines the length of the Cu/Zn trap has been significantly reduced (to 28 cm). A 12 mm diameter tube was used to facilitate easier gas movement through the trap and ensure there would be enough zinc surface area available to react with contaminants. The purpose of both the KBr and zinc trap is to eliminate any trace amounts of BrF_5 or other fluorine compounds that may react with the glass and grease of the sample tube to produce contaminants, such as SiF_4 and CF_4, that can interferes with analysis on the mass spectrometer (Ding, 2004). Oxygen gas cannot be passed through a zinc trap without oxidizing the zinc.

2.2.2.1 Reaction and extraction procedure

Samples are loaded into the reaction vessels under a constant flow of ultra-high purity dry nitrogen to prevent atmosphere from entering the line. Reaction vessels are heated to 100°C overnight under vacuum to remove water adsorbed to the surface of the sample or

the sides of the reaction vessel. The next day, 100mmHg of BrF_5 reagent is frozen into each reaction vessel and samples are reacted for 16 hours at 600°C (for 1mg of pure silica). The oxygen extraction must be performed first because SiF_4 freezes at a higher temperature than O_2. For each sample, the reaction vessel is frozen with liquid nitrogen, keeping the reagent, SiF_4, and any reaction products (e.g., BrF_3, CF_4, etc.) other than O_2 frozen in the vessel. The valve at the top of the reaction vessel is opened releasing O_2 into the rest of the line. The O_2 gas is passed through a series of cold traps (all at liquid nitrogen temperature) and a KBr trap to remove any contaminants that may escape the reaction vessel. The gas is collected in the yield finger using a 6Å molecular sieve onto which the O_2 gas is frozen. After the sample yield is determined, the O_2 is transferred from the yield tube to the sample collection tube at -100°C using a slurry of ethanol and liquid nitrogen. Any nitrogen present in the line or in the sample can react with BrF_5 to form NF_3. When ionized in the mass spectrometer if interferes with mass 33 ($^{16}O^{17}O$) resulting in inaccurate $\delta^{17}O$ values (Clayton and Mayeda 1983). The slurry traps NF_3 to ensure clean O_2 gas for analysis.

After extraction of O_2 from all the reaction vessels, they are prepared for extraction of SiF_4. For each reaction vessel, the lower half is frozen with liquid nitrogen and then allowed to warm up to -110°C using an ethanol-liquid nitrogen slurry. This releases the SiF_4 but keeps other reaction products frozen. The SiF_4 is frozen into trap 1 with liquid nitrogen (Fig. 2-2). After the bomb is closed and the line pumped, trap 1 is warmed to -110°C releasing the SiF_4 and allowing it to be frozen into the next cold trap down the line. This procedure is repeated until the SiF_4 has been moved through all three cold traps, and the Zn trap. After yield determination, the gas is frozen into a sample collection tube to be transported to the mass spectrometer for analysis.

Oxygen and silicon isotope analyses were performed on a MAT-253 mass spectrometer. The increased sensitivity of this instrument means that even with only the gas produced from 1mg of sample (16.7 μmol of O_2 and 16.7 umol of SiF_4), $\delta^{17}O$, $\delta^{18}O$, $\delta^{29}Si$, and $\delta^{30}Si$ values can be obtained. All oxygen isotope results were reported in the standard delta notation relative to VSMOW:

$$\delta^{17}O\ (‰) = [(^{17}O/^{16}O)_{sample}/(^{17}O/^{16}O)_{VSMOW} - 1] \times 10^3 \quad (2\text{-}2)$$

$$\delta^{18}O\ (‰) = [(^{18}O/^{16}O)_{sample}/(^{18}O/^{16}O)_{VSMOW} - 1] \times 10^3 \quad (2\text{-}3)$$

All silicon isotope results were reported in the standard delta notation relative to NBS-28:

$$\delta^{29}Si\ (‰) = [(^{29}Si/^{28}Si)_{sample}/(^{29}Si/^{28}Si)_{NBS\text{-}28} - 1] \times 10^3 \quad (2\text{-}4)$$

$$\delta^{30}Si\ (‰) = [(^{30}Si/^{28}Si)_{sample}/(^{30}Si/^{28}Si)_{NBS\text{-}28} - 1] \times 10^3 \quad (2\text{-}5)$$

SiF_4 is a hazardous gas and care must be taken in handling. After the analysis of SiF_4, the gas is not pumped through the mass spectrometer but frozen back into the sample tube and disposed of safely in a fume hood. This increases the life of the pump on the mass spectrometer and eliminates the need for ventilating the pumps on the mass spectrometer.

2.3 Results and Discussion

Historically, one of the challenges in fluorinating mineral samples for the extraction of gases is to ensure that there is little contamination added to the gas sample via reaction between the fluorinating gas and the interior of the reaction vessels and vacuum line. High precision can be achieved if the analyte gas is present in large enough quantities to remain undiluted by contaminants and if reaction temperatures are appropriate for mineral decomposition rather than reagent decomposition. The design of this line varies from the conventional line housed in the same facility and that of Leng and Sloane (2008) in several ways. The most notable difference is the volume of the line, particularly in the reaction section. Each reaction vessel has a volume of 5.23cm^3 compared to 28.94cm^3 on the conventional line. This makes it easier to process small sample sizes as the size of the blank in the line is reduced; 1mg of sample is analyzed compared to 8mg. Another important modification is the elimination of the step converting O_2 gas to CO_2 prior to analysis. Instead O_2 gas is frozen onto a 6Å molecular sieve in both the yield finger and sample tube. To determine the precision and accuracy of the isotope analyses using the modified apparatus, laboratory and international quartz and opal standards were analyzed over a period of one year.

2.3.1 Oxygen isotope analyses

The first measure of the quality of an isotope analysis of a silicate sample is the yield of the gas produced. Recovery of 100% of the expected gas volume is important to ensure that no isotope fractionation has occurred during combustion or collection of the gas through the extraction line. For example, 1 mg of pure SiO_2 should produce 16.66 μmol of O_2 gas and 16.66 μmol of SiF_4 gas. Over the course of this study, the average yield of oxygen gas was 17.0 ± 0.7 μmol/mg (n = 54) for NBS-28 (quartz), 17.1 ± 0.6 (n = 19) for ORX (quartz), 16.5 ± 1.2 (n = 6) for G95, 16.2 ± 0.2 for PS (n = 8) and 16.0 ± 0.6 (n = 7) for BFC. The standards G95, PS, and BFC are opal-A and can adsorb atmospheric water during weighing. As a result, samples of this type often have yields of less than 100% (e.g. Leng and Sloane 2008).

Initial testing resulted in poor sample yields and it was noted that there was little excess of BrF_5 or other condensable gases remaining in the reaction vessels after the reaction. After a reaction, the excess gas remaining in the reaction vessel may be BrF_5 reagent or some other product from the breakdown of BrF_5 at high temperatures or during reaction between BrF_5 and the interior walls of the apparatus. Too much reagent left in the reaction vessel can indicate incomplete sample reaction, while too little can suggest impure reagent, contaminants in the bomb or sample, or breakdown of reagent during heating. Remaining reagent amounts were low for almost all bombs. It was determined that the hot zone in each furnace was quite small. Both the sample and the tip of the thermocouple communicating with the furnace controller must be in the center of the hot zone to ensure the correct reaction temperature of 600°C. If the tip of the thermocouple was not in the hot zone the furnaces will heat up to more than 600°C resulting in the breakdown of reagent. This resulted in an incomplete reaction of the sample and produced high levels of non-condensables that can skew yield calculations of O_2 gas which are measured as total non-condensable gas volumes. Given the small size of the bombs care must be taken to ensure that the sample reaction is occurring in the hot zone so that temperatures elsewhere in the furnace are not too high.

Once adjustments were made to the position of the thermocouples, the following results were obtained. A plot of $\delta^{17}O$ versus $\delta^{18}O$ should have a slope of 0.50 to 0.52 if there is no mass independent fractionation occurring during purification of the gas in the extraction line. The results obtained for NBS-28 and the opal-A standards display the 1:2 relationship expected for these materials (Fig. 2-3).

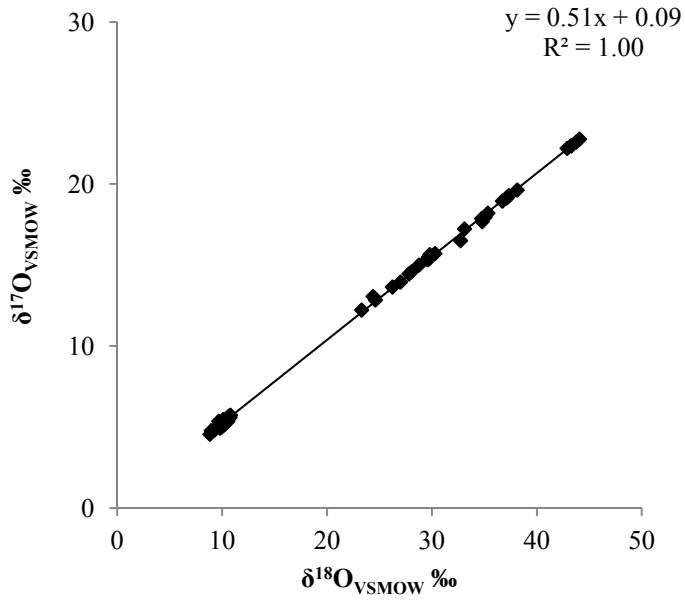

Figure 2-3. A plot of $\delta^{17}O$ to $\delta^{18}O$ for quartz (NBS-28) and opal-A standards (phytoliths (G95), diatoms (BFC), and precipitated amorphous silica (HT, PS)) displaying the approximate 1:2 relationship expected for terrestrial materials.

The $\delta^{18}O$ values of silicates are reported relative to the international standard VSMOW (see Eqn. 2-3). In practice, the $\delta^{18}O$ values of VSMOW are not measured with each oxygen isotope determination of a silicate mineral. Rather the $^{18}O/^{16}O$ ratio of O_2 gas derived from the sample is compared the $^{18}O/^{16}O$ ratio of a laboratory reference gas to produce a $\delta^{18}O$ value relative to the reference gas. These values are converted to VSMOW values via the construction of a calibration curve, which compares the measured $\delta^{18}O$ values (x-axis) to the $\delta^{18}O$ values expected for a standard (y-axis). Once developed for a set of standards, a calibration curve can be applied to samples to obtain

accurate $\delta^{18}O$ values relative to VSMOW. A calibration curve was created using the international quartz standard NBS-28, an in-house quartz standard, ORX, and a selection of biogenic silica samples and standards that had been prepared for analysis via controlled isotope exchange and iGFD (Fig. 2-4). For standards that were not used to construct the calibration curve the standard NBS-28 had an average $\delta^{18}O$ (VSMOW) value of 9.9 ± 0.6 ‰ (n = 47; expected value = 9.6 ‰ (Brand et al., 2014)). The internal quartz standard ORX had an average $\delta^{18}O$ value of 11.4 ± 0.6 ‰ (n = 17; expected value = 11.5 ‰). The standard Diatomite had an average $\delta^{18}O$ value of 22.3 ± 0.6 ‰ (n = 10). Diatomite is a silicon isotope standard and does not have a known $\delta^{18}O$ value reported in the literature. Its oxygen isotope composition was analysed here to test for precision only.

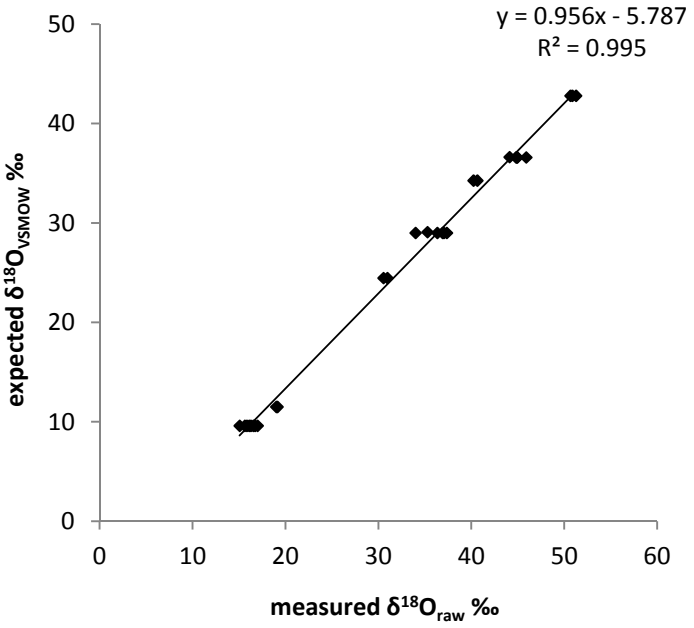

Figure 2-4. The calibration curve used to normalize oxygen isotope compositions to VSMOW. Standards included in the calibration curve are: NBS-28 and ORX (quartz) and a selection of biogenic silica standards treated via iGFD and samples with known $\delta^{18}O$ values treated via controlled isotope exchange.

To evaluate the effectiveness of the iGFD method a selection of opal-A standards with known values were analyzed. The standards used were BFC (lacustrine diatomite), PS (marine diatom sediment), and G95 (fresh grass phytoliths). These standards were

previously analysed by other researchers as part of an inter-laboratory comparison study evaluating the effectiveness of different pretreatment and analysis methods for the determination of the $\delta^{18}O$ values of opal-A (Chapligin et al., 2011). Our results are compared to the pooled results of multiple pretreatments from that study (Table 2-2). The $\delta^{18}O$ values obtained for all standards using nitrogen iGFD are within the range of accepted values, indicating that iGFD using nitrogen gas is an effective treatment for removing exchangeable oxygen from samples of biogenic silica for oxygen isotope analysis.

Table 2-2. Comparison of accepted opal-A standard $\delta^{18}O$ values (Chapligin et al. 2011) to those determined in this study.

Standard	**accepted $\delta^{18}O_{VSMOW}$ ‰**	**SD**	***n***	**$\delta^{18}O_{VSMOW}$ ‰**	**SD**	***n***
G95	36.6	0.3	7	36.1	0.6	6
PS	42.8	0.8	6	42.3	0.5	8
BFC	29	0.3	7	28.5	0.5	7

2.3.2 Silicon isotope analyses

The standards used to determine the efficacy of the SiF_4 extraction procedure were NBS-28 and Diatomite, a natural diatomite sample originally deposited as marine biogenic opal (Reynolds et al., 2007). The Diatomite standard was provided by Mark Brzezinski from the University of California. Over the course of the experiment the average yield of SiF_4 gas from NBS-28 was 17.4 ± 0.8 μmol/mg (n = 45). To determine whether the SiF_4 gas was free of contaminants we compared a mass scan of the gas evolved from a Diatomite sample to a scan of SiF_4 gas from the reference tank on a Finnegan MAT 253 mass spectrometer. In the source of the mass spectrometer the SiF_4 breaks down and is ionized. Hence, there will be fractions with different masses (e.g., F = 19, Si = 28, SiF = 47, SiF_2 = 66, and SiF_3 = 85). SiF_4 gas ionizes to SiF_3^+ in the source so the collectors are set to 85, 86 and 87 m/z for measurement. The similarities of the two scans suggest that the SiF_4 generated from samples was pure after treatment in the vacuum line (Fig. 2-5). The higher intensity peak at mass ~66 in the diatomite sample would suggest that the

slightly high yield measured for standards is the result of some of the gas being in the form of SiF_2. However, this does not appear to alter the $\delta^{30}Si$ value of the standard.

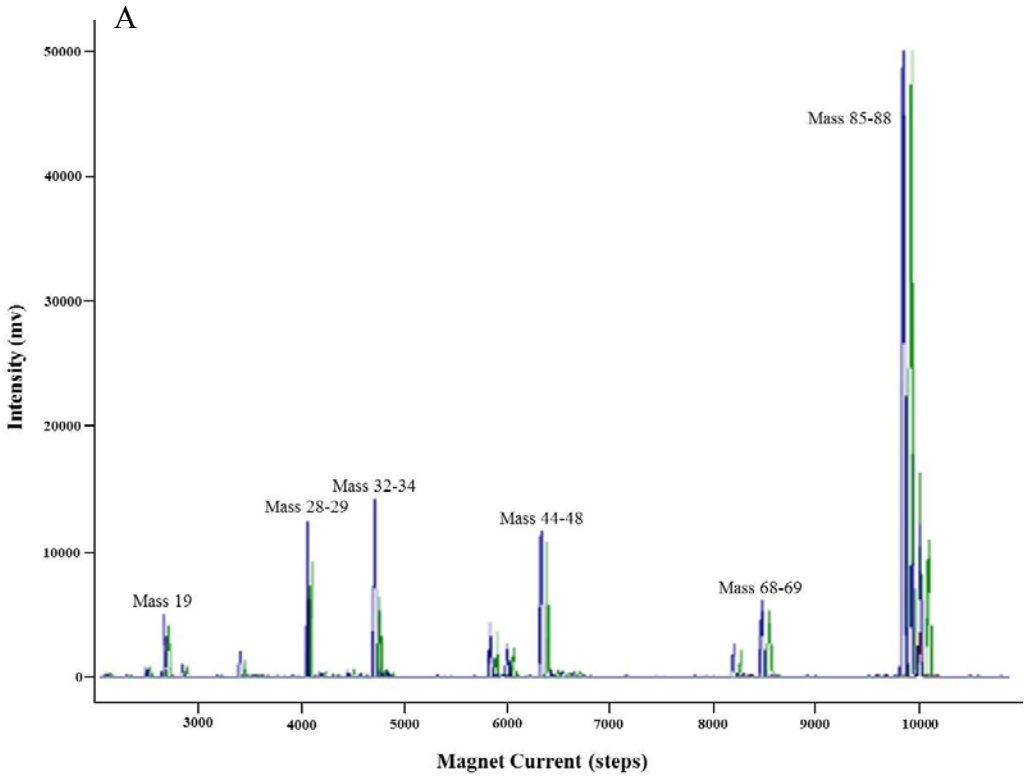

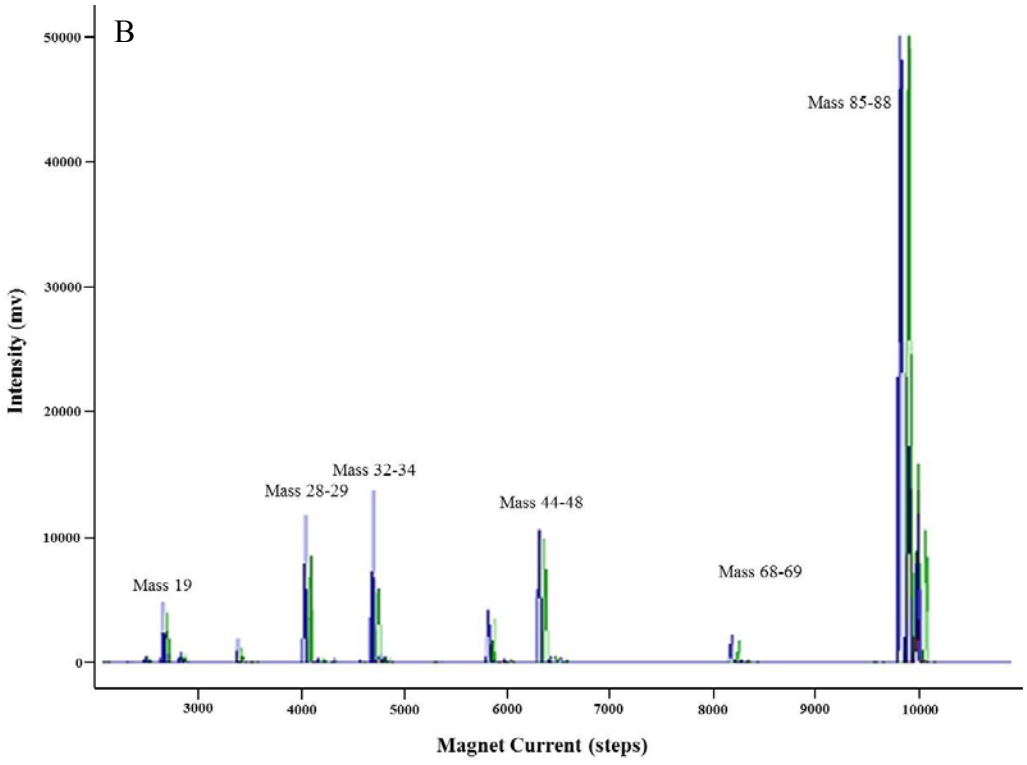

Figure 2-5. Mass scans of SiF_4 gas obtained from a sample of Diatomite standard (A) and SiF_4 reference gas (B).

Silicon isotope values are reported as $\delta^{29}Si$ and $\delta^{30}Si$ according to equations 2-4 and 2-5 using the average $^{30}Si/^{29}Si$ and $^{30}Si/^{28}Si$ ratios of NBS-28 gas collected from two samples on the same day. Over 8 months, the average $\delta^{29}Si$ and $\delta^{30}Si$ values for NBS-28 over all runs were 0.00 ± 0.03 ‰ and 0.00 ± 0.04 ‰, respectively (n = 47). The average corrected $\delta^{29}Si$ and $\delta^{30}Si$ values for Diatomite were 0.63 ± 0.05 ‰ and 1.24 ± 0.07 ‰, respectively (n = 10). The accepted $\delta^{29}Si$ and $\delta^{30}Si$ values for diatomite are 0.64 ± 0.07 ‰ and 1.26 ± 0.09 ‰, respectively (Reynolds et al., 2007). The precision associated with $\delta^{30}Si$ values of biogenic silica is comparable to those determined via traditional fluorination methods (± 0.10; Leng and Sloane 2008), laser fluorination (± 0.1; De La Rocha et al., 1997), and SIMS (± 0.75; Basile-Doelsch et al., 2005).

The relationship between $\delta^{29}Si$ and $\delta^{30}Si$ as a result of mass dependent isotope fractionation should be approximately 1:2 ($\delta^{29}Si = 0.51 \times \delta^{30}Si$), and can be used as an indicator of sample purity (Leng and Sloane 2008). Contaminant gases, such as COF_3^+ (mass 85), will result in anomalously low $\delta^{30}Si$ values, disrupting this relationship (Ding et al., 1996). This relationship for the standards NBS-28 and Diatomite is shown in figure 2-6. Also included in this figure are the $\delta^{29}Si$ and $\delta^{30}Si$ values of all phytolith silica analyzed for this thesis. These data are included to fill in the gap between NBS-28 and Diatomite values so that the trend line does not simply connect two clusters of data. These data conform to the predicted relationship indicating that any contaminant gases (e.g. COF_3^+) do not interfere with masses 85, 86, and 87 measured for silicon isotope analyses. The iGFD step required to prepare samples for oxygen isotope analysis involves heating the sample to 1100ºC. Any trace amounts of carbon would have been removed during this step.

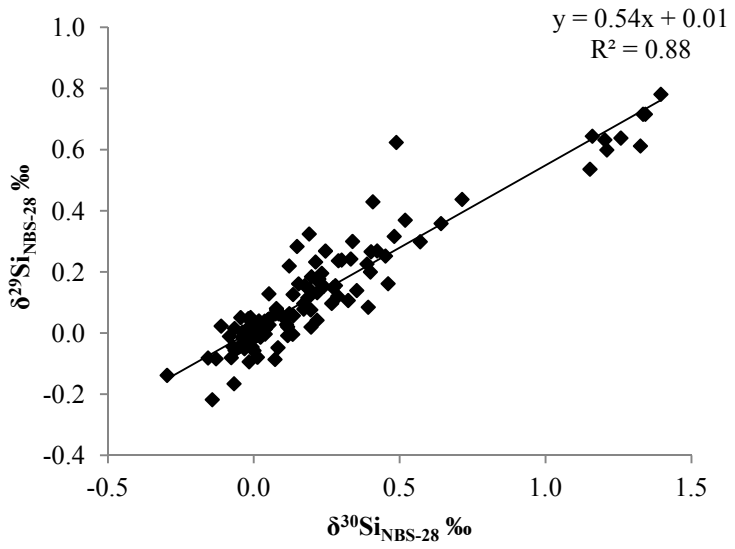

Figure 2-6. Cross-plot of $\delta^{30}Si$ and $\delta^{29}Si$ values of phytolith silica and the standards NBS-28 and Diatomite.

2.4 Summary

The oxygen and silicon isotope composition can be measured from the same ~1mg size sample using slightly modified conventional fluorination techniques. We have shown that accurate and reproducible $\delta^{18}O$ values (± 0.6 ‰) can be obtained from small samples of biogenic silica using BrF_5 fluorination and gas purification in a vacuum extraction line. The iGFD method of removing exchangeable oxygen developed by Chapligin et al. (2010) was modified, and has been proven effective using less expensive nitrogen gas in place of helium, a glass tube in place of ceramic, and a gas flow rate of ~4L/min. Very reproducible $\delta^{29}Si$ and $\delta^{30}Si$ values (± <0.1 ‰) were also obtained. Carbon contamination, which can affect yields of SiF_4 and can be an issue in the silicon isotope analysis of biogenic silica samples, was not a problem as it was removed during heating to 1100ºC during the inert-gas flow dehydration.

2.5 References

Alexandre A. (1996) Phytolithes, interactions sol-plante et paléoenvironnements. Ph.D. dissertation, Univ. d'Aix-Marseille III.

Basile-Doelsch, I., Meunier, J.D., Parron, C. (2005) Another continental pool in the terrestrial silicon cycle. Nature 433, 399-402.

Brand, W.A., Coplen. T.B., Vogl, J., Rosner, M., Prohaska, T. (2014) Assessment of international reference materials for isotope-ratio analysis (IUPAC Technical Report). Pure and Applied Chemistry 86, 425-467.

Brandriss, M.E., O'Neil, J.R., Edlund, M.B., Stoermer, E.F. (1998) Oxygen isotope fractionation between diatomaceous silica and water. Geochimica et Cosmochimica Acta 62(7), 1119-125.

Carter, J.A. (2009) Atmospheric carbon isotope signatures in phytolith-occluded carbon. Quaternary International 193, 20-29.

Chapligin, B., Meyer, H., Friedrichsen, H., Marent, A., Sohns, E., Hubberten, H.-W. (2010) A high-performance, safer and semi-automated approach for the $\delta^{18}O$ analysis of diatom silica and new methods for removing exchangeable oxygen. Rapid Communications in Mass Spectrometry 24, 2655-2664.

Chapligin, B., Leng, M.J., Webb, E., Alexandre, A., Dodd, J.P., Ijiri, A., Lücke, A., Shemesh, A., Abelmann, A., Herzschuh, U., Longstaffe, F.J., Meyer, H., Moschen, R., Okazaki, Y., Rees, N.H., Sharp, Z.D., Sloane, H.J., Sonzogni, S., Swann, G.E.A., Sylvestre, F., Tyler, J.J., Yarn, R. (2011) Inter-laboratory comparison of oxygen isotope compositions from biogenic silica. Geochimica et Cosmochimica Acta 75, 7242-7256.

Clayton, R.N. and Mayeda, T.K. (1983) Oxygen isotopes in eucrites, shergottites, nakhlites, and chassignites. Earth and Planetary Science Letters 62, 1-6.

Crespin. J., Alexandre, A., Sylvestre, F., Sonzogni, C., Paillès, C., Garreta, V. (2008) IR laser extraction technique applied to oxygen isotope analysis of small biogenic silica samples. Analytical Chemistry 80, 2372-2378.

De La Rocha, C.L., Brzezinski, M., and DeNiro, M.J. (1997) Fractionation of silicon intotopes by marine diatoms during biogenic silica formation. Geochimica et Cosmochimica Acta 61(23), 5051-5056.

De La Rocha, C.L. and Bickle, M.J. (2005) Sensitivity of silicon isotopes to whole-ocean changes in the silica cycle. Marine Geology 217, 267-282.

Demarest, M.S., Brzezinski, M.A., Beucher, C.P. (2009) Fractionation of silicon isotopes during biogenic silica dissolution. Geochimica et Cosmochimica Acta 73, 5572-5583.

Ding, T., Jiang, S., Wan, D., Li, Y., Li, J., Song, H., Liu, Z., Yao, X. (1996) Silicon Isotope Geochemistry. Geological Publishing House. Beijing, China.

Ding, T. (2004) Analytical methods for silicon isotope determinations. In P.A. de Groot (Ed.) Handbook of Stable Isotope Analytical Techniques, Volume 1. pp. 523-537 Elsevier Ltd. San Deigo, CA.

Ding, T.P., Zhou, J.X., Wan, D.F., Chen, Z.Y., Wan, C.Y., Zhang, F. (2009) Silicon isotope fractionation in bamboo and its significance to the biogeochmical cycle of silicon. Geochimica et Cosmochimica Acta 72, 1381-1395.

Dodd, J.P. and Sharp, Z.D. (2010) A laser fluorination method for oxygen isotope analysis of biogenic silica and a new oxygen isotope calibration of modern diatoms in freshwater environments. Geochimica et Cosmochimica Acta 74(4), 1381-1390.

Douthitt, C.B. (1982) The geochemistry of the stable isotopes of silicon. Geochimica et Cosmochimica Acta 46, 1449-1458.

Hamison, M. and Knauth, L.P. (1983) Stepwise fluorination – a useful approach for the isotopic analysis of hydrous minerals. Geochimica et Cosmochimica Acta 47, 1589-1595.

Jones, L.H.P. and Milne, A.A. (1963) Studies of silica in the oat plant I. Chemical and physical properties of the silica. Plant and Soil 18, 207-220.

Kelly, E.F., Amundson, R.G., Marino, B.D., and DeNiro, M.J. (1991) Stable isotope ratios of carbon in phytoliths as a quantitative method of monitoring vegetation and climate change. Quaternary Research 35, 222-233.

Kita, N.T., Ushikubo, T., Fu, B., Valley, J.W. (2009) High precision SIMS oxygen isotope analysis and the effect of sample topography. Chemical Geology 264, 43-57.

Labeyrie, L. (1987) New approach to surface seawater paleotemperatures using $^{18}O/^{16}O$ ratios in silica of diatom frustules. Nature 248, 40-42.

Labeyrie, L.D. and Juillet, A. (1982) Oxygen isotopic exchangeability of diatoms valve silica; interpretation and consequences for paleoclimatic studies. Geochimica et Cosmochimica Acta 46, 967-975.

Leng, M.J. and Barker, P.A. (2006) A review of the oxygen isotope composition of lacustrine diatom silica for palaeoclimate reconstruction. Earth Science Reviews 75, 5-27.

Leng, M.J. and Sloane, H.J. (2008) Combined oxygen and silicon isotope analysis of biogenic silica. Journal of Quaternary Science 23(4) 313-319.

Lentfer, C.J. and Boyd, W.E. (1998) A comparison of three methods for the extraction of phytoliths from sediments. Journal of Archaeological Science 25, 1159-1183.

Lücke, A., Moschen, R., Schleser, G.H. (2005) High-temperature carbon reduction of silica: A novel approach for oxygen isotope analysis of biogenic opal. Geochimica et Cosmochimica Acta 69, 1423-1433.

Matheney, R.K. and Knauth, P. (1989) Oxygen-isotope fractionation between marine biogenic silica and seawater. Geochimica et Cosmochimica Acta 53, 3207-3214.

Mattey, D. and Macpherson, C. (1993) High-precision oxygen isotope microanalysis of ferromagnesian minerals by laser-fluorination. Chemical Geology 105, 305-318.

Mopper, K. and Garlick, G.D. (1971) Oxygen isotope fractionation between biogenic silica and ocean water. Geochimica et Cosmochimica Acta 35, 1185-1187.

Morley, D.W., Leng, M.J., Mackay, A.W., Sloane, H.J., Rioual, P., Batterbee, R.W., 2004. Cleaning of lake sediment samples for diatom oxygen isotope analysis. Journal of Paleolimnology 31, 391-401.

Moschen, R., Lücke, A., Schleser, G.H. (2005) Sensitivity of biogenic silica oxygen isotopes to changes in surface water temperature and palaeoclimatology. Geophysical Research Letters 32, L07708.

Reynolds, B.C., Aggarwal, J., André, L., Baxter, D., Beucher, C., Brzezinski, M.A., Engström, E., Georg, R.B., Land, M., Leng, M.J., Opfergelt, S., Rodushkin, I., Sloane, H.J., van den Boorn, S.H.J.M., Vroon, P.Z., Cardinal, D. (2007) An inter-laboratory comparison of Si isotope reference materials. Journal of Analytical Atomic Spectrometry 22, 561-568.

Rings, A., Lücke, A., Schleser, G.H. (2004) A new method for the quantitative separation of diatoms frustules from lake sediments. Limnology and Oceanography 2, 25-34.

Piperno, D.R. (2006) Phytoliths: A Comprehensive Guide for Archaeologists and Paleoecologists. AltaMira Press.

Schleser, G.H., Lucke, A., Moschen, R., Rings, A., 2001. Separation of diatoms from sediment and oxygen isotope extraction from their siliceous valves – a new approach. Terra Nostra, 2001/3. Schriften der Alfred-Wegener-Stiftung (6th Workshop of the European Lake Drilling Program, Potsdam), pp. 187-191.

Shahack-Gross, R., Shemesh, A., Yakir, D., Weiner, S. (1996) Oxygen isotope composition of opaline phytoliths: Potential for terrestrial climatic reconstruction. Geochimica et Cosmochimica Acta 60(20), 3949-3953.

Sharp, Z.D. (1990) A laser-based microanalytical method for the insitu determination of oxygen isotope ratios of silicates and oxides. Geochimica et Cosmochimica Acta 54, 1353-1357.

Shemesh, A., Charles, C.D., Fairbanks, R.G. (1992) Oxygen isotopes in biogenic silica: Global changes in ocean temperature and isotopic composition. Science 256, 1434-1436.

Shemesh, A., Burckle, L.H., Hays, J.D., 1995. Late Pleistocene oxygen isotope records of biogenic silica from the Atlantic sector of the Southern Ocean. Paleoceanography 10, 179-196.

Webb, E.A. and Longstaffe, F.J. (2000) The oxygen isotope compositions of silica phytoliths and plant water in grasses: Implications for the study of paleoclimate. Geochimica et Cosmochimica Acta 64(5), 767-780.

Zhao, Z. and Pearsall, D.M. (1998) Experiments for improving phytolith extraction from soils. Journal of Archaeological Science 25, 587-598.

Zeigler, K., Chadwick, O.A., Brzezinski, M.A., Kelly, E.F. (2005) Natural variations of $\delta^{30}Si$ ratios during progressive basalt weathering, Hawaiian Islands. Geochimica et Cosmochimica Acta 69(17), 4597-4610.

3. The effect of progressive dissolution on the silicon isotope composition of opal-A

3.1 Introduction

Silicon isotopes can be used to trace silicon as it cycles through the biosphere and lithosphere and to study biomineralization and weathering processes (Basile-Doelsch 2006 and references therein). During weathering the lighter Si isotopes are preferentially released from minerals so that the δ^{30}Si value of dissolved Si in solution is lower than the original minerals by up to ~3 ‰ (Ziegler et al., 2005). The δ^{30}Si values of Si in soil solutions (and ultimately rivers and oceans over long time scales) vary with weathering rates that depend on temperature, humidity and the carbon dioxide concentration of the atmosphere (Ziegler et al., 2005). Silicon isotope values of materials like phytoliths, diatoms, and siliceous cements that precipitate from waters containing dissolved Si from weathering reactions and it has been suggested that their δ^{30}Si values can be used as a proxy for the availability of silicic acid in terrestrial and marine environments, where lower δ^{30}Si values would indicate a higher concentration of silicic acid (Ding et al., 2009; Basile-Doelsch et al., 2005; De La Rocha and Bickle 2005; De La Rocha et al., 1998). In this study we assess whether the δ^{30}Si values of phytoliths are preserved after partial dissolution has occurred.

Aqueous silicic acid is taken up by plants from soil water and precipitated inside plant tissues as silica phytoliths. The uptake of silicic acid by plants is associated with a biochemical Si-isotope fractionation of $\alpha_{plant\text{-}water} = 0.9988$, which means that phytoliths in plants have lower δ^{30}Si values that the silicic acid in soils (Ding et al., 2005, 2009). In addition, phytoliths become increasingly enriched in ^{30}Si from the lower to the upper parts of rice, bamboo, and banana plants as the pool of available silicic acid becomes depleted of ^{28}Si as phytolith deposition continues (Ding et al., 2005, 2009; Opfergelt et al., 2006). Phytolith δ^{30}Si values can vary by as much as 3.3 ‰ in a single plant (Ding et al., 2009). In addition to the variation in δ^{30}Si values in phytoliths across the entire plant,

there may be some heterogeneity within individual phytoliths because the pool of silicic acid from which they precipitate is constantly evolving (Ding et al., 2009). Although researchers have suggested that the $\delta^{30}Si$ values of phytoliths can be used to understand silicon availability during plant growth (Ding et al., 2009) this application is complicated by the isotopic heterogeneity of the phytoliths within a plant. However, the silicon released from the weathering of phytoliths is depleted in ^{30}Si relative to soil waters and can be used to trace the contribution of biogenic silica to the terrestrial silicon cycle (Ziegler et al., 2005; Meunier et al., 2010).

In the soil, post-depositional changes in the isotopic composition of biogenic silica over time could affect interpretations of silicon cycling rates. For example, higher $\delta^{30}Si$ values of phytolith silica would be associated with lower silicic acid availability which is associated with lower weathering rates (Ziegler et al., 2005; Derry et al., 2005). If phytoliths partially dissolve, if there is selective dissolution of some phytolith morphologies, or if there is isotopic exchange with soil water, the $\delta^{30}Si$ values of phytolith silica could be modified. For example, previous research has noted, that the $\delta^{18}O$ values of fresh diatom silica are 3-10 ‰ lower than diatom frustules extracted from sediments in the same environment (Brandriss et al., 1998; Schmidt et al., 2001). Changes have been observed in the surface structure of diatoms after digenesis, most notably the removal of surface OH groups by either partial dissolution or silica condensation reactions that occur after deposition in sediments (Brandriss et al., 1998; Schmidt et al., 2001) (Eqn. 3-1).

$$SiO_2 + 2\ H_2O \leftrightarrow Si(OH)_4 \qquad (3\text{-}1)$$

Sedimentary diatoms have slower dissolution rates and lower specific surface areas compared to fresh diatoms (Dixit and VanCappellen 2002; VanCappellen et al., 2002; Hurd et al., 1981; Barker et al., 1994). Experimental studies have shown that the $\delta^{30}Si$ values of fresh diatom silica, fossil diatom silica, and a synthetic silica powder did not change even after nearly 50% of the original mass had been dissolved (Demarest et al., 2009; Geilert et al., 2014; Wetzel et al., 2014).

While there are a few studies examining the kinetics of phytolith dissolution and its effect on phytolith physical properties (Fraysse et al., 2006a/b; 2009), none consider changes in isotopic composition. Because phytolith assemblages are more heterogeneous than diatoms, both in terms of the isotope composition and morphologies produced in a single species, the silicon-isotope composition of phytoliths may change more drastically than that of diatoms during partial or selective dissolution. The recycling rate of phytoliths in soils can be variable. Well preserved phytoliths have been recovered from Pliocene-aged deposits, while in some tropical soils the bulk of phytolith input turns over within 6 months (Baker, 1960; Jones, 1964; Alexandre et al., 1997). Alexander et al. (1994) examined phytoliths found in the litter and upper layer of a tropical soil and found that the surfaces of phytoliths remaining were rugulose or stippled indicating partial dissolution affects phytoliths. In this study the effects of dissolution on the silicon-isotope composition of phytoliths will be assessed through dissolution experiments performed under a range of temperature and pH conditions.

3.2 Methods

3.2.1 Source material

Samples of biogenic silica were obtained from whole horsetails (*Equisetum arvense*) collected at Long Point Conservation Area in Southwestern Ontario, Canada in a single season (2009). Whole plants were used because soil phytolith assemblages contain phytoliths from all plant parts. Plant material was washed with distilled water to remove soil particles and dried at 65°C. Phytoliths were isolated from the dried plant material by digestion in an excess of 99% sulphuric acid until tissues were dissolved completely. Organic matter was then oxidized with 30% hydrogen peroxide until only silica remained (Geis, 1973). Silica was rinsed with distilled water using high-speed centrifugation to remove sulphuric acid.

Samples were examined by x-ray diffraction and contained primarily opal-A with low amounts of gypsum and anhydrite. These minerals can form during treatment with

sulfuric acid if calcium oxalate is present in plant tissues. Gypsum and anhydrite was removed from the sample by reaction with HCl.

3.2.2 Characterization of phytoliths

Physical properties of the bulk phytolith sample were assessed prior to and after dissolution. Specific surface area (SSA) was determined via single-point N_2 adsorption using a Micrometrics ASAP 2010 BET surface area analyzer. Grain size analysis was performed on phytoliths in suspension using a Malvern Mastersizer 2000. Phytolith surface features were examined via scanning electron microscope. Samples were mounted on SEM stubs by dispersing phytoliths in acetone and applying a drop to the stub. SEM stubs were carbon coated. Images were taken using a Hitachi S2500 tungsten source SEM at an accelerating voltage of 10kv and a working distance of 4mm.

3.2.3 Dissolution experiment

Dissolution experiments were conducted by reacting a series of 150mg subsamples of silica phytolith with 125mL of Millipore water in sealed high-density polyethylene bottles that had been treated with 10% HCl for 24 hours to ensure that they were free of contaminants. Subsamples were allowed to react for 2 to 70 days. Experiments were conducted at pH 4, 6, 8, and 10 and temperatures of 4, 19, 35, and 44°C. Individual experiments were set up for each time interval. Low pH and temperature conditions were selected to approximate the conditions in soils, while experiments at high pH and temperature encouraged a faster dissolution rate and ensured that at least some experiments resulted in substantial dissolution of silica. Acidic conditions were achieved by the addition of HCl, and high pH conditions by the addition of NaOH to Millipore water. At the end of each experiment the contents of each bottle were filtered through a 5μm sieve to separate the solution from the remaining solid silica.

The dissolved silicon concentration of each solution was determined via inductively coupled plasma atomic emission spectroscopy (ICP-AES) using a Perkin-Elmer Optima-3000 dual view ICP-Atomic Emission Spectrometer. The percent of dissolved solid for each subsample was calculated based on dissolved silicon concentration assuming that the original phytoliths had a SiO_2 stoichiometry.

3.2.4 Measurement of $\delta^{30}Si$ values

Silicon isotope determinations were made by converting 1 mg of biogenic SiO_2 to SiF_4 gas via reaction with BrF_5 heated in reaction vessels and gas purification in a vacuum extraction line (Ding, 2004; Leng and Sloane, 2008). Prior to reaction, all samples were heated to 1100°C under a flow of nitrogen gas to remove hydroxyl groups and combust occluded carbon (Chapligin et al., 2010; Chapter 2). All stable isotope results are expressed in the standard δ-notation, relative to NBS-28 (Brand et al., 2014) where

$$\delta = \left[\left(\frac{R_{sample}}{R_{standard}}\right) - 1\right] \times 1000\ (‰) \qquad (3\text{-}2)$$

and R represents $^{30}Si/^{28}Si$. A dual inlet triple-collecting Finnegan MAT 253 isotope ratio mass spectrometer was used for all measurements. The $\delta^{30}Si$ value for the standard opal-A Diatomite was 1.24 ± 0.07 ‰ (*n* = 10), in agreement with the accepted value of 1.26 ‰ (Reynolds et al., 2007). The reproducibility averaged ± 0.07 ‰ on sample duplicates and ± 0.04 ‰ on untreated phytoliths (n=3).

3.3 Results

3.3.1 Degree of dissolution:

The degree of dissolution for samples reacted under different conditions varied between a few percent to nearly 30% of the total amount of solid (Fig. 3-1). As expected, the degree of dissolution generally increased as the experiments progressed, and was more pronounced at high temperature and pH. The samples reacted under the most extreme conditions (pH = 10, T = 44°C) dissolved the most in the shortest period of time. Samples reacted at 4°C never lost more than 5% of the solid to the solution over the full range of pH (4-10).

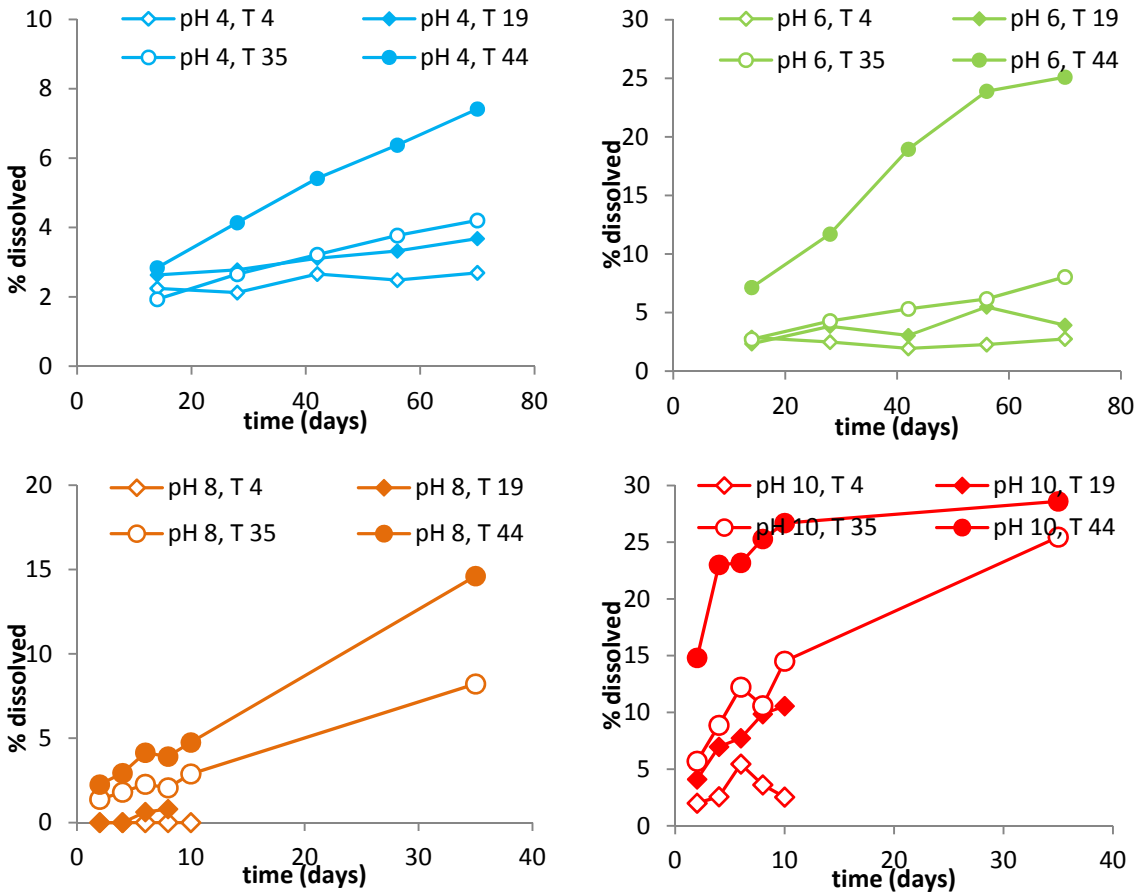

Figure 3-1. Percent of the solid dissolved plotted versus reaction time for pH 4 (A), pH 6 (B), pH 8 (C), and pH 10 (D).

Figure 3-1 indicates that under some conditions (e.g. pH 10) dissolution rates are faster at the beginning of the experiment and decrease with time. The average dissolution rate was calculated from the silicon concentration in solution at the end of each sampling interval (Fig. 3-2 below). These results demonstrate that for high pH the rates are initially faster and decrease as the system approaches steady state (Fig. 3-2). Experiments conducted at pH 4 and 6 display the same trend but dissolution rates are an order of magnitude slower than at high pH (Fig. 3-2b). Experiments conducted at pH 6, 44°C and pH 10, 19, 35, and 44°C reached saturation by the time each experiment was terminated. Throughout the experiments the pH of the solution in each bottle should have shifted as silicic acid concentrations increased. The change in pH in each bottle was modeled over the course of the experiments based on the concentration of silicon in solution and the initial pH (set at the beginning of the experiment). For experiments in which enough

silica was dissolved to alter the pH of the solution, pH decreased over time lowering the concentration of dissolved silicic acid required to reach saturation. The maximum concentration of silica that the solution could contain at the calculated pH was then used to determine if the experiment had reached saturation.

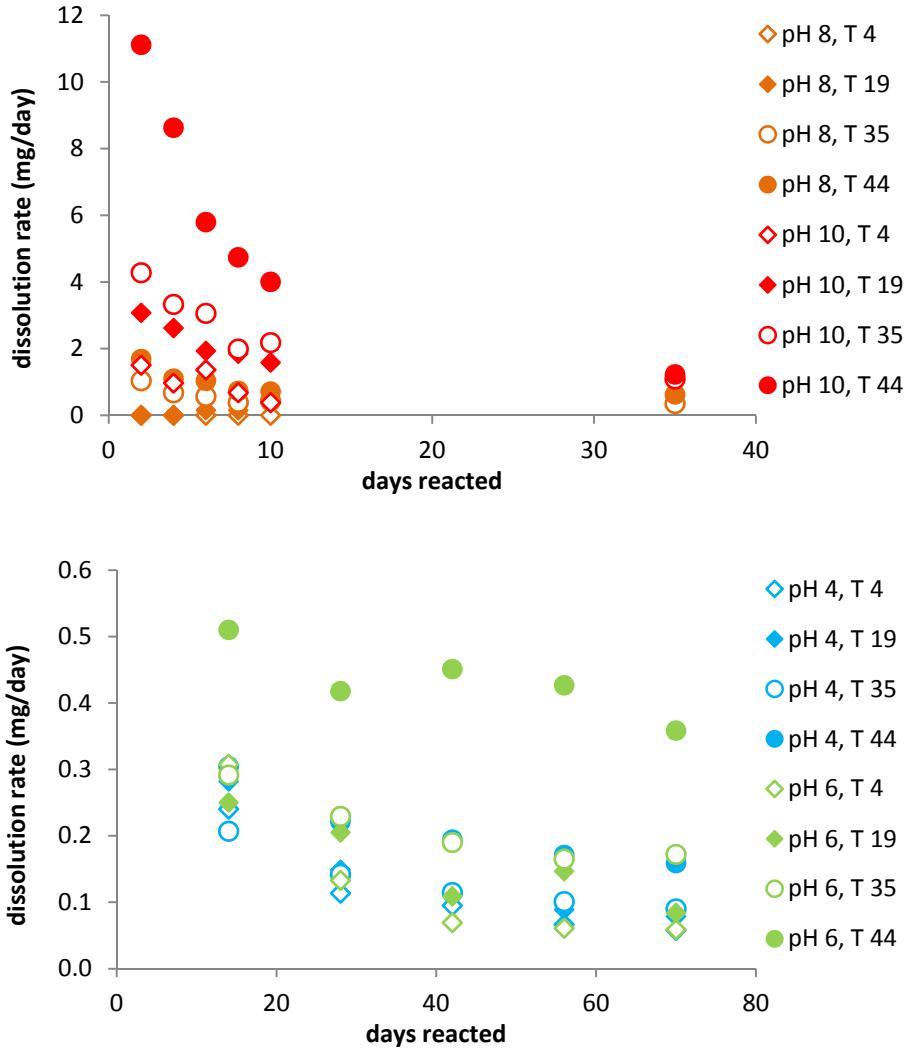

Figure 3-2. Phytolith dissolution rate versus number of day reacted for experiments conducted at pH 8 and 10 (A), and at pH 4 and 6 (B).

3.3.2 Changes in physical characteristics:

Prior to dissolution most phytolith surfaces were relatively smooth with some smaller particles attached to the surface. Images in Appendix A show a group of horsetail phytoliths that are representative of the range of morphologies present in the undissolved

bulk sample. The phytoliths pictured range in size from 10 to 60 μm. Most are fragments of phytoliths that were produced during centrifugation, but rounded phytoliths are also visible (Appendix A, A-1A, A-1F). Figures A-2 to A-7 in Appendix A show a selection of images of phytoliths that underwent dissolution under a range of pH and temperature conditions. Phytoliths post-dissolution have more pitted and irregular surface features than those examined prior to dissolution. Some specimens dissolved under high pH and temperature conditions appear to have undergone surface alteration such as surface pitting, which in some cases is extreme (Appendix A, A-3A, A-6D).

The unreacted bulk phytolith sample had a SSA of 313.0 m^2/g. All reacted samples had a SSA lower than that of the original, falling between 191.3 and 271.9 m2/g. There is a negative relationship between SSA and $\delta^{30}Si$ values of partially dissolved samples (r = 0.51, n = 21, $p < 0.05$). The mean particle size of phytoliths prior to dissolution was 33.8 μm and increased up to a maximum of 40.6 μm post-dissolution (Appendix B). Mean particle size increased as dissolution progressed (n = 25, r = 0.49, $p < 0.05$). The relationship between average particle size and $\delta^{30}Si$ of phytoliths was not significant (n = 25, r = 0.14, $p > 0.05$).

3.3.3 $\delta^{30}Si$ values of phytoliths

The bulk unaltered phytolith sample had an initial $\delta^{30}Si$ value of 0.09 ± 0.04 ‰ (n = 4). After different degrees of dissolution, most experiments produced phytoliths with $\delta^{30}Si$ values higher than or the same as the undissolved sample (Fig. 3-3). At pH 4 almost all $\delta^{30}Si$ values of biogenic silica remained the same within error as the starting material. Three of the samples treated at pH 4 exceed the $\delta^{30}Si$ value of the untreated sample, but were still enriched in ^{30}Si less than 0.35 ‰ (Fig. 3-3A). The maximum amount of material dissolved was 7.4%. When two phytolith samples were treated under identical conditions (pH = 10, T = 35, time = 35 days) the reproducibility on the amount of Si in solution was ± 0.40 μg/ml and ± 0.2 for $\delta^{30}Si$ values.

At pH 6 there was an increase in the $\delta^{30}Si$ values of biogenic silica by up to 0.63 ‰ in the initial stages of dissolution (3.7 to 7.8% dissolved, or 31 to 46% saturation) for all experiments, after which $\delta^{30}Si_{silica}$ values began to decrease to within the range of $\delta^{30}Si$

values measured for untreated phytoliths (Fig. 3-3B). For all temperatures the highest $\delta^{30}Si$ value occurred after the solution had become at least 30% saturated with respect to dissolved silicon (Fig. 3-4B).

Although dissolution did not proceed as far as some of the other experiments due to the shorter reaction time, at pH 8 there was often a slight increase in the $\delta^{30}Si$ values (maximum 0.37 ‰) of the remaining silica around 1% dissolved, or 5 to 15% saturation (Fig. 3-3C, 3-4C). For the 35°C experiment the maximum $\delta^{30}Si_{silica}$ value was reached at 2.9% dissolved, similar to the experiment conducted at pH 6 for the same temperature. The $\delta^{30}Si$ value of silica reacted at 44°C did not change from that of the starting material over the course of the experiment, despite dissolution of nearly 15% of the initial mass of sample. Experiments conducted at pH 10 behave in a similar manner to those conducted at pH 6, with the exception of samples dissolved at 44°C (Fig. 3-3D). At temperatures of 4, 19, and 35°C the $\delta^{30}Si$ value of remaining phytoliths increases until the solution reaches roughly 40% saturation, at which point silica $\delta^{30}Si$ values begin to decrease (Fig. 3-4D). Samples reacted at 44°C behave differently in that the $\delta^{30}Si$ value of remaining silica is always the same as or lower (by up to 0.39 ‰) than that of the starting material.

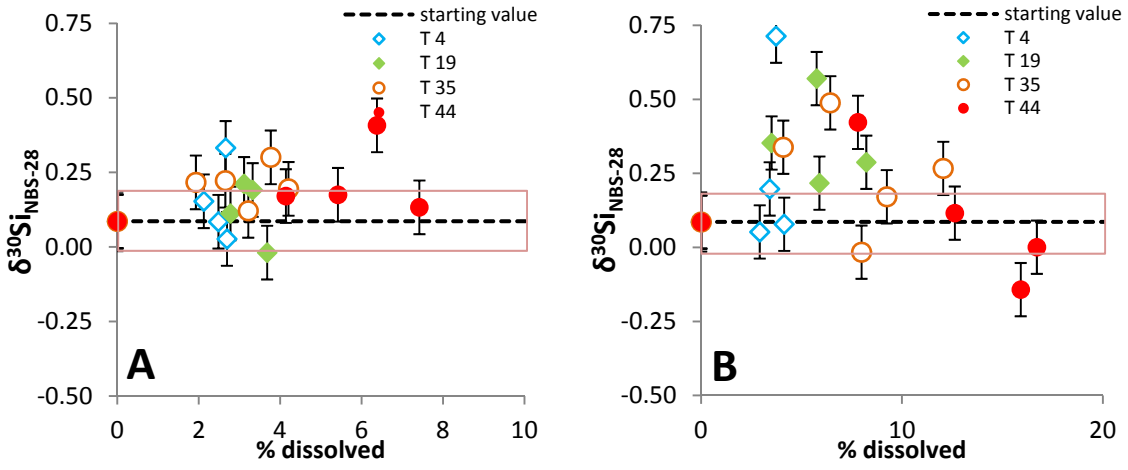

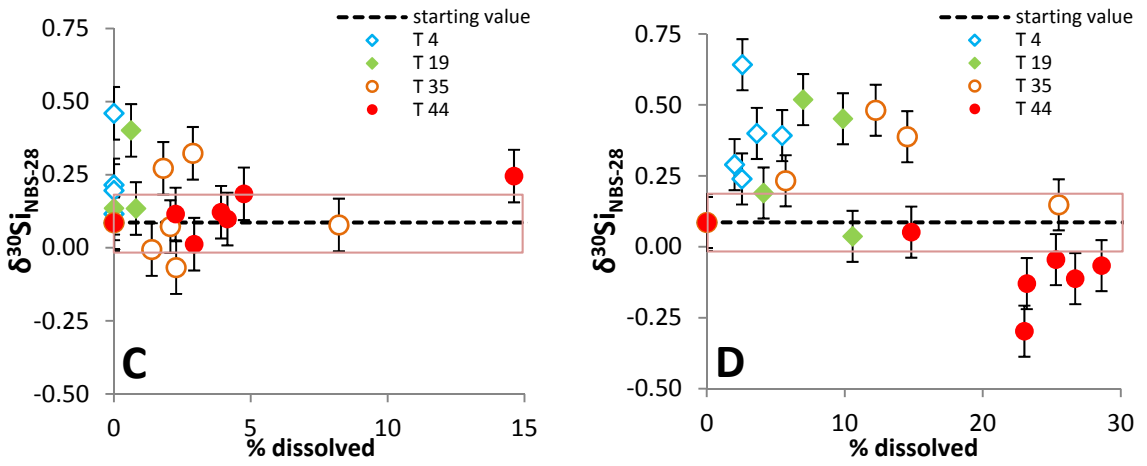

Figure 3-3. $\delta^{30}Si$ values of partially dissolved phytoliths versus the % of the solid dissolved for each experiment conducted at pH 4 (A), pH 6 (B), pH 8 (C), and pH 10 (D). the dashed line denotes the $\delta^{30}Si$ value of the untreated sample and the box the error associated with that measurement.

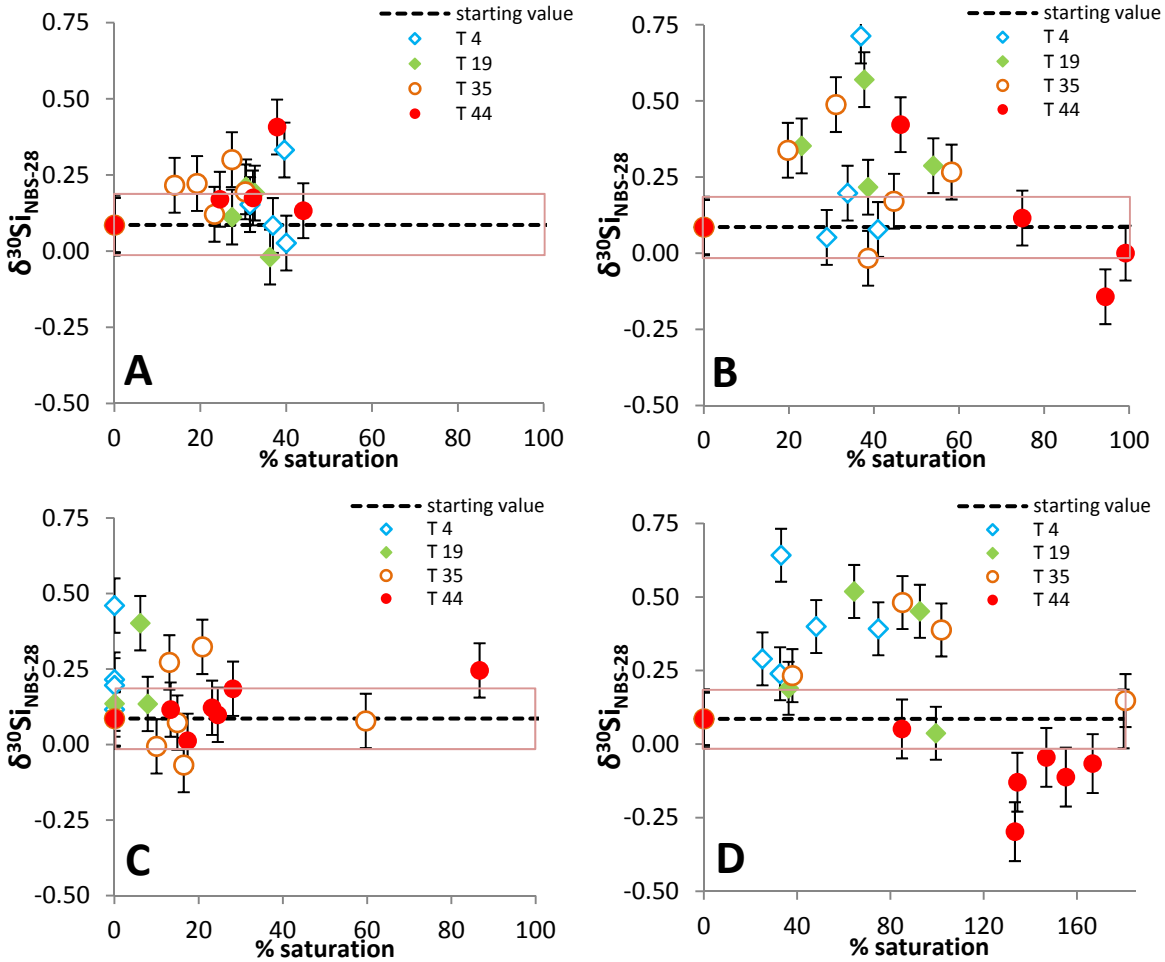

Figure 3-4. δ^{30}Si values of partially dissolved phytoliths versus % saturation with respect to dissolved silica for each experiment conducted at pH 4 (A), pH 6 (B), pH 8 (C), and pH 10 (D).

3.4 Discussion

Whether or not significant changes in the δ^{30}Si values of phytoliths were observed during partial dissolution was dependant on the amount of silica that dissolved and may reflect varying processes of dissolution and ultimately re-precipitation when the system approached equilibrium.

3.4.1 Dissolution behaviour

Phytolith dissolution begins rapidly, as high as 10 to 74 mg/g/day at pH 10, and then slows as the reaction approaches steady state. Under the conditions in this experiment rapid dissolution occurred within the first 10 days. Other studies of amorphous silica dissolution have also observed an initial, rapid loss of material (e.g. Fraysse et al., 2006b, 2009; Demarest et al., 2009; .Fraysse et al., 2009; Brady and Walther 1990). After the first stage of rapid dissolution, rates slow to about 0.5 to 3.0 mg/g/day after approximately the first 10 days, even though saturation was not reached in most experiments. In this study, steady state is reached in two of the experiments: pH 10, 35°C and pH 10, 44°C. Taking into account the evolution of solution pH with the release of silicic acid as dissolution progresses, these experiments reached saturation with respect to silicic acid at 10 days and 4 days respectively, but dissolution rates did not slow until after 10 days.

Other researchers have observed initial rapid rates of dissolution of diatom or phytolith silica (Barker et al., 1994; Van Cappellen et al., 2002; Fraysse et al., 2006a/b; 2009). A comparison of dissolution rates is difficult because experiments were under variable conditions; batch versus flow-through reactors; saltwater versus fresh water, temperature, pH, and silica aluminum content all varied between experiments. In this study, dissolution rates dropped exponentially from initial values of 74.0 to 2.7 mg/g/day when

10% of the silica was dissolved. When dissolution was greater than 10%, dissolution rates were between 8.2 and 0.5 mg/g/day. In batch experiments similar to those in the current study Fraysse et al. (2006a) report dissolution rates for horsetail phytoliths at pH 6 of 0.40-0.75 mg/g/day, which is comparable to that observed for pH 6 in this study (1.01-2.90 mg/g/day) when differences in specific surface area are considered (92.8 versus 313.0 m^2/g in this study). Both SSA and dissolution rates are approximately 3 times higher in this study than in Fraysse et al. (2006a).

Others have suggested that the initial rapid dissolution is a result of the dissolution of fine structures and small particles (<2 μm) adsorbed to the phytolith surfaces (Fraysse et al., 2009). If a similar dissolution of adsorbed particles or fine surface features were occurring in this study we would expect to see decrease in SSA in addition to the observed initial rapid dissolution. By the end of each treatment SSA of the remaining phytoliths had dropped by 11 to 30 percent across all experiments which represents 3 to 30% dissolution. If fine particles were being preferentially dissolved we would expect to see an increase in the average grain size of the dissolved samples. Grain size analysis provides the relative distribution of grain sizes within a sample. The analysis is performed on a dispersed sample and the process would dislodge adsorbed particles and decrease the average grain size reported. If adsorbed particles are removed by dissolution the proportion of larger grains should increase. If fine structures are being dissolved grain sizes should decrease and the reported average grain size should be lower. There is a positive relationship between mean grain size and the percent of solid dissolved ($r = 0.40$, $n = 24$, $p < 0.05$) which suggests rapid dissolution is not the result of the removal of fine surface features. However, this relationship cannot entirely be explained by the loss of small particles. Because both the untreated and dissolved samples are filtered through a 5 μm sieve prior to analysis the bulk of each sample should be comprised of particles larger than 5 μm. Particles smaller than 5 μm may be adsorbed particle that were dislodged during the dispersion. In most samples, even those that have experienced >10% dissolution, 4-5% of particles are less than 5 μm in size. This means that fine particles are not being progressively removed during initial rapid dissolution. In addition, the < 5 μm particles make up less than 5% by volume of the original sample and cannot account

for the 10% mass loss observed during the first stage of dissolution. It is possible that the initial rapid dissolution is the result of a reactive surface layer which may be proven by examining the behaviour of silicon isotopes.

3.4.2 Effect of dissolution on phytolith $\delta^{30}Si$ values

3.4.2.1 Initial dissolution

At the beginning of dissolution the $\delta^{30}Si$ values of the remaining solid rapidly increase despite only seeing dissolution of a few percent (Fig 3-3). Investigations using transmission electron microscopy, N_2 adsorption, and oxygen isotopes suggest the presence of a highly reactive surface layer in marine biogenic silica (Hurd et al., 1981; Barker et al., 1994; Brandriss et al., 1998). The dramatic decrease in dissolution rate of phytoliths as dissolution progresses, both in this study and others (Fraysse et al., 2006a/b; 2009) may be explained by the removal a layer of more reactive silica on phytolith surfaces. The increase in $\delta^{30}Si$ values may be related to the dissolution of a highly reactive surface layer.

The amount of ^{30}Si enrichment observed during initial stages of dissolution was not correlated to the rate of dissolution ($r = 0.28$). If silicon fractionation during dissolution was rate dependent we would expect to see greater ^{30}Si enrichment at slower dissolution rates (Wetzel et al., 2014). $\delta^{30}Si$ values continue to increase until approximately 30-40% saturation even in cases where dissolution rates slowed prior to this point. The increase in $\delta^{30}Si$ values as dissolution progressed, as seen during initial dissolution, indicates dissolution dominated silicon isotope fractionation until this point. While other opal-dissolution studies have not observed significant changes in the $\delta^{30}Si$ value of remaining solid silica, the $\delta^{30}Si$ values of dissolved silica evolve as dissolution progresses (Geilert et al., 2014; Ziegler et al., 2005). During dissolution of synthetic amorphous silica, Geilert et al. (2014) observed that the initial $\delta^{30}Si$ values of Si in solution were lower than the $\delta^{30}Si$ values of the dissolving solid, and these values increased as dissolution progressed and the reactive surface became depleted of ^{28}Si. The $\delta^{30}Si$ values for silica in solution were calculated for the current study using the $\delta^{30}Si$ values of the remaining solid, the concentration of silica in solution, and a mass balance equation. The $\delta^{30}Si$ values of silica

in solution increased as dissolution progressed as observed by Geilert et al (2014) for synthetic opal and Ziegler et al. (2005) for the dissolution of phytoliths. In addition, the difference between the $\delta^{30}Si$ values of solid and dissolved silica ($\Delta^{30}Si_{solid\text{-}dissolved}$) is positive during the initial stage of dissolution, indicating the preferential movement of ^{28}Si into the liquid phase (Demarest et al., 2009; De Paolo 2011; Geilert et al., 2014, Appendix B).

3.4.2.2 Approach to steady state dissolution

Almost all experiments that show a significant change in the $\delta^{30}Si$ value of remaining silica during dissolution follow the same trend; there is an initial increase in the $\delta^{30}Si$ values of silica followed by a decrease that, in some cases, brings the $\delta^{30}Si_{silica}$ values back to that of the starting phytolith material by the time the experiments were terminated (Fig. 3-4). We observe a decrease in $\delta^{30}Si$ values after approximately 30-40% saturation is reached while continuing to see a net transfer of silica from the solid phase to the dissolved phase. This indicates that precipitation and/or adsorption reactions are important. The decrease in the $\delta^{30}Si$ values as dissolution progresses might reflect condensation reaction (or the "backward reaction" in Equation 1). Preferential incorporation of ^{28}Si into or onto the surface of the solid phase in precipitation experiments has been reported previously (Zeigler et al., 2005; Delstanche et al., 2009; Opfergelt et al., 2009; Geilert et al., 2014; Oelze et al., 2014). Despite the negative surface charge, there is an adsorption of silicic acid to silica surfaces even in basic media (Weres et al., 1981). Back-reactions can occur even in significantly undersaturated conditions (Truesdale et al., 2005). The peak in $\delta^{30}Si$ values observed at approximately 30-40% saturation and the subsequent decrease in $\delta^{30}Si$ of the solid silica (Fig. 3-4) indicates the point at which back reactions become important and begin to alter the $\delta^{30}Si$ value of the remaining solid. Because the relative amounts of dissolution and precipitation are unknown it is not possible to calculate the $\delta^{30}Si$ value of precipitated silica from these experiments. However, in one case (pH 10, T 4ºC) the amount of silica in solution increased to 30.6 ug/mL until 6 days and then decreased to 14.3 ug/mL by 10 days. Precipitation of silica would have been facilitated by the cooler temperature. If we assume that only precipitation was occurring we can calculate the $\delta^{30}Si$ value of the

precipitated silica based on a mass balance between the $\delta^{30}Si$ values of the silica at the point of maximum Si in solution and the end of the experiment. This results in a $\delta^{30}Si$ value of -4.61 ‰ for precipitated silica. Precipitation of silica with $\delta^{30}Si$ values that are much lower than the $\delta^{30}Si$ value of the initial solid can explain the decrease in $\delta^{30}Si$ values of phytoliths when the fluid had reached more than 30% saturation.

Four of the experiments from this study approached saturation; 19, 35 and 44°C at pH 10, and 44°C at pH 6. Using calculated $\delta^{30}Si_{dissolved}$ values, under these conditions, $\Delta^{30}Si_{solid\text{-}dissolved}$ was determined to be -0.46 ‰, -0.95 ‰, -0.53 ‰, and -0.51 ‰, respectively (average = -0.61 ‰) after the experiments had reached saturation. Others have reported negative values for $\Delta_{solid\text{-}dissolved}$ for silicon isotopes in silica and silicic acid and for calcium isotopes between calcite and Ca^{2+} in solution (DePaolo 2011; Geilert et al., 2014). When precipitation becomes dominant $\Delta^{30}Si_{solid\text{-}dissolved}$ is negative as the lighter isotope is partitioned into the solid phase, depleting the liquid of ^{28}Si (DePaolo 2011).

Others have noted that dissolved silica partially re-adsorbs onto the surface of undissolved particles (Flower 1993), this may also be occurring in our experiments. Sorption of silica onto mineral surfaces is associated with an increase in the $\delta^{30}Si$ value of dissolved silica as ^{28}Si is sorbed to mineral surfaces (Delstanche et al., 2009; Oelze et al., 2014). This sorption of isotopically light silicon onto the phytolith surface could also explain the decrease in $\delta^{30}Si$ values of the solid that occurs before the fluid reaches saturation with respect to silica, but at a similar point in the reaction in each experiment (i.e. 30-40% saturation).

Contrary to other studies of amorphous silica dissolution, we report a significant difference in the $\delta^{30}Si$ value of remaining silica compared to that of the starting phytolith material (Demarest et al., 2009; Geilert et al., 2014; Wetzel et al., 2014). In this study, the maximum change in $\delta^{30}Si$ of phytolith silica post-dissolution was + 0.63 ‰ and occurred after less than 5% of the original material had dissolved (Fig. 3-3). In contrast, Demarest et al. (2009) observed a maximum change in $\delta^{30}Si$ of fresh diatom silica of +0.27 ‰ which occurred at 50% dissolution. In that study most of the sampling intervals occurred after more than 10% of the solid had been dissolved and the $\delta^{30}Si$ values were unchanged from the initial values. Wetzel et al. (2014) report that ~3-12% dissolution of

sedimentary diatom silica was not accompanied by a statistically significant change in the δ^{30}Si values of the residual silica. However, in that study most of the experiments were conducted at pH 10.7 and 100ºC resulting in up to 7% of the starting mass dissolving in minutes. It is likely that these studies failed to capture the initial increase in δ^{30}Si values of solid silica observed in the current study as a result of their sampling interval and experimental conditions. In our experiment at pH 10, 44ºC the first sampling occurred after 15% of the silica dissolved and at that point it appeared that the δ^{30}Si value of solid silica had not changed (Fig. 3-3D).

All experiments, with the exception of those at pH 4, dissolved enough silica to alter the pH of the solution. This change was much more extreme for experiments conducted at pH 10 (up to 2.08 pH units), and has an influence on silica saturation. In the case of the 44°C experiment, saturation of the solution with respect to silicic acid was reached sometime between day 2 and 4 (14.8 and 23.0% dissolved on figure 3-3D), which corresponds to the shift in isotopic composition of the solid to lower values. As pH decreases silica precipitates, preferentially incorporating ^{28}Si into the solid. As the system approaches steady state between the forward and backward reactions in equation 1 there is a constant exchange of Si-isotopes between the solid and the liquid phase with more and more ^{28}Si is accumulating the solid. The liquid phase becomes progressively enriched in ^{30}Si during this process. Precipitation of silica drives the δ^{30}Si value of the solid towards lower values. A similar effect is likely occurring in all of the experiments but is more evident at high pH and temperature because the solution reaches saturation. While both dissolution and precipitation reactions eventually occur in each experiment, when saturation is reached the backward reaction (precipitation) becomes more important than the forward reaction (dissolution). At this point the overall direction of movement of ^{28}Si between the solid and liquid phase switches and the net result is a decrease in the δ^{30}Si value of the solid (DePaolo 2011).

3.5 Concluding Remarks

The results from this study, while consistent with the data of others, provide new information of the evolution of the δ^{30}Si values of biogenic silica during progressive dissolution. We show that dissolution can alter the δ^{30}Si value of remaining silica. This

change is most pronounced in the early phases of dissolution when less than 10% of the silica has dissolved; the remaining solid silica can be up to 0.63 ‰ higher than its original value. The dissolved silica during this phase of dissolution will have δ^{30}Si values that are much lower than those of typical soil waters (generally about -1.0 ‰ to +2.0 ‰) (Ziegler et al., 2005). For example, under reasonable soil conditions (pH = 6, T = 19˚C) the δ^{30}Si value of silicic acid produced by phytolith dissolution in these experiments was calculated to be about -12 ‰ when 6% of the silica dissolved. Once precipitation reactions became significant, as evidenced by a decrease in the δ^{30}Si values of the solid, the δ^{30}Si value of silicon in solution increased to -3 ‰. The δ^{30}Si values of silicic acid in soils are generally higher because they are heavily influenced by the precipitation of secondary minerals and, in upper soil horizons, plant uptake, both of which enrich the dissolved Si pool in ^{30}Si (Ziegler et al., 2005). This study has demonstrated that the weathering of opal-A is capable of producing dissolved silica with very low δ^{30}Si values. The overall δ^{30}Si values of silicic acid in soils will depend on the balance of dissolution and precipitation reactions for a myriad of minerals. However, this study suggests that the δ^{30}Si values of silica in solution may be lower in arid environments where soils are dry and dissolution rates are low. It has been hypothesized that the δ^{30}Si values of phytoliths could be used as an indicator of silicic acid availability to the plant during growth. This study suggests that these studies would be complicated for phytoliths extracted from soils that had undoubtedly experienced some dissolution.

3.6 References

Alexandre, A., Colin, F., Meunier, J.D. (1994) Phytoliths as indicators of the biogeochemical turnover of silicon in equatorial rainforest. Comptes Rendus de l'Académie des Sciences: Série Geoscience 319(2), 453-458.

Alexandre, A., Meunier, J.D., Colin, F., Koud, J.M. (1997) Plant impact on the biogeochemical cycle of silicon and related weathering. Geochimica et Cosmochimica Acta 61(3), 677-682.

Baker, G. (1960) Fossil opal-phytoliths. Micropaleontology 6(1), 79-85.

Barker, P., Fontes, J.C., Gasse, F., Druart, J.C. (1994) Experimental dissolution of diatom silica in concentrated salt solutions and implications for paleoenvironmental reconstruction. Limnology and Oceanography 39, 99-110.

Bartoli, F., Wilding, L.P. (1980) Dissolution of biogenic opal as a function of its physical and chemical properties. Soil Science Society of America Proceedings 44, 873-878.

Basile-Doelsch, I., Meunier, J.D., Parron, C. (2005) Another continental pool in the terrestrial silicon cycle. Nature 433, 399-402.

Basile-Doelsch, I. (2006) Si stable isotope in the Earth's surface: A review. Journal of Geochemical Exploration 88, 252-256.

Brady, P.V. and Walther, J.V. (1990) Kinetics of quartz dissolution at low temperatures. Chemical Geology 82, 253-264.

Brand, W.A., Coplen. T.B., Vogl, J., Rosner, M., Prohaska, T. (2014) Assessment of international reference materials for isotope-ratio analysis (IUPAC Technical Report). Pure and Applied Chemistry 86, 425-467.

Brandriss, M.E., O'Neil, J.R., Edlund, M.B., Stoermer, E.F. (1998) Oxygen isotope fractionation between diatomaceous silica and water. Geochimica et Cosmochimica Acta 62(7), 1119-125.

Chapligin, B., Meyer, H., Friedrichsen, H., Marent, A., Sohns, E., Hubberten, H.-W. (2010) A high-performance, safer and semi-automated approach for the $\delta^{18}O$ analysis of diatom silica and new methods for removing exchangeable oxygen. Rapid Communications in Mass Spectrometry 24, 2655-2664.

De La Rocha, C.L., Brzezinski, M.A., DeNiro, M.J., Shemesh, A. (1998) Silicon-isotope composition of diatoms as an indicator of past oceanic change. Nature 395, 680-683.

De La Rocha, C.L. and Bickle, M.J. (2005) Sensitivity of silicon isotopes to whole-ocean changes in the silica cycle. Marine Geology 217, 267-282.

Delstanche, S., Opfergelt, S., Cardinal, D., Elsass, F., Andre, L., Delvaux, B. (2009) Silicon isotope fractionation during adsorption of aqueous monosilicic acid onto iron oxide. Geochimica et Cosmochimica Acta 73, 923-934.

Demarest, M.S., Brzezinski, M.A., Beucher, C.P. (2009) Fractionation of silicon isotopes during biogenic silica dissolution. Geochimica et Cosmochimica Acta 73, 5572-5583.

DePaolo, D.J. (2011) Surface kinetic model for isotopic and trace element fractionation during precipitation of calcite from aqueous solutions. Geochimica et Cosmochimica Acta 75, 1039-1056.

Derry, L.A., Kurtz, A.C., Ziegler, K., Chadwick, O.A. (2005) Biological control of terrestrial silica cycling and export fluxes to watersheds. Nature 433, 728-731

Ding, T. (2004) Analytical methods for silicon isotope determinations. In P.A. de Groot (Ed.) Handbook of Stable Isotope Analytical Techniques, Volume 1. pp. 523-537 Elsevier Ltd. San Deigo, CA.

Ding, T.P., Ma, G.R., Shui, M.X., Wan, D.F., Li, R.H. (2005) Silicon isotope study on rice plants from the Zhejiang province, China. Chemical Geology 218, 41-50.

Ding, T.P., Zhou, J.X., Wan, D.F., Chen, Z.Y., Wan, C.Y., Zhang, F. (2009) Silicon isotope fractionation in bamboo and its significance to the biogeochmical cycle of silicon. Geochimica et Cosmochimica Acta 72, 1381-1395.

Dixit, S. and Van Cappellen, P. (2002) Surface chemistry and reactivity of biogenic silica. Geochimica et Cosmochimica Acta 66, 2559-2568.

Flower, R.J. (1993) Diatom preservation: experiments and observations on dissolution and breakage in modern and fossil material. Hydrobiologia 269/270, 473-484.

Fraysse, F., Cantais, F., Pokrovsky, O.S., Schott, J., Meunier, J.D. (2006a) Aqueous reactivity of phytoliths and plant litter: Physico-chemical constraints on terrestrial biogeochemical cycle of silicon. Journal of Geochemical Exploration 88, 202-205.

Fraysse, F., Pokrovsky, O.S., Schott, J., Meunier, J.D. (2006b) Surface properties, solubility, and dissolution kinetics of bamboo phytoliths. Geochimica et Cosmochimica Acta 70, 1939-1951.

Fraysse, F., Pokrovsky, O.S., Schott, J., Meunier, J.D. (2009) Surface chemistry and reactivity of plant phytoliths in aqueous solutions. Chemical Geology 258, 197-206.

Geilert, S., Vroon, P.Z., Roerdink, D.L., Van Cappellen, P., van Bergen, M.J. (2014) Silicon isotope fractionation during abiotic silica precipitation at low temperatures: Inferences from flow-through experiments. Geochimica et Cosmochimica Acta 142, 95-114.

Geis, J.W. (1973) Biogenic silica in selected species of deciduous angiosperms. Soil Science 116, 113-130.

Hurd, D.C., Pankratz, H.S., Asper, V., Fugate, J., Morrow, H. (1981) Changes in the physical and chemical properties of biogenic silica from the central equatorial Pacific: Part III, specific pore volume, mean pore size, and skeletal ultrastructure of acid-cleaned samples. America Journal of Science 281, 833-895.

Jones, R.L. (1964) Note on occurrence of opal phytoliths in some Cenozoic sedimentary rocks. Journal of Paleontology 38, 773-775.

Leng, M.J. and Sloane, H.J. (2008) Combined oxygen and silicon isotope analysis of biogenic silica. Journal of Quaternary Science 23(4), 313-319.

Meunier, J.D., Kirman, S., Strasberg, D., Nicolini, E., Delcher, E., Keller, C. (2010) The output and bio-cycling of Si in a tropical rain forest developed on young basalt flows (La Reunion Island). Geoderma 159, 431-439.

Oelze, M., von Blanckenburg, F., Hoellen, D., Dietzel, M., Bouchez, J. (2014) Si stable isotope fractionation during adsorption and the competition between kinetic and equilibrium isotope fractionation: Implications for weathering systems. Chemical Geology 380, 161-171.

Opfergelt, S., Cardinal, D., Henriet, C., Andre, L., Delvaux, B. (2006) Silicon isotopic fractionation by banana (Musa spp.) grown in a continuous nutrient flow device. Plant and Soil 285, 333-345.

Perry, C.C. and Fraser, M.A. (1991) Silica deposition and ultrastructure in the cell wall of *Equisetum arvense*: the importance of cell wall structures and flow control in biosilicification? Philosophical Transactions of the Royal Society B 334, 149-157.

Reynolds, B.C., Aggarwal, J., André, L., Baxter, D., Beucher, C., Brzezinski, M.A., Engström, E., Georg, R.B., Land, M., Leng, M.J., Opfergelt, S., Rodushkin, I., Sloane, H.J., van den Boorn, S.H.J.M., Vroon, P.Z., Cardinal, D. (2007) An inter-laboratory comparison of Si isotope reference materials. Journal of Analytical Atomic Spectrometry 22, 561-568.

Schmidt, M., Botz, R., Rickert, D., Bohrmann, G., Hall, S.R., Mann, S. (2001) Oxygen isotopes of marine diatoms and relations to opal-A maturation. Geochimica et Cosmochimica Acta 65(2), 201-211.

Truesdale V.W., Greenwood J.E., Rendell A. (2005) The rate-equation for biogenic silica dissolution in seawater – New hypotheses. *Aquatic Geochemistry* **11**, 319-343

Van Cappellen, P., Dixit, S., van Beusekom, J. (2002) Biogenic silica dissolution in the oceans: Reconciling experimental and field-based dissolution rates. Global Biogeochemical Cycles 16, 1-10.

Weres, O., Yee, A., Tsao, L. (1981) Kinetics of silica polymerization. Journal of Colloidal Interface Science 84, 379-402.

Wetzel, F., de Souza, G.F., Reynolds, B.C. (2014) What controls silicon isotope fractionation during dissolution of diatom opal? Geochimica et Cosmochimica Acta 131, 128-137.

Zeigler, K., Chadwick, O.A., Brzezinski, M.A., Kelly, E.F. (2005) Natural variations of δ^{30}Si ratios during progressive basalt weathering, Hawaiian Islands. Geochimica et Cosmochimica Acta 69(17), 4597-4610.

4. The effect of progressive dissolution on the oxygen isotope composition of opal-A

4.1 Introduction

Phytoliths are micron-sized particles of hydrated amorphous silica ($SiO_2 \cdot nH_2O$) that form inside plants. This form of biogenic silica is important in both terrestrial and global silicon cycles (see Alexandre et al., 1997, Derry et al., 2005, Basile-Doelsch 2006). The phytolith content of plants ranges from less than 0.5% up to 15% depending on species, plant part, and environmental conditions controlling the amount of silica available to the plant. Phytolith content in plants ranges from about 0.5% or less in dicotyledons, 1-3% in dryland grasses, and up to 10-15% in some wetland species (Epstein 1994). When plants die and decay the silica component remains in the soil. Phytolith accumulation can be significant and, in some cases, can comprise almost 100% of the silica in a soil horizon (Meunier et al., 1999). Opal-A has a higher dissolution rate than most silicates. Fraysse et al. (2006a) showed that horsetail phytoliths reacted at pH 6 had a dissolution rate of 0.40 to 0.75 mg/g/day. Because of their higher solubility phytoliths contribute a large proportion of dissolved silica to the soil solution. For example, in Congolese soils phytoliths released from decayed plants contributed three times more dissolved silica to runoff than non-biogenic minerals (Alexandre et al., 1997).

Despite the high solubility rates and generous contribution of phytolith Si to the terrestrial Si cycle, biogenic silica can be preserved in soils and sediment for thousands of years (Baker, 1960; Jones; 1964). The preservation of phytoliths in soils varies widely. Well preserved phytoliths have been recovered from Pliocene-aged deposits, while in some tropical soils the bulk of phytolith input turns over within 6 months (Baker, 1960; Jones; 1964; Alexandre et al., 1997). Phytoliths recovered from the soil have been valuable in studies of ecosystem or climate reconstruction. For example, at many archaeological sites phytolith morphology is used to determine the dominant vegetation growing on a soil in the past (e.g. Pearsall and Trimble 1984; Tsartsidou et al., 2008; Cabanes et al., 2012). In addition, the $\delta^{18}O$ values of phytoliths can be related to the $\delta^{18}O$

values of plant water and temperature of plant growth (Shahack-Gross et al., 1996). Hence, the $\delta^{18}O$ values of phytoliths extracted from soils have great potential as a paleoclimatic indicator (Shahack-Gross et al., 1996; Webb and Longstaffe 2002; Alexandre et al., 2012). However, the reliability of using the $\delta^{18}O$ values of soil phytoliths as climate indicators depends on the preservation of the isotope signal.

Other studies have demonstrated that the $\delta^{18}O$ values of opal-A diatoms are up to 10 ‰ enriched in ^{18}O in fossil assemblages relative to their modern counterparts (Brandriss et al., 1998). This shift may be attributed to silica condensation reactions in the sediment (Schmidt et al., 2001). This process removes surface hydroxyl groups and allows water from sediment pores to exchange with the silica surface. Because the condensation reactions occur in waters that have a similar temperature and $\delta^{18}O$ value as the water in which the diatoms originally formed differences in $\delta^{18}O$ values between fossil and fresh diatoms are not always observed. Contemporaneous diatoms formed from the same water at the same temperatures will have similar $\delta^{18}O$ values and fossil assemblages are isotopically homogeneous. In contrast, phytolith $\delta^{18}O$ values vary up to 15.6 ‰ among plant parts as a result of the ^{18}O enrichment of plant water during transpiration in the leaves (Webb and Longstaffe 2002). In addition, phytolith shapes can be highly variable among different plants and plant parts. If dissolution of phytoliths selectively removes phytoliths with different morphologies there is a potential to shift the overall $\delta^{18}O$ value of a soil phytolith assemblage.

Previous work on the dissolution behaviour of phytoliths has suggested that phytolith dissolution rate is independent of topology and the geometry of local structures (Fraysse et al., 2006a). This suggests that there are no preferential dissolution sites on the surface of phytoliths. Structural aluminum incorporated in the phytolith may or may not protect the phytolith from dissolution (Bartoli and Wilding, 1980; Fraysse et al., 2009). Further investigation into the stability of opal-A in soils is necessary in order to use the $\delta^{18}O$ values of soil-phytolith assemblages successfully as paleoclimate indicators. Issues such as isotope fractionation during partial (thinner parts of the phytolith may dissolve first) or selective dissolution of phytoliths of different shapes must be investigated as they have the potential to alter the isotope compositions of opal-A and influence paleoclimate

estimates. This study will investigate changes in the $\delta^{18}O$ values of a bulk phytolith sample as dissolution proceeds.

4.2 Methods

Samples were collected from horsetails (*Equestium arvense*) growing at Long Point Provincial Park, Southwestern Ontario, in November 2009. Horsetails were chosen because they are high silica accumulators, comprising up to 10% silica by dry weight. Phytoliths were isolated from organic matter via acid digestion (Geis, 1973). Samples were examined using x-ray diffraction to ensure sample purity.

Dissolution experiments were performed on silica phytoliths, as outlined in Chapter 3. Briefly, 150mg of phytoliths were reacted with 125 mL of Millipore water at 4, 19, 35, and 44°C. At the beginning of each experiment the water pH was set to 4, 6, 8, or 10 through the addition of either HCl or NaOH. Reaction times were between 2 and 70 days.

The dissolved silicon concentration of each solution was determined via inductively coupled plasma atomic emission spectroscopy (ICP-AES) using a Perkin-Elmer Optima-3000 dual view ICP-Atomic Emission Spectrometer. The percent of dissolved solid for each subsample was calculated based on dissolved silicon concentration assuming that the original phytoliths had a SiO_2 stoichiometry. Additionally, percent saturation with respect to silicic acid was calculated based on the concentration of dissolved silicon and the pH of the solution, adjusted for the addition of silicic acid during dissolution.

4.2.1 Removal of OH groups

All samples were subjected to inert gas flow dehydration (iGFD) prior to isotopic analysis to remove exchangeable OH groups that can alter the $\delta^{18}O$ values of biogenic silica (Mopper and Garlick 1971; Chapligin et al., 2010; Chapter 2). When opal is dehydrated in air hydroxyl groups can be incorporated into the silica structure through the formation of new Si-O-Si bonds (Labeyrie and Juillet 1980). This process is reversible until at least 400°C (Alexandre 1996). Inert gas flow dehydration removes the exchangeable components of hydrated silica by ramp degassing up to a temperature of 1100°C under a constant flow of inert gas (Chapligin et al., 2010). All samples were

heated to 1100˚C, held at that temperature for 1.5 hours, and then allowed to cool. The procedure was conducted under a constant flow of nitrogen gas. The details of the procedure used here are discussed in chapter 2 of this thesis.

4.2.2 Measurement of $\delta^{18}O$ values

Oxygen isotope values were determined by converting SiO_2 to O_2 gas by reaction with BrF_5 at 600 °C prior to purification in a vacuum extraction line. All stable isotope results are expressed in the standard δ-notation, relative to VSMOW where

$$\delta = \left[\left(\frac{R_{sample}}{R_{standard}}\right) - 1\right] \times 1000\ (‰) \qquad (4\text{-}1)$$

and *R* represents $^{18}O/^{16}O$. A dual inlet triple-collecting isotope ratio mass spectrometer was used for all measurements. Over the course of the analyses, the standard NBS-28 had an average $\delta^{18}O$ value of 9.9 ± 0.6 ‰ (*n* = 53; expected value = 9.6 ‰ (Brand et al., 2014)). The internal quartz standard ORX had an average $\delta^{18}O$ value of 11.4 ± 0.6 ‰ (*n* = 19; expected value = 11.5 ‰). Dehydrated opal-A had $\delta^{18}O$ values of 36.1 ± 0.6 ‰ (*n* = 6), 42.3 ± 0.5 ‰ (*n* = 8), and 28.5 ± 0.5 ‰ (*n* = 7) for standards G95, PS, and BFC, respectively. The accepted values for these materials are 36.6 ‰ (G95), 42.8 ‰ (PS), and 29.0 ‰ (BFC) (Chapligin et al., 2011). Reproducibility on sample duplicates was ±0.6 ‰ (*n* pairs = 16).

A subset of samples was sent for particle size and specific surface area analysis. Particle size analysis was performed on suspended particles using a Malvern Mastersizer 2000. Specific surface area was determined by single point N_2 adsorption using a Mircometrics ASAP 2010 BET surface area analyzer.

4.3 Results

4.3.1 Amount of dissolution

The amount and rate of dissolution that occurred during each experiment (Chapter 3, Figs. 3-1 and 3-2), as well as specific surface area (SSA) and grain size analysis results have been discussed previously. In general, the amount of sample dissolved increased, to

a maximum of 28.6 %, over time (up to 10 days or 10 weeks depending on the pH of the solution) (Chapter 3, Figure 3-1). This trend was more pronounced at higher temperature and pH. The percent saturation reached with respect to dissolved silica for each of the experiments is also presented in Chapter 3, figure 3-4. Saturation was reached in one experiment at pH 6 (44˚C) and two at pH 10 (35˚C and 44˚C).

The specific surface area of the unreacted bulk phytolith sample was 313.0 m^2/g. The specific surface area of reacted samples was lower than that of the unreacted sample, with values ranging between 191.3 and 271.9 m^2/g. There is no relationship between amount dissolved (percent of solid) and SSA ($n = 20$, $r = 20$, $p = 0.21$). The unreacted phytolith sample had a mean grain size of 33.8 μm. Mean grain sizes of partially dissolved samples range between 32.7 and 43.6 μm. There is a statistically significant relationship between amount dissolved and mean grain size (Appendix B); samples that lost more of the solid material to the dissolved phase have a larger mean grain size ($n = 24$, $r = 0.40$, $p < 0.05$).

4.3.2 Oxygen isotope composition of opal-A

The $\delta^{18}O$ value of the untreated sample used in all dissolution experiments was 28.9 ± 0.5 ‰ prior to dissolution ($n = 3$). In one case an enrichment in ^{18}O of 5.3 ‰ was observed for a sample treated for 4 days at pH 8. This sample did not show any evidence of Si in solution and will not be discussed further. Most often, samples that underwent dissolution had higher $\delta^{18}O$ values than the untreated material by up to 3.9 ‰ (Fig. 4-1). For example, at pH 10, almost all partially dissolved samples have $\delta^{18}O$ values higher than the starting value (Fig. 4-1D). However, ^{18}O enrichment is most pronounced at lower temperatures; the experiments conducted at 44°C have both the smallest overall change and the smallest range in $\delta^{18}O$ values (Fig. 4-1).

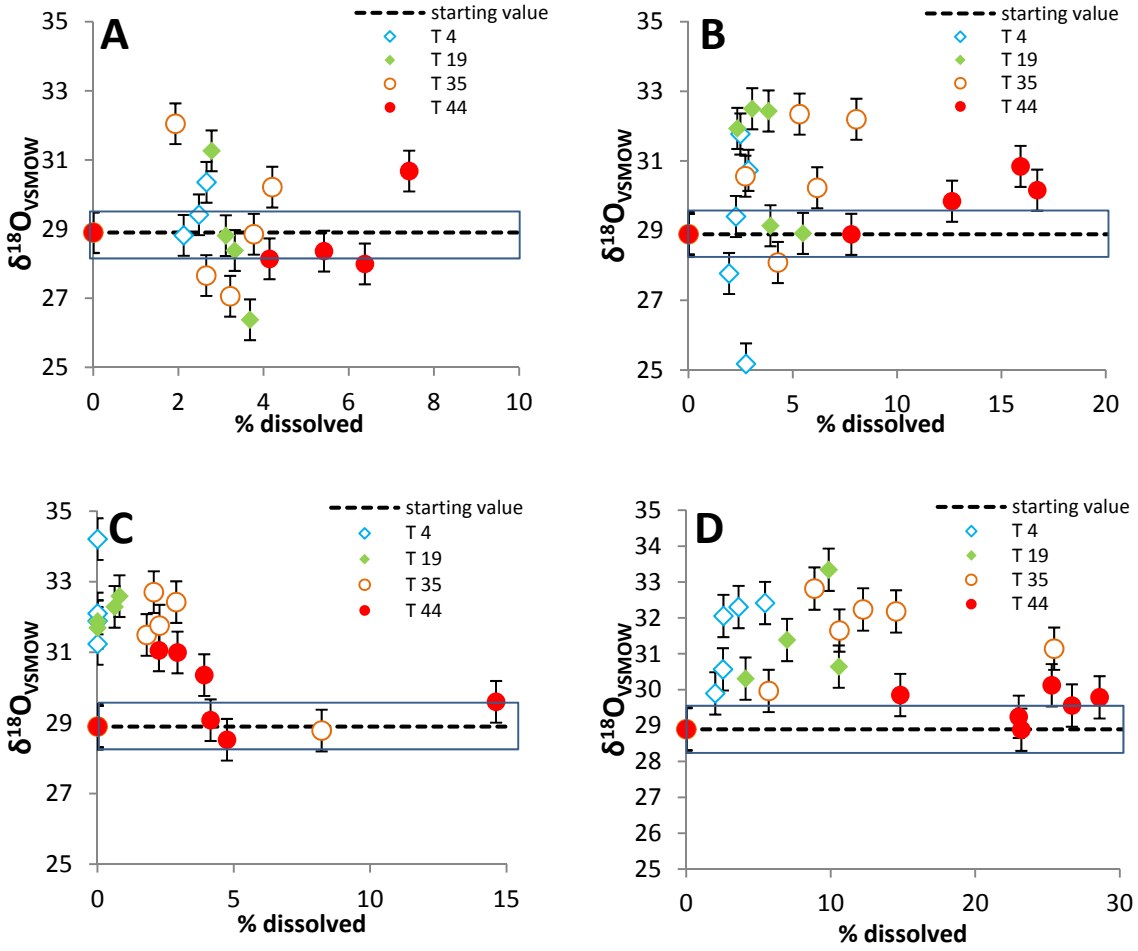

Figure 4-1. $\delta^{18}O$ values of partially dissolved phytolith silica plotted against % of the solid dissolved for all temperatures at pH 4 (A), 6 (B), 8 (C), and 10 (D). The blue box shows the standard deviation on the mean $\delta^{18}O$ value of the untreated phytolith material (dashed line).

For the experiments conducted at pH 4, most phytolith samples had little material removed by dissolution (up to 7.4% dissolved) and $\delta^{18}O$ values are unchanged or slightly higher than the starting material. All samples treated at pH 4, except those conducted at 44°C, had $\delta^{18}O$ values that reached a maximum in ^{18}O-enrichment of 1.4 to 3.0 ‰ when dissolution was 2 to 3 %. Further dissolution resulted in phytolith $\delta^{18}O$ values that became progressively lower until they were equal to or in some cases were lower than the $\delta^{18}O$ values of the starting material. At 44°C, the first set of phytoliths removed from

solution had already reached 4% dissolution and it is unknown whether the $\delta^{18}O$ values of these samples increased before this point.

At pH 6, samples for all experiments had $\delta^{18}O$ values that were higher than the starting value, with the exception of those conducted at 4°C. The total range in $\delta^{18}O$ values (7.3 ‰) of the reacted samples is similar to that observed for samples from experiments conducted at pH 4 (5.6 ‰), but the average $\delta^{18}O$ values for the data series are 30.2 ‰ and 29.0 ‰ for pH 6 and pH 4, respectively. Two of the experiments conducted at pH 6 (temperature 4°C and 19°C) display a decrease in the amount of sample dissolved partway through the experiment (Fig. 4-1B). In both cases this occurs at approximately 40% saturation with respect to silicic acid (Fig. 4-2B). This roughly coincides with a shift to lower $\delta^{18}O$ values of the remaining solid.

At pH 8, all reacted samples have $\delta^{18}O$ values that are the same as or higher than the starting material by up to 3.7 ‰ as the system approached 20% saturation (Fig. 4-2C). Samples reacted at lower temperatures show a greater change from the original oxygen isotope composition than those reacted at higher temperature (Fig. 4-1C). Samples reacted at 44°C have the smallest change in $\delta^{18}O$ values, a maximum of 2.1 ‰ higher than the original value. Twenty percent saturation was reached at 2.1 and 2.9 % dissolution for 35 and 44 °C respectively, and it is at this point that the highest $\delta^{18}O$ values are observed. Beyond 20% saturation the $\delta^{18}O$ values of the phytoliths decline until returning to the original $\delta^{18}O$ value by the time the solution reached a maximum of 87 % saturation.

At 4°C (pH 8), the concentration of dissolved silica was below the ICP-AES detection level even after reaction for 10 days. However, there was still a change in the $\delta^{18}O$ values of the solid sample. The changes in $\delta^{18}O$ values of the solid increase to 34.2 ‰ after four days and then begin to decrease, always remaining higher than the $\delta^{18}O$ value of the original phytolith material. Samples reacted at 19°C also have very low dissolved silica concentrations. After 8 days only 0.8 % of the solid had dissolved. The $\delta^{18}O$ values of this sample series increase as dissolution progresses.

At pH 10 at all temperatures the $\delta^{18}O$ values of partially dissolved silica increased up to 4.3 ‰ during early dissolution (10 % loss or 60-90% saturation). As dissolution continues the phytolith $\delta^{18}O$ values begin to decrease until they were at or within 2 ‰ of the $\delta^{18}O$ value of the original material (Fig. 4-1D). At 4°C and 19°C the sample with the highest $\delta^{18}O$ value also nears the highest percent saturation (~90%) (Fig. 4-2D). In the experiment conducted at 4°C both the amount of material dissolved and the $\delta^{18}O$ values of remaining phytoliths begin to decrease after the peak in $\delta^{18}O$ values (Fig. 4-2D). In the experiment conducted at 35°C the highest $\delta^{18}O$ value is reached when the percent

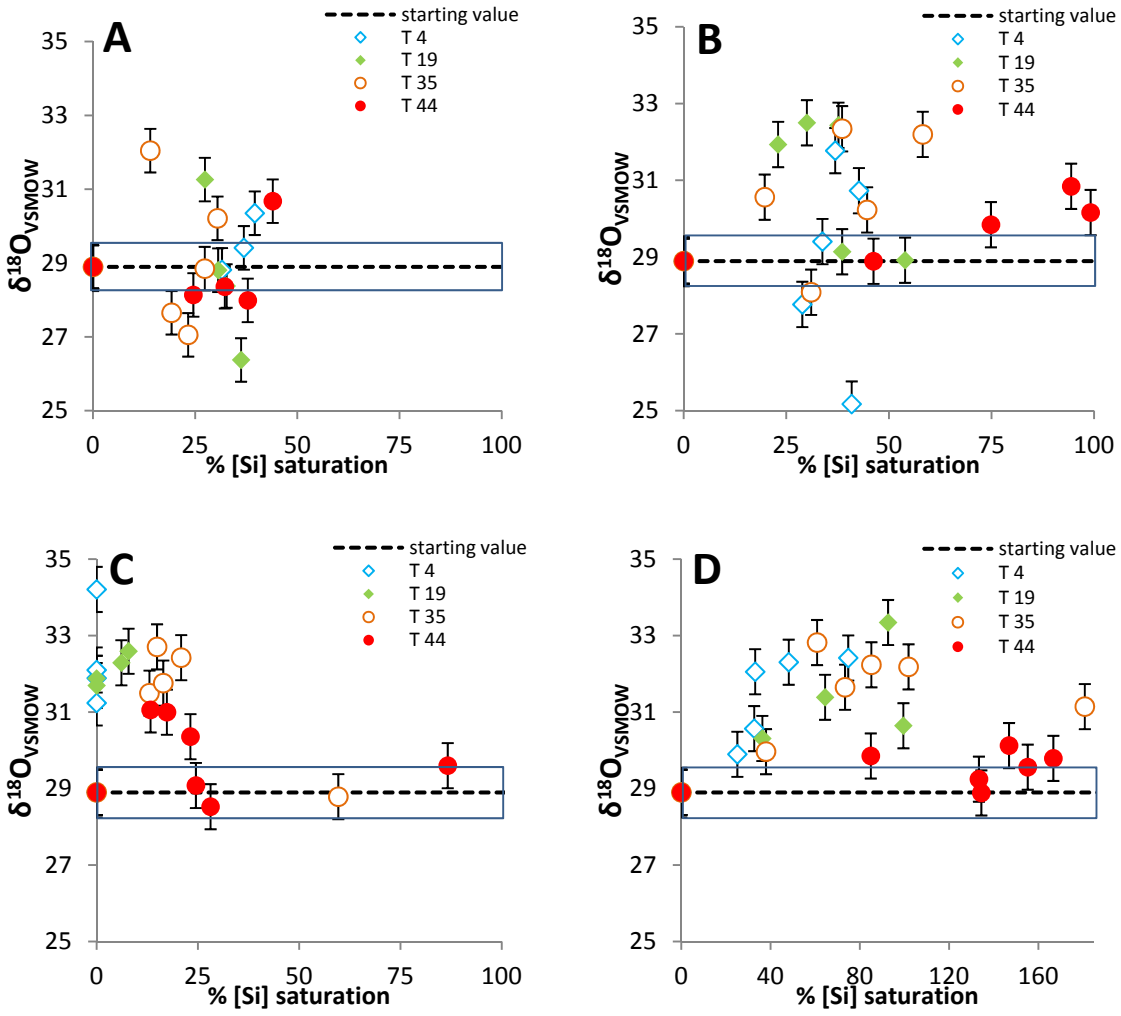

Figure 4-2. $\delta^{18}O$ values of partially dissolved phytolith silica plotted with percent saturation of the solution with respect to dissolved silica for all temperatures at pH 4 (A), 6 (B), 8 (C), and 10 (D). Blue boxes represent the standard deviation associated with the $\delta^{18}O$ value of untreated phytolith material.

saturation is at ~60% despite the fact that the degree of saturation continues to increase, eventually reaching over 100% (Fig. 4-2D). The experiment conducted at 44°C has notably different results from those conducted at lower temperatures, with almost all samples having $\delta^{18}O$ values that are the same as the starting material.

There is no direct relationship between $\delta^{18}O$ values of partially dissolved silica and SSA ($n = 28$, $r = 0.22$, $p = 0.17$) or mean grain size ($n = 32$, $r = 0.17$, $p = 0.21$). Analysis of variance between groups that underwent different treatments indicated that samples dissolved at pH 4 had $\delta^{18}O$ values lower (closer to the original value) than the other groups. From the perspective of temperature, samples dissolved at 44°C had $\delta^{18}O$ values that were lower than those of the other temperature groups. This trend was least pronounced for all temperatures at pH 4.

4.4 Discussion

The results of these experiments along with the previous results observed for changes in $\delta^{30}Si$ values of the same samples indicate that dissolution appears to have occurred in two stages. The removal of a reactive surface layer is followed by a second stage of dissolution of the bulk sample which, in some cases involves re-precipitation. This has also been proposed by others for opal-A (Juillet 1980; Barker et al., 1994; Truesdale et al., 2005; Fraysse et al., 2009). A two-stage dissolution is supported in this study by 1) changes in dissolution rates, 2) changes in SSA, 3) a decrease in percent saturation under extreme conditions, and 4) $\delta^{18}O$ values that initially increase and then decrease again. As the sample begins to dissolve there is an initial increase in $\delta^{18}O$ values followed by a decrease. Over the course of dissolution SSA decreases. Suggested causes of a two-stage dissolution have been the initial dissolution of small particles adsorbed to the surface (Fraysse et al., 2009), early removal of a reactive surface layer (Juillet 1980; Truesdale et

al., 2005), and re-precipitation as the system approaches saturation (Truesdale et al., 2005).

4.4.1 Adsorption of small particles

The possibility of initial rapid dissolution of small particles contributing to the first stage of dissolution was discussed in Chapter 3. Examination of dissolution rates within the context of changes in phytolith SSA and mean particle size indicate that the loss of small particles from the phytolith assemblage was not responsible for the initial rapid dissolution rate observed for all experiments.

4.4.2 The reactive surface layer

Much of the literature discussing the presence of a reactive surface layer on biogenic silica comes from the study of diatom silica, and the results are inconclusive. The relationship between $\delta^{18}O$ values of water, diatoms and temperature vary depending on the age of the deposit, with fossil diatoms having $\delta^{18}O$ values 3-10 ‰ higher than fresh diatoms (Brandriss et al., 1998; Schmidt et al., 1997). The presence of an isotopically light (Brandriss et al., 1998; Juillet 1980) and more reactive (Hurd et al., 1981; Barker et al., 1994; Brandriss et al., 1998) surface layer on fresh diatoms has been suggested. Based on weight loss during dehydration, Brandriss et al. (1998) found that there was substantially more loosely adsorbed water on the surfaces of fresh diatoms compared to diatomite, and suggested that the surface of fresh frustules is more hydrous and reactive than fossil diatoms. Partial dissolution would alter the diatom surface at submicroscopic levels. The surface area to volume ratio of diatom frustules decreased as dissolution progressed, indicating selective, surface-controlled dissolution (Barker et al., 1994). The study of biogenic silica (radiolarians) via transmission electron microscopy and nitrogen adsorption suggests the presence of a non-porous and a more porous fraction of silica, with older assemblages having a lower proportion of porous material than younger assemblages (Hurd et al., 1981). Removal of such a surface layer when fresh diatoms were partially dissolved in hot acid resulted in $\delta^{18}O$ values that were up to 5.3 ‰ higher than unaltered diatoms (Juillet 1980). This suggests that diagenesis removes this less stable surface layer. However, in similar studies, acid treatments that removed up to 29%

of fresh diatom silica or 7% of fossil diatom silica did not change the $\delta^{18}O$ value of the diatoms (Schmidt et al., 2001). The work of Truesdale et al. (2005) also supports the existence of a more reactive fraction of silica in diatoms. They model diatom dissolution by having fractions of fast and slow dissolving silica. In these models, the fast dissolving silica comprised between 60% and 99.9% of the sample.

In this study, the SSA of dissolved samples always decreases by about 30% relative to the unreacted sample. Removal of a porous reactive surface layer would explain this observation (Hurd et al., 1981). During initial phytolith dissolution $\delta^{18}O$ values increase to up to 33.3 ‰ until or before 10% dissolution occurs (Fig. 4-1). This is equivalent to 30-40% saturation of the solution with respect to dissolved silica for pH 4 and 6 (Fig. 4-2). Peak $\delta^{18}O$ values were reached by 15% saturation at pH 8 and above 60% saturation at pH 10. Juillet (1980) also saw an increase in $\delta^{18}O$ of diatoms after dissolution and attributed it to the removal or isotopically light hydroxyl groups. In a study examining the alteration of glasses in aqueous solution, the breakdown of the surface resulted in the formation of a gel layer which increased with depth over time (Valle et al., 2010). This layer was enriched in ^{18}O relative to the pristine sample (Valle et al., 2010). This is similar to the initial increase in the $\delta^{18}O$ value of silica observed for horsetail phytoliths. However, an isotopically light surface layer is not a necessity to explain the increase in $\delta^{18}O$ of remaining silica observed in this study. Initial dissolution is rapid and condensation reactions were prohibited as the initial solution contained no dissolved silicic acid. This alone will favour the movement of ^{16}O from the solid to the solution causing the $\delta^{18}O$ values of remaining silica to increase.

4.4.3 Progressive dissolution

Although the majority of post-dissolution $\delta^{18}O_{silica}$ values are higher than that of the starting material, the $\delta^{18}O$ value of silica begins to decrease in the later stages of the experiment. This is likely the result of silica precipitation. The silica-water thermometer of Dodd and Sharp (2010) were used to estimate the $\delta^{18}O$ values of re-precipitated silica, using a $\delta^{18}O$ for Millipore water of -7 ‰. This thermometer is applicable because dissolved silicic acid equilibrates isotopically with water in less than one second at 25°C

(Felipe et al., 2004). This means that silicic acid involved in re-precipitation is not affected by the isotopic composition of the solid from which it dissolved. The re-precipitated silica would have values of 29.9 and 25.9 ‰ in equilibrium with Millipore water at 4 and 19°C. Silica that was precipitated at 35°C and 44°C would have $\delta^{18}O$ values of approximately 22.4 and 21.0 ‰, respectively. This indicates that if re-precipitation of material was the controlling factor, the $\delta^{18}O$ values of the newly formed silica would be lower that the $\delta^{18}O$ value of the bulk sample. Any precipitated silica would cause the $\delta^{18}O$ value of the solid to decrease, regardless of the temperature at which precipitation occurred.

Based on the data presented here, precipitation begins to affect the $\delta^{18}O$ value of the solid once experiments reach approximately 30-40% saturation with respect to silicic acid at pH 4 and 6 and 15% saturation at pH 8 (Fig. 4-2). The beginning of precipitation at pH 10 is difficult to identify with the current data set because of the sampling intervals. Condensation/precipitation reactions are thought to be a factor in the dissolution of silica even in undersaturated conditions (Truesdale et al., 2005). The magnitude of the back reaction is correlated with the concentration of silicic acid in the solution (Truesdale et al., 2005). In this study, shifts in the direction of change in $\delta^{18}O$ occur before saturation with respect to silicic acid.

We suggest that as the precipitation of new silica progresses, the silica deposited on the surface creates a new layer that has an isotopic composition that is different from that of the bulk solid. The $\delta^{18}O$ value of the precipitated silica will depend on the temperature of the experiment, but should always be equal to or lower than the initial phytolith $\delta^{18}O$ value. The $\delta^{18}O$ values of post-dissolution silica analysed from the 44°C experiments is much lower than those conducted at lower temperatures. This observation is in agreement with the above theory, as the silica deposited in this experiment would have $\delta^{18}O$ values nearly 10 ‰ lower than that deposited at 4°C. A simple mass balance equation allows us to calculate what percentage of the remaining silica (1-*f*) is comprised of newly precipitated material at the end of the experiments.

$$\delta^{18}O_{final} = f(\delta^{18}O_{peak}) + (1-f)\delta^{18}O_{new} \qquad (4\text{-}2)$$

An important assumption in this calculation is that peak $\delta^{18}O$ values of partially dissolved silica were captured with our sampling interval. For experiments conducted at pH 10, temperature 19 and 35°C, where we are confident that peak $\delta^{18}O$ values were captured, precipitated silica comprised 36 and 16% of the analysed sample, respectively. More silica was precipitated at lower temperatures where solubility is reduced. Over an extended period of time, it is expected that the $\delta^{18}O$ values of silica would shift towards the expected $\delta^{18}O$ values for silica forming in equilibrium for the given temperatures.

The relative rates of the forward (dissolution) and backward (precipitation) reaction is always important when considering the effect of dissolution on the isotopic composition of minerals (DePaolo 2011). Here, the effect of each is particularly pronounced at the beginning versus the end of the experiment. In soil water, where phytoliths are in constant contact with pore waters back reactions may occur even during the initial phase of rapid dissolution, but the system used here is different. There is no silicic acid in solution to contribute to a back reaction at the outset of the experiment. The pool of available silicic acid accumulates as the phytoliths dissolve. This pool is the source of silicic acid for precipitation that moves oxygen that is depleted of ^{18}O, relative to the starting material, into the solid. This effect becomes evident when the solution becomes over 15% saturated when pH is less than 8, which is typical of natural soil conditions. ^{16}O is preferentially removed from the solid in the initial phase of dissolution, resulting in an increase in $\delta^{18}O$ values of the remaining phytoliths. If back reactions begin during this phase they are negligible. As the pool of dissolved silicic acid grows precipitation reactions become more important and we begin to see the isotopic composition of the remaining phytolith silica decrease, even though the net reaction is moving forward in the direction of dissolution.

4.5 Concluding remarks

We have demonstrated that when ~3-10% of the silica has dissolved phytolith $\delta^{18}O$ values increase by up to 3.9 ‰. Using the temperature equation of Dodd and Sharp (2010), that relates the $\delta^{18}O$ value of opal-A to temperature, an increase in the $\delta^{18}O$ values of phytoliths of 3.9 ‰ would result in an underestimation of growing temperature

by nearly 20˚C. In this study, phytolith $\delta^{18}O$ values began to decrease after approximately 10% of the silica had dissolved and approached their initial $\delta^{18}O$ value. However, this occurs as a result of precipitation of silica in isotopic equilibrium with water in the bottles. In the soil environment, if pore waters are less than 15% saturated with respect to silicic acid re-precipitation is less likely to occur and phytolith $\delta^{18}O$ values may remain high. In highly undersaturated conditions $\delta^{18}O$ values may continue to increase as dissolution progresses, albeit at a slower rate as the rate of dissolution decreased. This pattern of dissolution has been observed in phytolith dissolution experiments under flow-through conditions (Fraysse et al., 2009). If soil water is in contact with phytoliths for a sufficient period of time phytolith $\delta^{18}O$ values will decrease as silica in isotopic equilibrium with soil water is precipitated. This scenario involves the formation of a silica coating that would potentially protect the core (original phytolith silica) from further alteration. For the dissolution conditions in this study phytolith $\delta^{18}O$ values at the end of the experiments are similar to the original phytoliths. This might not be the case in natural systems. For a soil whose average temperature is 19˚C and soil water $\delta^{18}O$ values are -7 ‰ precipitated silica has a $\delta^{18}O$ value of 26 ‰. The contribution of this new silica to a phytolith with an original $\delta^{18}O$ value of 29 ‰ would decrease the overall $\delta^{18}O$ value as seen in this study. However, the $\delta^{18}O$ values of soil phytolith assemblages produced by grasses have been estimated to range from 25 to 31 ‰ based on a weighted average contribution of phytoliths from various plant parts (Webb and Longstaffe 2002). Re-precipitation of silica with a $\delta^{18}O$ value of 26 ‰ could either increase or decrease $\delta^{18}O$ values of phytoliths in soils depending on their original composition. However, at one location the $\delta^{18}O$ value of silica precipitated in soil conditions will have a lower $\delta^{18}O$ value than phytoliths produced from ^{18}O-enriched plant water. If the $\delta^{18}O$ values of phytoliths drop below the original value during diagenesis temperatures calculated from these values will be too high. Any interpretation of paleoclimate based on the $\delta^{18}O$ values of phytoliths should also look for evidence of phytolith alteration.

4.5 References

Alexandre, A., Colin, F., Meunier, J.D. (1994) Phytoliths as indicators of the biogeochemical turnover of silicon in equatorial rainforest. Comptes Rendus de l'Académie des Sciences: Série Geoscience 319(2), 453-458.

Alexandre A. (1996) Phytolithes, interactions sol-plante et paléoenvironnements. Ph.D. dissertation, Univ. d'Aix-Marseille III.

Alexandre, A., Meunier, J.D., Colin, F., Koud, J.M. (1997) Plant impact on the biogeochemical cycle of silicon and related weathering. Geochimica et Cosmochimica Acta 61(3), 677-682.

Baker, G. (1960) Fossil opal-phytoliths. Micropaleontology 6(1), 79-85.

Barker, P., Fontes, J.C., Gasse, F., Druart, J.C. (1994) Experimental dissolution of diatom silica in concentrated salt solutions and implications for paleoenvironmental reconstruction. Limnology and Oceanography 39, 99-110.

Barnes C.J. and Allison G.B. (1983) The distribution of deuterium and ^{18}O in dry soils. Journal of Hydrology 60, 141-156.

Bartoli, F. (1985) Crystallochemistry and surface properties of biogenic opal. Journal of Soil Science 36, 335-350.

Bartoli, F., Wilding, L.P. (1980) Dissolution of biogenic opal as a function of its physical and chemical properties. Soil Science Society of America Proceedings 44, 873-878.

Basile-Doelsch, I. (2006) Si stable isotope in the Earth's surface: A review. Journal of Geochemical Exploration 88, 252-256.

Brand, W.A., Coplen. T.B., Vogl, J., Rosner, M., Prohaska, T. (2014) Assessment of international reference materials for isotope-ratio analysis (IUPAC Technical Report). Pure and Applied Chemistry 86, 425-467.

Brandriss, M.E., O'Neil, J.R., Edlund, M.B., Stoermer, E.F. (1998) Oxygen isotope fractionation between diatomaceous silica and water. Geochimica et Cosmochimica Acta 62(7), 1119-125.

Chapligin, B., Meyer, H., Friedrichsen, H., Marent, A., Sohns, E., Hubberten, H.-W. (2010) A high-performance, safer and semi-automated approach for the $\delta^{18}O$ analysis of diatom silica and new methods for removing exchangeable oxygen. Rapid Communications in Mass Spectrometry 24, 2655-2664.

Chapligin, B., Leng, M.J., Webb, E., Alexandre, A., Dodd, J.P., Ijiri, A., Lücke, A., Shemesh, A., Abelmann, A., Herzschuh, U., Longstaffe, F.J., Meyer, H., Moschen, R., Okazaki, Y., Rees, N.H., Sharp, Z.D., Sloane, H.J., Sonzogni, S., Swann, G.E.A., Sylvestre, F., Tyler, J.J., Yarn, R. (2011) Inter-laboratory comparison of oxygen isotope compositions from biogenic silica. Geochimica et Cosmochimica Acta 75, 7242-7256.

Dawson, T.E., Pausch, R.E., Parker, H.M. (1998) Chapter 11: The role of hydrogen and oxygen stable isotopes in understanding water movement along the soil-plant-atmosphere continuum. In: Griffiths H. (Ed.) Stable Isotopes: Integration of biological, ecological, and geochemical processes. pp. 169-183.

DePaolo, D.J. (2011) Surface kinetic model for isotopic and trace element fractionation during precipitation of calcite from aqueous solutions. Geochimica et Cosmochimica Acta 75, 1039-1056.

Derry, L.A., Kurtz, A.C., Ziegler, K., Chadwick, O.A. (2005) Biological control of terrestrial silica cycling and export fluxes to watersheds. Nature 433, 728-731

Dodd, J.P. and Sharp, Z.D. (2010) A laser fluorination method for oxygen isotope analysis of biogenic silica and a new oxygen isotope calibration of modern diatoms in freshwater environments. Geochimica et Cosmochimica Acta 74, 1381-1390.

Epstein 1994 – I think this ref is in Piperno 2006 book

Farris, F. And Strain, B.R. (1978) The effect of water-stress on leaf $H2^{18}O$ enrichments. Radiation and Environmental Biophysics 15(2), 167-202.

Felipe, M.A., Kubicki, J.D., Rye, D.M. (2004) Oxygen isotope exchange kinetics between H2O and H4SiO4 from ab initio calculations. Geochimica et Cosmochimica Acta 68, 949-958.

Fraysse, F., Cantais, F., Pokrovsky, O.S., Schott, J., Meunier, J.D. (2006a) Aqueous reactivity of phytoliths and plant litter: Physico-chemical constraints on terrestrial biogeochemical cycle of silicon. Journal of Geochemical Exploration 88, 202-205.

Fraysse, F., Pokrovsky, O.S., Schott, J., Meunier, J.D. (2006b) Surface properties, solubility, and dissolution kinetics of bamboo phytoliths. Geochimica et Cosmochimica Acta 70, 1939-1951.

Fraysse, F., Pokrovsky, O.S., Schott, J., Meunier, J.D. (2009) Surface chemistry and reactivity of plant phytoliths in aqueous solutions. Chemical Geology 258, 197-206.

Gat, J.R. (1998) Chapter 23: Stable isotopes, the hydrological cycle and the terrestrial biosphere. In: Griffiths H. (Ed.) Stable Isotopes: Integration of biological, ecological and geochemical processes. pp. 397-407.

Geis, J.W. (1973) Biogenic silica in selected species of deciduous angiosperms. Soil Science 116, 113-130.

Hurd, D.C., Pankratz, H.S., Asper, V., Fugate, J., Morrow, H. (1981) Changes in the physical and chemical properties of biogenic silica from the central equatorial Pacific: Part III, specific pore volume, mean pore size, and skeletal ultrastructure of acid-cleaned samples. America Journal of Science 281, 833-895.

Jones, R.L. (1964) Note on occurrence of opal phytoliths in some Cenozoic sedimentary rocks. Journal of Paleontology 38, 773-775.

Juillet, A. (1980) Structure de la silice biogénique: nouvelles données apportées par l'analyse isotopique de l'oxygène. Comptes Rendus de l'Académie des Sciences 290 D, 1237-1239.

Labeyrie, L.D. and Juillet, A. (1982) Oxygen isotopic exchangeability of diatoms valve silica; interpretation and consequences for paleoclimatic studies. Geochimica et Cosmochimica Acta 46, 967-975.

Meunier, J.D., Colin, F., Alarcon, C. (1997) Biogenic silica storage in soils. Geology 27, 835-838.

Mopper, K. and Garlick, G.D. (1971) Oxygen isotope fractionation between biogenic silica and ocean water. Geochimica et Cosmochimica Acta 35, 1185-1187.

Piperno, D.R. (2006) Phytoliths: A Comprehensive Guide for Archaeologists and Paleoecologists. AltaMira Press.

Schmidt, M., Botz, R., Stoffers, P., Anders, T., Bohrmann, G. (1997) Oxygen isotopes in marine diatoms: A comparative study of techniques and new results on the isotopic composition of recent marine diatoms. Geochimica et Cosmochimica Acta 61, 2275-2280.

Schmidt, M., Botz, R., Rickert, D., Bohrmann, G., Hall, S.R., Mann, S. (2001) Oxygen isotopes of marine diatoms and relations to opal-A maturation. Geochimica et Cosmochimica Acta 65(2), 201-211.

Shahack-Gross, R., Shemesh, A., Yakir, D., Weiner, S. (1996) Oxygen isotopic composition of opaline phytoliths: Potential for terrestrial climatic reconstruction. Geochimica et Cosmochimica Acta 60(20), 3949-3953.

Truesdale, V.W., Greenwood, J.E., Rendell, A. (2005) The rate-equation for biogenic silica dissolution in seawater – new hypotheses. Aquatic Geochemistry 11, 319-343.

Valle, N., Verney-Carron, A., Sterpenich, J., Libourel, G., Deloule, E., Jollivet, P. (2010) Elemental and isotopic (^{29}Si and ^{18}O) tracing of glass alteration mechanisms. Geochimica et Cosmochimica Acta 74, 3412-3431.

Webb, E.A. and Longstaffe, F.J. (2002) Climatic influences on the isotopic composition of biogenic silica in prairie grass. Geochimica et Cosmochimica Acta 66(11), 1891-1904.

Yakir, D. (1998) Chapter 10: Oxygen-18 of leaf water: a crossroad for plant-associated isotopic signals. In: Griffiths H. (Ed.) Stable Isotopes: Integration of biological, ecological and geochemical processes. pp. 147-167.

5. The effect of burning on the dissolution behaviour and silicon and oxygen isotope composition of phytolith silica

5.1 Introduction

Wildfires are an important component in the maintenance of many ecosystems. Many ecosystems thrive when periodic burning clears undergrowth and recycles nutrients (Wilson and Shay, 1990; McPherson 1995). As fires play a role in the cycling of vegetation they contribute to the deposition of phytoliths in soil. When there is fire there is both burning of above ground vegetation and heating of the underlying soil. The maximum temperature of grassland fires is typically 700ºC (Engle et al., 1989; McPherson 1995). Wildfires can alter plant community structure, often in favour of grasses (Vilà et al., 2001; Wilson and Shay 1990). Grasses are well-adapted to fire in that their growing tips are located below the soil and they have a short life cycle (Woodcock 1992). Grasslands provide plenty of fuel and allow fire to easily propagate (Woodcock 1992). Because they are also high silica accumulators relative to woody vegetation, it is important to understand how burning changes the physical and chemical properties of phytolith silica, as they can be affected by fire both during the combustion of vegetation and after deposition in soil.

Phytoliths are a useful source of information in archaeological contexts as human activities can concentrate phytoliths in archaeological deposits (e.g. Albert et al., 2003; Tsartsidou et al., 2008). When diagnostic phytolith morphologies are present analysis of phytolith assemblages can provide information on the types of vegetation used in agriculture, structures, and as fuel for cooking (Albert et al., 2003; Tsartsidou et al., 2008). In addition, the oxygen and silicon isotope compositions of phytoliths can be used to glean information about past environmental conditions and changes in the silicon cycle. Phytoliths are concentrated in hearths when vegetation, including wood, bark and grass, is burned and several studies have examined changes in the morphological and physical characteristics of phytoliths collected from these deposits (e.g. Cabanes et al., 2011, 2012; Elbaum et al., 2003). Changes in the morphology of some fine-featured

epidermal and hair-cell phytoliths upon heating above 600 °C under laboratory conditions have been observed (Runge, 1998). Some phytoliths are more heat-resistant than others. For example, phytoliths from different rice species and plant parts lost their diagnostic morphologies at significantly different temperatures (600°C-1000°C) (Wu et al., 2012).

The results of work examining the effect of burning on phytolith dissolution behaviour are contradictory. Phytoliths burned at 500ºC for 5 hours were found to be more soluble than their unburned counterparts, while phytoliths burned at 450ºC for 6 hours had no change in solubility (Cabanes et al., 2011; Fraysse et al., 2006). Studies that examine the effects of heating on phytolith isotopic compositions are uncommon, and primarily concerned with determining the temperature at which OH^- groups are no longer exchangeable (Alexandre 1996). Heating phytoliths to 400ºC results in the removal of hydrogen bonded surface OH groups, a reaction that is partially reversible at that temperature (Alexandre 1996). Because wildfires can easily reach temperatures in excess of 400°C this may have a serious impact on the reliability of phytoliths isotopic composition in areas prone to burning if oxygen from these OH groups is incorporated into the silica structure during dehydroxylation. It has been suggested that changes in phytoliths refractive index upon burning are the result of the incorporation of water molecules into the silica structure (Elbaum et al., 2003), and this may affect both the dissolution behaviour and $\delta^{18}O$ values of heated phytoliths. The effect of burning on the $\delta^{30}Si$ values of phytoliths has not been studied. The silicon in the phytoliths should not be lost or fractionated during the burning process. In fact, some pre-treatments of phytoliths prior to silicon isotope analyses heat the silica to 1100°C with no change in $\delta^{30}Si$ values (Chapter 2). However, reorganization of the bonds at the surface of the phytolith upon heating may alter dissolution behaviours that can fractionate Si-isotopes. This study assesses the effects of heating on phytolith oxygen and silicon isotopic compositions, dissolution rate and changes in isotopic composition after partial dissolution.

5.2 Methods

Phytoliths were extracted from horsetails (*Equisetum arvense*) as they are one of the highest silica accumulators. Phytoliths were isolated via acid digestion (Geis 1973) and

sample purity (i.e. only amorphous silica) was determined using x-ray diffraction. A subset of the bulk phytolith sample used in the dissolution experiments described in chapters 3 and 4 was heated in a muffle furnace from room temperature to 700°C, held at that temperature for 4 hours, and then cooled. This temperature was chosen because grass fires usually reach a maximum temperature of 700°C (McPherson, 1995). This provided the bulk burned phytolith sample used in the dissolution experiments described here.

Dissolution experiments were conducted by reacting a series of 150mg subsamples of burned phytolith silica with 125mL of Millipore water in high-density polyethylene bottles. Samples were reacted for 2 to 56 days depending on the pH of the solution used. Experiments conducted at pH 8 (T = 4°C or 19°C) reacted for 2, 4, 6, 8, and 10 days. Experiments conducted at pH 4 or 6 (T = 4°C or 19°C) reacted for 14, 28, 42, and 56 days. At the end of the designated time a small aliquot of the solution was taken from each bottle for the determination of dissolved silicon concentration, and the contents of each bottle run through a 5μm sieve, separating the solid from the liquid and terminating the experiment.

The dissolved silicon concentration was determined via inductively coupled plasma emission spectroscopy (ICP-AES), the results of which were used to determine the percent of the solid dissolved in each dissolution experiment and % saturation calculated the concentration of dissolved silica and the temperature and pH of the solution at the beginning of the experiment. Specific surface area and particle size was determined for some of the samples. Specific surface area was determined by single point N_2 adsorption using a Micrometrics ASAP 2010 BET surface area analyser. Particle size analysis was performed on suspended particles using a Malvern Mastersizer 2000.

Oxygen and silicon isotope values were measured on the same sample via reaction with BrF_5 at 600 °C to convert phytolith SiO_2 to O_2 and SiF_4. These gases were purified in a vacuum extraction line (Ding, 2004; Leng and Sloane 2008; Chapter 2). All samples were subjected to inert gas flow dehydration (iGFD) to remove exchangeable oxygen prior to analysis (Chapligin et al., 2010; Chapter 2). All stable isotope results are expressed in the standard delta notation relative to either VSMOW or NBS-28, where

$$\delta = \left[\left(\frac{R_{sample}}{R_{standard}}\right) - 1\right] \times 1000\ (‰)$$

and *R* represents either $^{18}O/^{16}O$ or $^{30}Si/^{28}Si$. A dual inlet triple-collecting Finnigan MAT 253 isotope ratio mass spectrometer was used for all measurements. Over the course of the analyses, the standard NBS-28 had an average $\delta^{18}O$ value of 9.9 ± 0.6 ‰ (*n* = 53; expected value = 9.6 ‰; Brand et al., 2014). The internal quartz standard ORX had an average $\delta^{18}O$ value of 11.4 ± 0.6 ‰ (*n* = 19; expected value = 11.5 ‰). The average $\delta^{30}Si$ value for the standard Diatomite was 1.24 ± 0.07 ‰ (*n* = 10; expected value = 1.26 ‰; Reynolds et al., 2007). Reproducibility on sample duplicates was ±0.6 ‰ and ±0.07 ‰ (*n* = 16 pairs) for $\delta^{18}O$ and $\delta^{30}Si$, respectively.

5.3 Results

Silica dissolution rates for the various experiments are shown in Figure 5-1. For all experiments, the rate of dissolution was higher initially and decreased over time. The concentration of dissolved silica increased as dissolution progressed, reaching a maximum of 53.8 µg/mL. The higher initial dissolution rates observed for samples treated at pH 8 was observed in the first 10 days of reaction and cannot be compared directly to samples treated at pH 4 and 6 which were not sampled during this interval. However, taken together, the dissolution rate of all samples from all treatments demonstrate that silica dissolution occurs quickly when the samples are first placed in water and slows as the system progresses towards equilibrium. A comparison between treatments shows that the rate of phytolith dissolution was higher with increasing temperature and pH.

The dissolution rates of burned versus non-burned samples are compared in Figure 5-2. Under higher pH and temperature conditions, when both burned and unburned samples dissolve at higher rates, it is evident that the burned samples dissolve faster than their unburned counterparts. At pH = 8 the dissolution rates could only be calculated for two of the unburned samples because dissolution occurred so slowly, whereas dissolved Si was produced immediately for the burned samples dissolved at pH= 8 in all instances. When

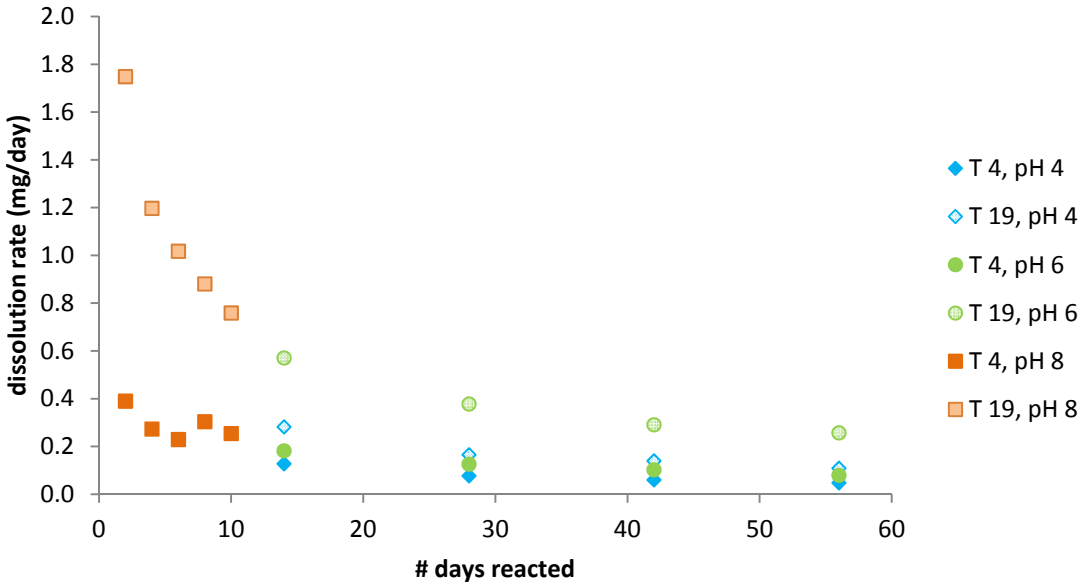

Figure 5-1. Dissolution rate of burned phytoliths over the course of dissolution.

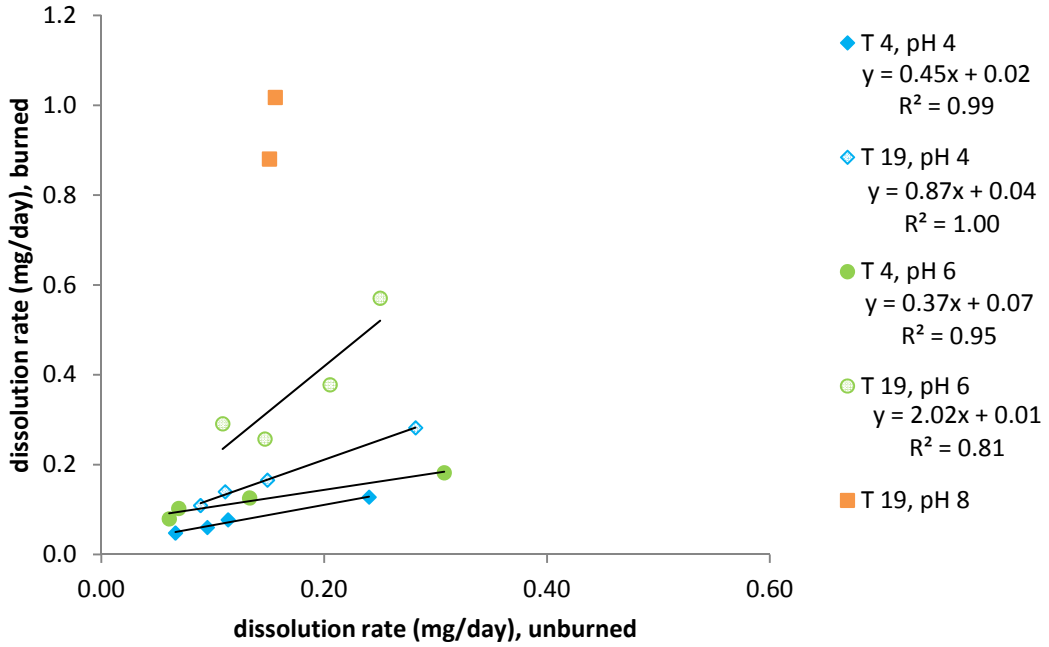

Figure 5-2. Comparison of dissolution rates between burned and unburned phytoliths over the course of dissolution. The sampling interval was the same for both burned and unburned dissolution experiments.

pH = 6 and temperature = 4°C, or pH= 4 at both temperatures, dissolution rates for both burned and unburned samples are less than 0.31 mg/day, and the unburned phytoliths dissolve more quickly than the burned phytoliths treated at the same conditions (Fig. 5-2).

The specific surface area of the undissolved burned sample, 250.1 m^2/g, is significantly lower than that of the unburned sample (313.0 m^2/g). The average grain size of the sample material before dissolution is the same for both the burned and unburned sample (33.3 μm and 33.8 μm, respectively).

The $\delta^{18}O$ value of the burned bulk sample was 26.3 ‰, which is 2.6 ‰ lower than that of the unburned sample. Figure 5-3 shows the change in $\delta^{18}O$ values of the remaining solid silica of the burned samples as dissolution progressed, along with the $\delta^{18}O$ value of the both burned and unburned starting material. Phytolith $\delta^{18}O$ values all initially increase after dissolution. $\delta^{18}O$ values of partially dissolved phytoliths from all experiments but one (T = 4ºC, pH 6) then decrease. This pattern is similar to what was observed for unburned phytoliths (Chapter 4). The average shift in $\delta^{18}O$ values of burned phytoliths at peak values is +1.1 ‰, compared to +1.8 ‰ for unburned samples reacted under the same conditions. The shift to higher $\delta^{18}O$ values occurs between about 1-5% dissolved (Fig. 5-3A) or 15-45% saturation (Fig. 5-3B).

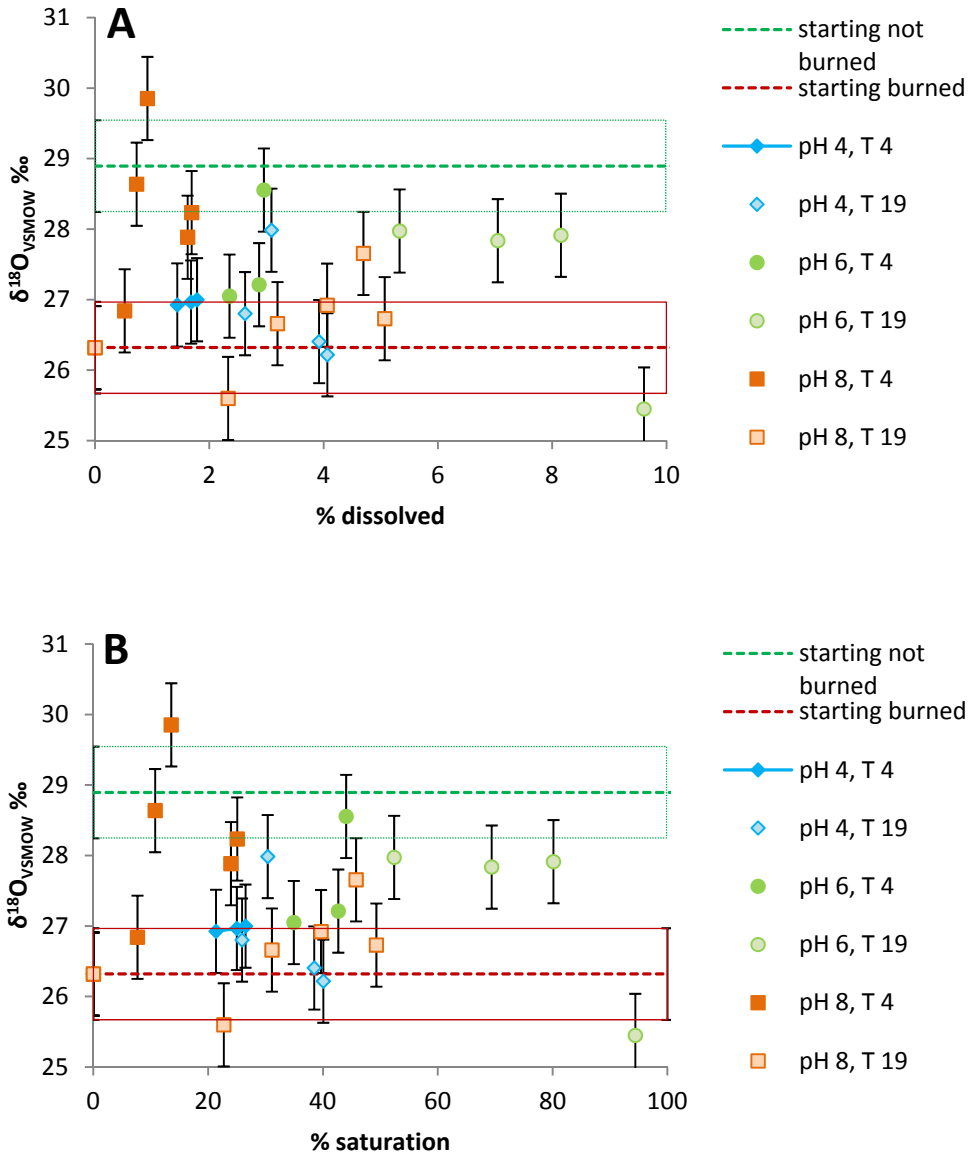

Figure 5-3. The change in $\delta^{18}O$ of partially dissolved phytoliths plotted against the percent of the solid dissolved (A) and percent saturation (B).

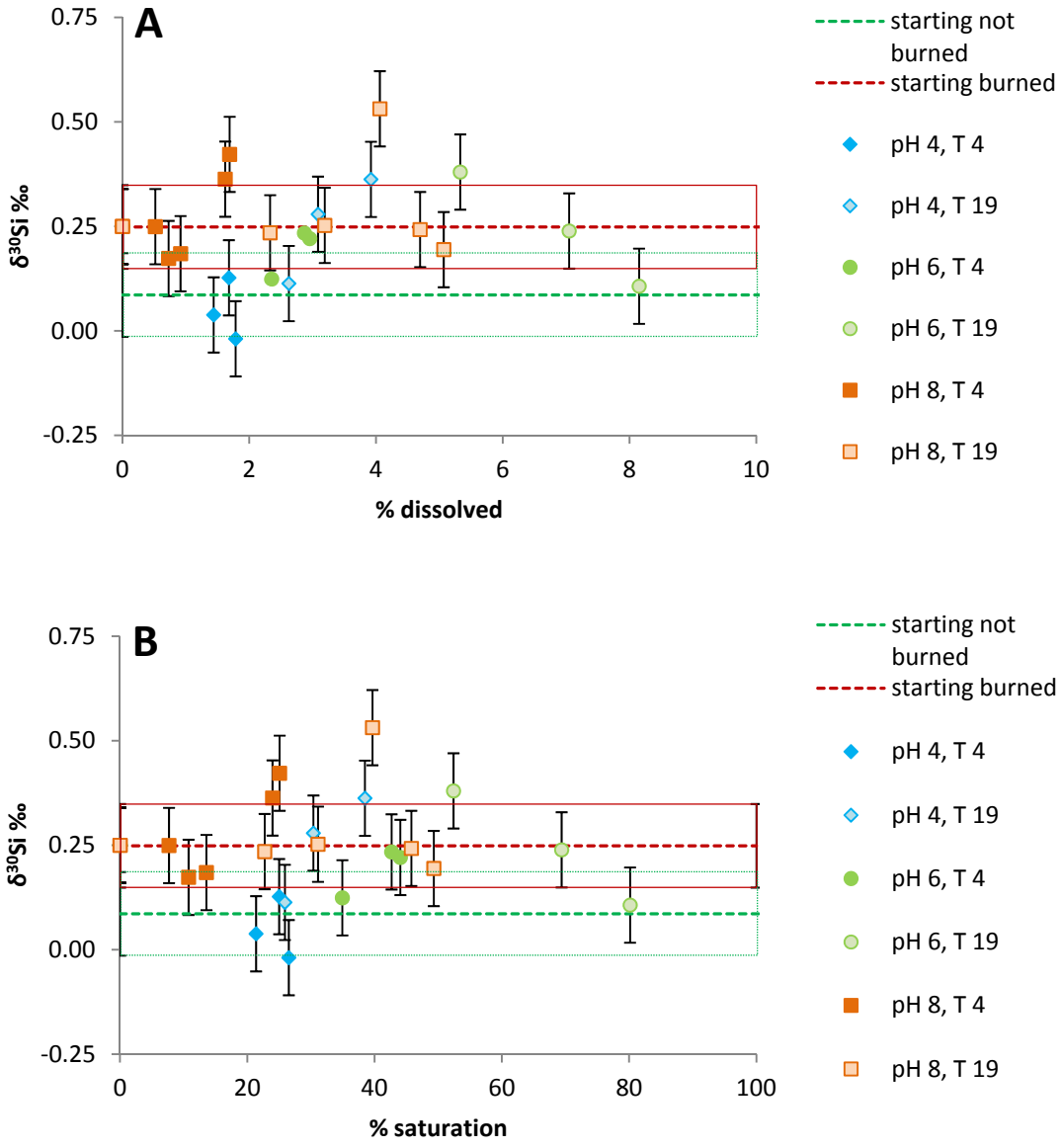

Figure 5-4. The change in $\delta^{30}Si$ of partially dissolved phytoliths plotted against the percent of the solid dissolved (A) and percent saturation (B).

Figure 5-4 shows the $\delta^{30}Si$ values of both the burned and unburned starting material, and the change in $\delta^{30}Si$ of samples as dissolution progressed. The $\delta^{30}Si$ value of the burned bulk sample is the same, within error, as that of the unburned material. The experiment conducted at T = 19ºC, pH 8 displays the increase in $\delta^{30}Si$ values until ~4% of the material is dissolved, followed by a decrease in $\delta^{30}Si$ as dissolution continues that was

observed for oxygen isotopes. This trend is similar to what was observed for unburned phytolith silica. All other experiments, with the exception of T = 4, pH 4, do not display a change in $\delta^{30}Si$ with dissolution. The maximum change in $\delta^{30}Si$ with dissolution was +0.33 ‰ for burned samples and +0.63 ‰ for unburned samples.

5.4 Discussion

5.4.1 Differences in the rate of dissolution

The decrease in SAA from 313.0 to 250.1 m^2/g after the phytoliths were burned is likely a result of partial annealing of the porous surface layer. This observation is in contrast to a study by Fraysse et al. (2006) who demonstrated that the SAA of soil phytoliths heated to 450°C increased from 5.2 ± 0.1 m^2/g to 6.5 ± 0.1 m^2/g. However, in that study the SAA of the phytoliths was low to begin with reflecting the loss of fine structures and thin cell walls during several hundred years in the soil (Fraysse et al., 2006).

Because the SSA of the burned sample is lower than the unburned sample we expected that the rate of dissolution would also be lower. This is the case for low temperature and pH conditions when dissolution rates are below ~0.30 mg/day. However, the opposite is true at higher pH and temperature conditions when dissolution rates are above ~0.30 mg/day (Fig. 5-2). Hence, the change in SAA that occurs upon burning cannot alone explain the differences in dissolution rates observed for burned versus unburned samples. The decrease in SSA is not accompanied by a change in the average grain size of the sample, suggesting that heating the phytoliths changed the nature of the surface layer (Truesdale et al., 2005; Schmidt et al., 2001). The presence of a highly reactive surface layer on the surface of marine biogenic silica has been discussed by other authors (Hurd et al., 1981; Barker et al., 1994; Brandriss et al., 1998) and suggested as being important in the dissolution trends of phytolith silica (Chapter 3, 4). Heating the silica to 700°C may have partially reorganized some of the bonds in the surface layer making them easier to break. Alexandre (1996) showed that heating to just 400ºC resulted in some permanent alteration of phytolith surfaces at the molecular level as the silica was not able to recover its initial hydroxyl and molecular water content. However, if bond re-organization were the only factor affecting dissolution the burned silica would be easier to dissolve even at

the lower pH and temperature conditions. We must consider three types of material being dissolved: the reactive surface layer of unburned phytoliths, the rest/bulk of the phytolith, and, in the case of burned phytoliths, partially reorganized silica. Examination of SSA and average grain size has suggested that the reactive surface layer is absent or greatly reduced on the burned phytoliths. At low pH and temperature conditions when dissolution rates are slower the dominant process in unburned phytoliths is removal of the reactive surface layer. Burned phytoliths, therefore, have a slower dissolution rate under these conditions because the reactive surface material has been completely or partially altered during the burning process. When pH and temperature conditions promote faster dissolution, the reactive surface layer of the unburned phytoliths is quickly removed, and the re-organized surface of the burned samples dissolves faster than the bulk silica of the unburned phytoliths.

During heating of biogenic opal, surface water and OH^- groups are removed and new reaction sites can be created. It was noted by Fraysse et al. (2006) that heated phytoliths had a surprisingly high negative surface charge. They suggest, following Hiemstra et al. (1996), that this may be the result of the presence of singly co-ordinated silanol groups ($Si\text{-}O^-$) that were created throughout the solid (Fraysse et al., 2006). Phytolith silica is amorphous so not all bond angles are ideal (Neuefeind and Liss, 1996). Bonds at unfavourable angles will be more prone to breaking during heating, exposing oxygen that is not fully co-ordinated. This process, in essence, provides new reaction sites without drastically changing SSA, as the creation of these new "surfaces" is at an atomic scale. In other studies, a higher proportion of singly-coordinated oxygen on the surface of quartz has been correlated dissolution rate (Brady and Walther 1990). From the pH of the zero point of charge (pH ~2.5) to high pH, the proportion of the surface species $Si\text{-}O^-$ controls dissolution rate (Walther 2009).

5.4.2 Isotopic composition of burned and unburned phytoliths

The $\delta^{18}O$ value of the bulk heated phytolith sample is 2.6 ‰ lower than that of the bulk sample before heating. The incorporation of ^{18}O-depleted hydroxyl oxygen as silica is heated would cause the $\delta^{18}O$ value of phytolith silica to decrease in a manner similar to

that observed here (Juillet 1980; Brandriss et al., 1998). This is not unexpected since hydroxyl oxygen starts to become a permanent part of the amorphous silica structure by 400°C (Labeyrie and Juillet 1980; Alexandre 1996). The decrease in the $\delta^{18}O$ value of the burned compared to fresh phytoliths is not accompanied by a change in the $\delta^{30}Si$ values suggesting that the incorporation of hydroxyl groups is likely the cause.

The silicon isotope composition of heated phytoliths changes very little during dissolution (Fig. 5-4). Almost all partially dissolved samples have $\delta^{30}Si$ values that fall within the range of error on the $\delta^{30}Si$ value of the undissolved material. This is different from the results of the unburned samples. During the dissolution of fresh phytolith silica $\delta^{30}Si$ values of the remaining solid increase until up to ~10% of the material has dissolved, after which $\delta^{30}Si$ values begin to decrease (Fig. 5-5). There are three possible reasons that this trend is not observed during the dissolution of burned phytoliths. The maximum % dissolved over the course of dissolution of burned phytoliths was 8.2% (Fig. 5-4). Because the increase in $\delta^{30}Si$ values of the unburned partially dissolved phytoliths occurred very early in the experiment it is possible that the peak in $\delta^{30}Si$ of the burned samples was missed by our sampling intervals. However, because higher $\delta^{18}O$ values are observed with the dissolution of burned phytoliths it is not likely that changes in $\delta^{30}Si$ of burned silica were missed (Fig. 5-3). The second possibility concerns the role of the reactive layer in the change in $\delta^{30}Si$ values with dissolution. The initial increase on the $\delta^{30}Si$ value of unburned silica was observed as the reactive layer was being removed. If the reactive layer was altered on phytoliths that have been burned making it less susceptible to dissolution then a shift to higher $\delta^{30}Si$ with dissolution may not be observed. Third, there may have been some fractionation of silicon isotopes during dissolution but of a magnitude that was too small to be detected.

The oxygen isotope composition of partially dissolved, heated phytoliths behave in a similar way to the unburned experiments – they initially increase by ~1-2 ‰ until approximately 5-8% of the solid has been dissolved (15-45% saturation) after which $\delta^{18}O$ values begin to decrease until they are at or below the $\delta^{18}O$ value of the initial material. In the unburned samples this was the result of preferential dissolution of ^{16}O followed by precipitation reactions (Chapter 4). For the unburned samples (Chapter 4), as dissolution

progressed the isotopic composition of the remaining silica continued towards lower $\delta^{18}O$ and $\delta^{30}Si$ values. The overall magnitude of change in $\delta^{18}O$ values with dissolution is less for burned phytoliths than for unburned phytoliths (Fig. 5-5).

Examining the results of both the oxygen and silicon isotope composition of phytoliths as dissolution progresses, it appears that the re-organization of silica at the phytolith surface has changed the way the silica dissolves. Burning creates new reaction sites on the silica surface that dissolve more quickly than the bulk silica and this process results in a smaller fractionation between the bulk silica and silicic acid. As a result, it is possible that $\delta^{30}Si$ values of burned phytoliths also changed with initial dissolution but that these changes were not detectable. The relative mass difference between the isotopes of silicon is less than for lighter elements and, as a result, the magnitude of fractionation during reactions is lower. It is possible that any silicon isotope fractionation that occurred during the dissolution of burned phytoliths was too small to be measured.

Figure 5-5 (next page). The $\delta^{18}O$ and $\delta^{30}Si$ values of partially dissolved burned and unburned phytoliths reacted for the same length of time at pH 4 (A), pH 6 (B), and pH 8 (C).

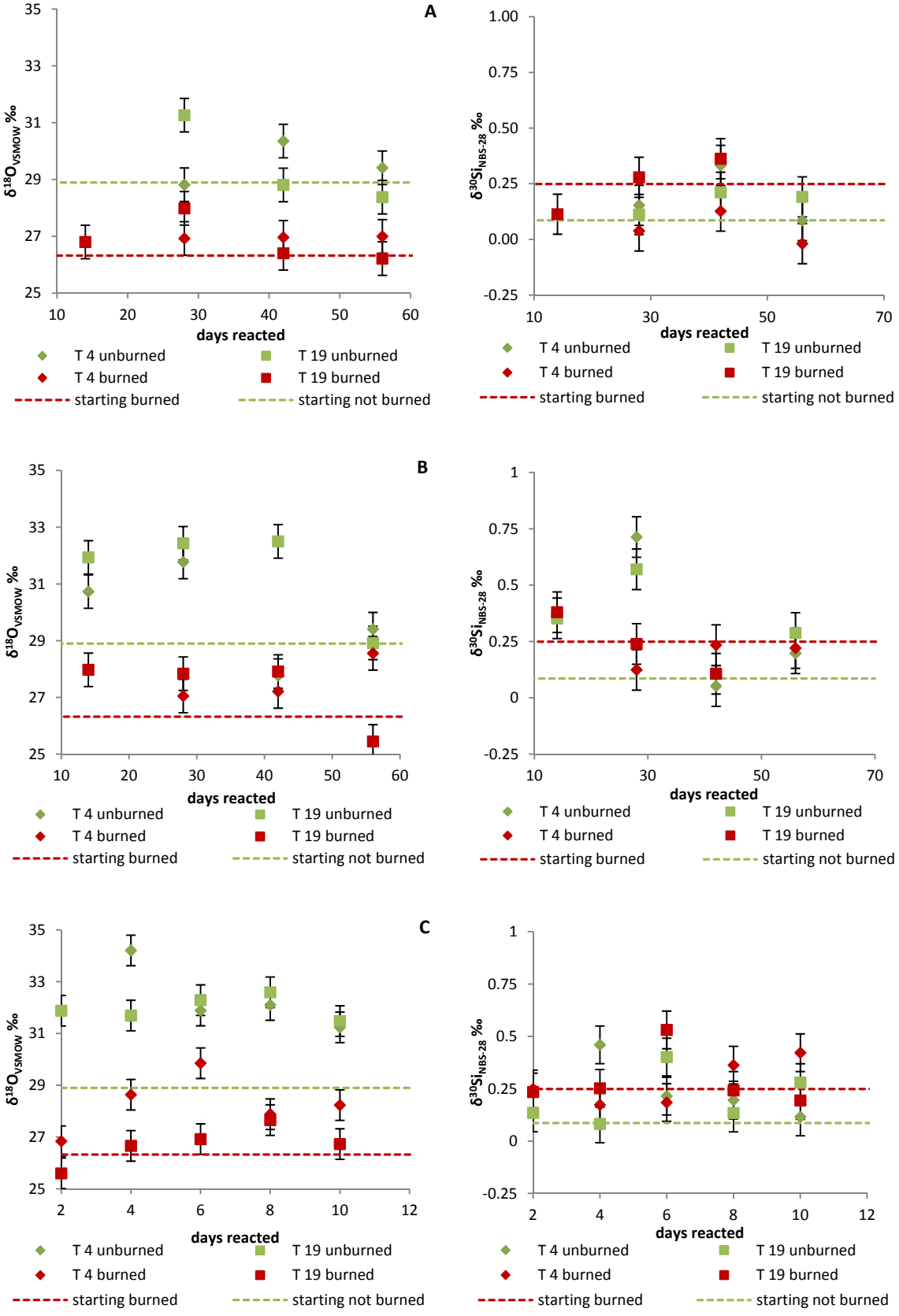
A
B
C
δ18OVSMOW ‰
δ30SiNBS-28 ‰
days reacted
T 4 unburned
T 19 unburned
T 4 burned
T 19 burned
starting burned
starting not burned

5.5 Concluding Remarks

The results presented here indicate that burning phytoliths at 700ºC results in changes in their oxygen isotope composition and the manner in which they dissolve. When conditions favour the rapid dissolution of silica (i.e. higher temperature and pH) burned phytoliths dissolve faster than unburned phytoliths. When conditions for silica dissolution are less favourable unburned phytoliths dissolve more quickly, likely a result of the reactive surface layer which constitutes less of the total volume of silica in burned phytoliths. Burned phytoliths have $\delta^{18}O$ values that are lower than their unburned counterparts by 2.6 ‰ while $\delta^{30}Si$ values are unchanged. Changes to lower $\delta^{18}O$ values of burned versus unburned phytolith silica would result in overestimations of temperature and would complicate interpretations of relative changes in $\delta^{18}O$ over time. In addition, under some conditions burned phytoliths may be less well preserved than unburned phytoliths.

5.6 References

Albert, R.M., Bar-Yosef, L., Weiner, S. (2003) Quantitative phytolith study of hearths from the Natufian and Middle Paleolithic levels of Hayonim Cave (Galilee, Israel). Journal of Archaeological Science 30, 461-480.

Alexandre A. (1996) Phytolithes, interactions sol-plante et paléoenvironnements. Ph.D. dissertation, Univ. d'Aix-Marseille III.

Alexandre, A., Crespin, J., Sylvestre, F., Sonzogni, C., Hilbert, D.W. (2012) The oxygen isotopic composition of phytoliths assemblages from tropical rainforest soil tops (Queensland, Australia): validation of a new paleoenvironmental tool. Climate of the Past 8, 307-324.

Barker, P., Fontes, J.C., Gasse, F., Druart, J.C. (1994) Experimental dissolution of diatom silica in concentrated salt solutions and implications for paleoenvironmental reconstruction. Limnology and Oceanography 39, 99-110.

Brady, P.V. and Walther, J.V. (1990) Kinetics of quartz dissolution at low temperatures. Chemical Geology 82, 253-264.

Brand, W.A., Coplen. T.B., Vogl, J., Rosner, M., Prohaska, T. (2014) Assessment of international reference materials for isotope-ratio analysis (IUPAC Technical Report). Pure and Applied Chemistry 86, 425-467.

Brandriss, M.E., O'Neil, J.R., Edlund, M.B., Stoermer, E.F. (1998) Oxygen isotope fractionation between diatomaceous silica and water. Geochimica et Cosmochimica Acta 62(7), 1119-125.

Cabanes, D., Weiner, S., Shahack-Gross, R. (2011) Stability of phytoliths in the archaeological record: a dissolution study of modern and fossil phytoliths. Journal of Archaeological Science 38(9), 2480-2490.

Cabanes, D., Gadot, Y., Cabanes, M., Finkelstein, I., Weiner, S., Shahack-Gross, R. (2012) Human impact around settlement sites: a phytoliths and mineralogical study for assessing site boundaries, phytolith preservation, and implications for spatial reconstructions using plant remains. Journal of Archaeological Science 39, 2697-2705.

Chapligin, B., Meyer, H., Friedrichsen, H., Marent, A., Sohns, E., Hubberten, H.-W. (2010) A high-performance, safer and semi-automated approach for the $\delta^{18}O$ analysis of diatom silica and new methods for removing exchangeable oxygen. Rapid Communications in Mass Spectrometry 24, 2655-2664.

Ding, T. (2004) Analytical methods for silicon isotope determinations. In P.A. de Groot (Ed.) Handbook of Stable Isotope Analytical Techniques, Volume 1. pp. 523-537 Elsevier Ltd. San Deigo, CA.

Elbaum, R., Weiner, S., Albert, R.M., Elbaum, M. (2003) Detection of burning of plant materials in the archaeological record by changes in the refractive indices of siliceous phytoliths. Journal of Archaeological Science 30(2), 217-226.

Engle, D.M., Bidwell, T.G., Ewing, A.L., Williams, J.R. (1989) A technique for quantifying fire behaviour in grassland fire ecology studies. The Southwestern Naturalist 34, 79-84.

Fraysse, F., Cantais, F., Pokrovsky, O.S., Schott, J., Meunier, J.D. (2006) Aqueous reactivity of phytoliths and plant litter: Physico-chemical constraints on terrestrial biogeochemical cycle of silicon. Journal of Geochemical Exploration 88, 202-205.

Geis, J.W. (1973) Biogenic silica in selected species of deciduous angiosperms. Soil Science 116, 113-130.

Hiemstra, T., Venema, P., Van Riemsdijk, W.H. (1996) Intrinsic proton affinity of reactive surface groups of metal (hydr)oxides: the bond valence principle. Journal of Colloid and Interface Science 184, 680-692.

Hurd, D.C., Pankratz, H.S., Asper, V., Fugate, J., Morrow, H. (1981) Changes in the physical and chemical properties of biogenic silica from the central equatorial Pacific: Part III, specific pore volume, mean pore size, and skeletal ultrastructure of acid-cleaned samples. America Journal of Science 281, 833-895.

Juillet, A. (1980) Structure de la silice biogénique: nouvelles données apportées par l'analyse isotopique de l'oxygène. Comptes Rendus de l'Académie des Sciences 290 D, 1237-1239.

Leng, M.J. and Sloane, H.J. (2008) Combined oxygen and silicon isotope analysis of biogenic silica. Journal of Quaternary Science 23(4), 313-319.

McPherson, G.R. (1995) The role of fire in the Desert Grasslands. In: McClaran, M.P. and Van Devender, T.R. (eds.) The Desert Grassland pp. 130-151. University of Arizona Press, Tuscon, AZ, USA.

Neuefeind and Liss 1996

Reynolds, B.C., Aggarwal, J., André, L., Baxter, D., Beucher, C., Brzezinski, M.A., Engström, E., Georg, R.B., Land, M., Leng, M.J., Opfergelt, S., Rodushkin, I., Sloane, H.J., van den Boorn, S.H.J.M., Vroon, P.Z., Cardinal, D. (2007) An inter-laboratory comparison of Si isotope reference materials. Journal of Analytical Atomic Spectrometry 22, 561-568.

Runge, F. (1998) The effects of dry oxidation temperatures (500-800ºC) and of natural corrosion on opal phytoliths. In J.D. Meunier, F. Colin, and L. Faure-Denard (Eds.), The phytoliths: Applications in earth science and human history pp. 73. Aix en Provence, France: CEREGE.

Schiegl, S., Stockhammer, P., Scott, C., Wadley, L. (2004). A mineralogical and phytolith study of the Middle Stone Age hearths in Sibudu Cave, KwaZulu-Natal, South Africa. South African Journal of Science 100, 185-194.

Schmidt, M., Botz, R., Rickert, D., Bohrmann, G., Hall, S.R., Mann, S. (2001) Oxygen isotopes of marine diatoms and relations to opal-A maturation. Geochimica et Cosmochimica Acta 65(2), 201-211.

Truesdale V.W., Greenwood J.E., Rendell A. (2005) The rate-equation for biogenic silica dissolution in seawater – New hypotheses. *Aquatic Geochemistry* **11**, 319-343.

Tsartsidou, G., Lev-Yadun, S., Efstratiou, N., Weiner, S. (2008) Enthoarchaeological study of phytolith assemblages from an agro-pastoral village in Northern Greece (Sarakini): development and application of a Phytolith Difference Index. Journal of Archaeological Science 35, 600-613.

Vilà, M., Lloret, F., Ogheri, E., Terradas, J. (2001) Positive fire-grass feedback in Mediterranean Basin woodlands. Forest Ecology and Management 147, 3-14.

Walther, J.V. (2009) Essentials of Geochemistry, Second Edition. Jones and Bartlett Publishers.

Wilson, S.D. and Shay, J.M. (1990) Competition, fire, and nutrients in a mixed-grass prairie. Ecology 71, 1959-1967.

Woodcock, D.W. (1992) The rain on the plain: Are there vegetation-climate feedbacks? Palaeogeography, Palaeoclimatology, Palaeoecology 97, 191-201.

Wu, Y., Wang, C., Hill, D.V. (2012) The transformation of phytolith morphology as the result of their exposure to high temperature. Microscopy Research and Technique 75, 852-855.

6. Summary

Phytoliths are a highly soluble source of silicon relative to other minerals and can be important contributors of silicic acid to soil water. Their oxygen and silicon isotope compositions are potentially useful tools for examining past environmental conditions. Phytolith $\delta^{18}O$ values can be related to their temperature of formation and modern soil phytolith $\delta^{18}O$ values have been related directly to mean annual temperature and the oxygen isotope composition of precipitation (Alexandre et al., 2012). However, phytoliths are subject to dissolution after their deposition in the soil, and it is important to understand phytolith dissolution behaviour and its effect on the $\delta^{18}O$ and $\delta^{30}Si$ values before phytoliths can be used to provide reliable information regarding past environmental conditions. This study demonstrates that both $\delta^{18}O$ and $\delta^{30}Si$ values of phytoliths are modified when phytoliths partially dissolve.

Phytolith $\delta^{30}Si$ values increase by up to 0.63 ‰ with partial dissolution. As a result, the alteration of phytolith $\delta^{30}Si$ values in the soil will complicate attempts to use phytoliths to examine silicic acid availability to plants, as proposed by Ding et al. (2009). However, phytolith $\delta^{30}Si$ values do not change after burning, and burned phytoliths generally retain their original $\delta^{30}Si$ values after 8% dissolution. This indicates that burned soil or hearth phytolith assemblages may be useful in investigations of silicic acid availability.

The dissolution of phytolith silica produces dissolved silicic acid with $\delta^{30}Si$ values that are much lower than those commonly reported for soil solutions (Ziegler et al., 2005). Many authors have investigated the $\delta^{30}Si$ values of soil solutions and the solid material from which they are derived and have discussed the importance of precipitation of new mineral phases and preferential adsorption of ^{28}Si onto mineral surfaces in modifying the $\delta^{30}Si$ values of soil solutions (Zeigler et al., 2005; Delstanche et al., 2009; Opfergelt et al., 2009; Geilert et al., 2014; Oelze et al., 2014). Based on the extremely low $\delta^{30}Si$ values calculated for dissolved silica in this study, we suggest that soil solutions that contain silicic acid derived from phytoliths must be highly modified by precipitation reactions, adsorption of silicic acid into mineral surfaces, and preferential plant uptake of ^{28}Si.

Phytoliths that have undergone partial dissolution have $\delta^{18}O$ values that are up to 3.9 ‰ higher than unaltered phytoliths, which translates into an underestimation of temperature by nearly 20˚C. However, precipitation of silica in isotopic equilibrium with water onto phytolith surfaces acted to drive overall phytolith $\delta^{18}O$ values down once the solution was 30-40% saturated with respect to silicic acid. In soil environments, if soil water is in contact with phytoliths for a sufficient period of time, a silica coating may form on the outside of the phytolith that has $\delta^{18}O$ values that are in isotopic equilibrium with soil water. In most cases, the newly precipitated silica would have $\delta^{18}O$ values that are lower than those of phytoliths precipitated from ^{18}O-enriched plant water. This could potentially result in overestimations of past growing temperature.

Clearly the extent of alteration of a soil phytolith assemblage needs to be assessed prior to the use of their isotopic composition in paleoclimate models. While other authors have observed the loss of fine features and adsorbed particles on the surface of phytoliths subjected to dissolution (e.g. Fraysse et al., 2006), in this study dissolution features were not consistently observed on the surfaces of partially dissolved phytoliths. Cabanes et al. (2011) have suggested that partially dissolved phytolith assemblages can be identified based on their solubility. However, phytoliths produced in different plants can have widely variable dissolution rates so this method may not always be accurate. It may be possible to use the proportion of Si-O-Si to Si-OH bonds in phytolith silica to determine if they have undergone extensive alteration. For example, Schmidt et al. (2001) found that the ratio of Si-O-Si to Si-OH bond was higher in fossil diatoms than in fresh ones and was related to an increase in the $\delta^{18}O$ value of the sample. However, this method would need to be calibrated on a range of phytolith assemblages because percent of exchangeable oxygen is variable even in fresh samples (Webb and Longstaffe 2002).

Heating phytoliths to 700˚C results in a decrease in phytolith $\delta^{18}O$ values by 2.6 ‰ as ^{18}O-depleted hydroxyl oxygen is incorporated into the silica structure. As a result, archaeological hearth deposits, which often concentrate phytoliths, are not ideal source of phytolith silica if the aim is to use $\delta^{18}O$ values to determine paleotemperature. Burned phytoliths can be identified based on their refractive index (Elbaum et al., 2003), so it is

possible to identify assemblages that are not suitable for oxygen isotope analysis as a result of burning.

Despite similar visual trends in the $\delta^{18}O$ and $\delta^{30}Si$ values of unburned phytoliths as dissolution progressed, there is no significant relationship between phytolith $\delta^{18}O$ and $\delta^{30}Si$ values from the same sample. This is likely because the experiments discussed in this study were conducted in batch reactors and the precipitation of new silica was observed. The controls on the partitioning of silicon and oxygen isotopes during silica precipitation are different. The $\delta^{18}O$ values of newly precipitated silica were controlled by the $\delta^{18}O$ value of the water and the temperature of each experiment. Silicon isotope fractionation is not temperature dependent. The $\delta^{30}Si$ values of newly precipitated silica depend on the $\delta^{30}Si$ value of the solution from which precipitation occurs. In these experiments the $\delta^{30}Si$ value of the solution was variable, depending on how much silica had dissolved. We suspect that had experiments been conducted in flow-through reactors both $\delta^{18}O$ and $\delta^{30}Si$ values of phytoliths would have continued to increase for the duration of the experiment, and a correlation between the oxygen and silicon isotope composition of remaining silica would have been observed.

Recommended future work would monitor phytolith dissolution with earlier sampling at low pH and longer sampling over a range of pH conditions. This would provide more information on the dissolution behaviour of phytoliths when they first reach the soil and allow us to observe trends in $\delta^{18}O$ and $\delta^{30}Si$ values of silica over an extended period of precipitation. In this study, the effects of burning on the isotopic composition of phytoliths was only determined for the relatively high temperature of 700˚C. Examining changes in the isotopic composition of phytoliths burned at a range of lower temperatures would allow us to determine at what temperature burning begins to interfere with the use of phytoliths for paleothermometry. Finally, examination of single large fresh and soil phytoliths, perhaps from bamboo, for evidence of isotopic zoning would allow us to determine if phytoliths are isotopically homogenous and determine if soil phytoliths develop a coating of silica precipitated once they are deposited in the soil.

6.1 References

Alexandre, A., Crespin, J., Sylvestre, F., Sonzogni, C., Hilbert, D.W. (2012) The oxygen isotopic composition of phytolith assemblages from tropical rainforest soil tops (Queensland, Australia): validation of a new palaeoenvironmental tool. Climate of the Past 8, 307-324.

Cabanes, D., Weiner, S., Shahack-Gross, R. (2011) Stability of phytoliths in the archaeological record: a dissolution study of modern and fossil phytoliths. Journal of Archaeological Science 38, 2480-2490.

Delstanche, S., Opfergelt, S., Cardinal, D., Elsass, F., Andre, L., Delvaux, B. (2009) Silicon isotope fractionation during adsorption of aqueous monosilicic acid onto iron oxide. Geochimica et Cosmochimica Acta 73, 923-934.

Elbaum, M. (2003) Detection of burning of plant materials in the archaeological record by changes in the refractive indices of siliceous phytoliths. Journal of Archaeological Science 30, 217-226.

Fraysse, F., Pokrovsky, O.S., Schott, J., Meunier, J.D. (2006) Surface properties, solubility, and dissolution kinetics of bamboo phytoliths. Geochimica et Cosmochimica Acta 70, 1939-1951

Geilert, S., Vroon, P.Z., Roerdink, D.L., Van Cappellen, P., van Bergen, M.J. (2014) Silicon isotope fractionation during abiotic silica precipitation at low temperatures: Inferences from flow-through experiments. Geochimica et Cosmochimica Acta 142, 95-114.

Oelze, M., von Blanckenburg, F., Hoellen, D., Dietzel, M., Bouchez, J. (2014) Si stable isotope fractionation during adsorption and the competition between kinetic and equilibrium isotope fractionation: Implications for weathering systems. Chemical Geology 380, 161-171.

Opfergelt, S., Delvaux, B., André, L., Cardinal, D. (2009) Plant silicon isotopic signature might reflect soil weathering degree. Biogeochemistry 91, 163-175.

Schmidt, M., Botz, R., Rickert, D., Bohrmann, G., Hall, S.R., Mann, S. (2001) Oxygen isotopes of marine diatoms and relations to opal-A maturation. Geochimica et Cosmochimica Acta 65(2), 201-211.

Webb, E.A. and Longstaffe, F.J. (2002) Climatic influences on the isotopic composition of biogenic silica in prairie grass. Geochimica et Cosmochimica Acta 66(11), 1891-1904.

Zeigler, K., Chadwick, O.A., Brzezinski, M.A., Kelly, E.F. (2005) Natural variations of δ^{30}Si ratios during progressive basalt weathering, Hawaiian Islands. Geochimica et Cosmochimica Acta 69(17), 4597-4610.

Appendix A

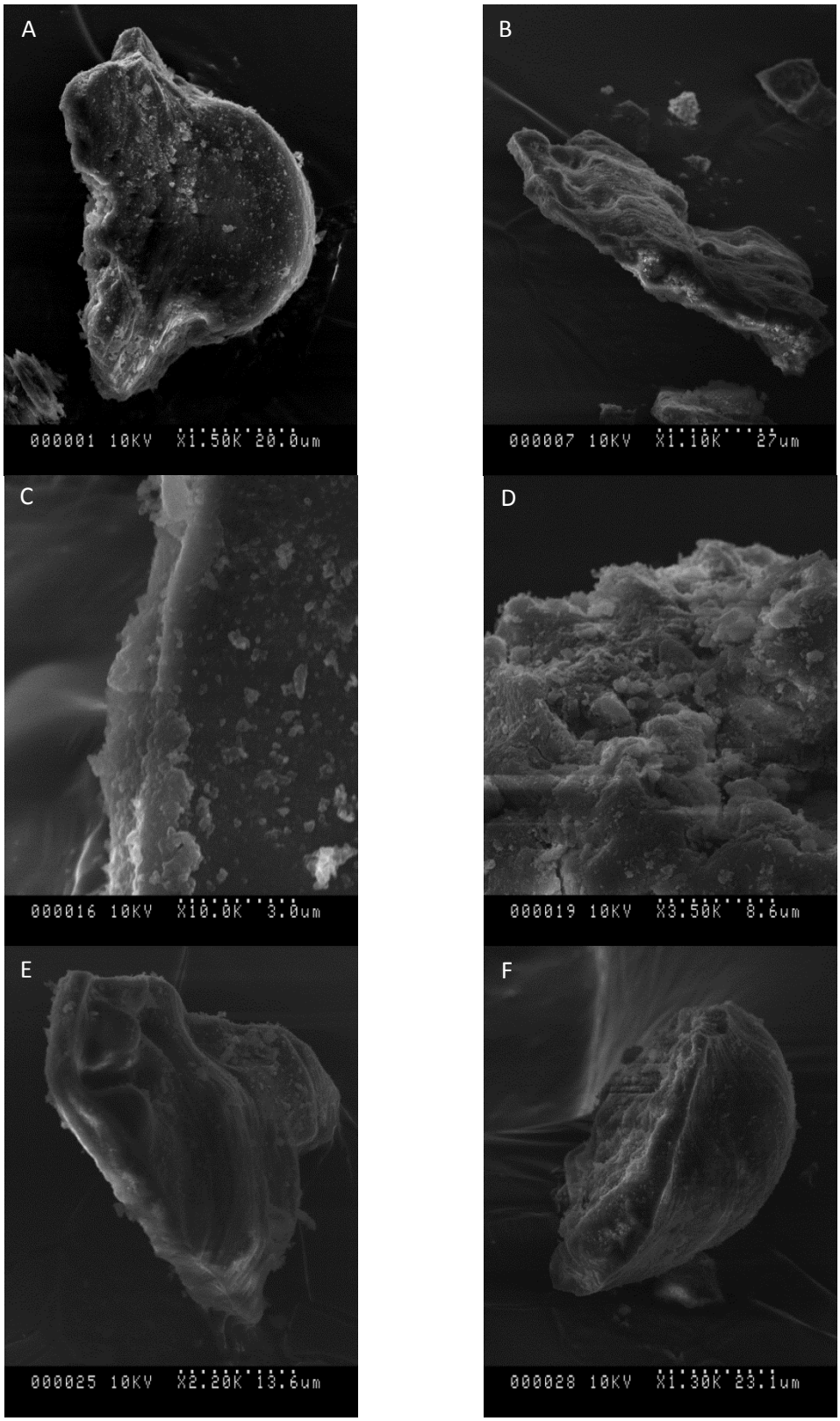

A-1. SEM images of phytoliths prior to dissolution.

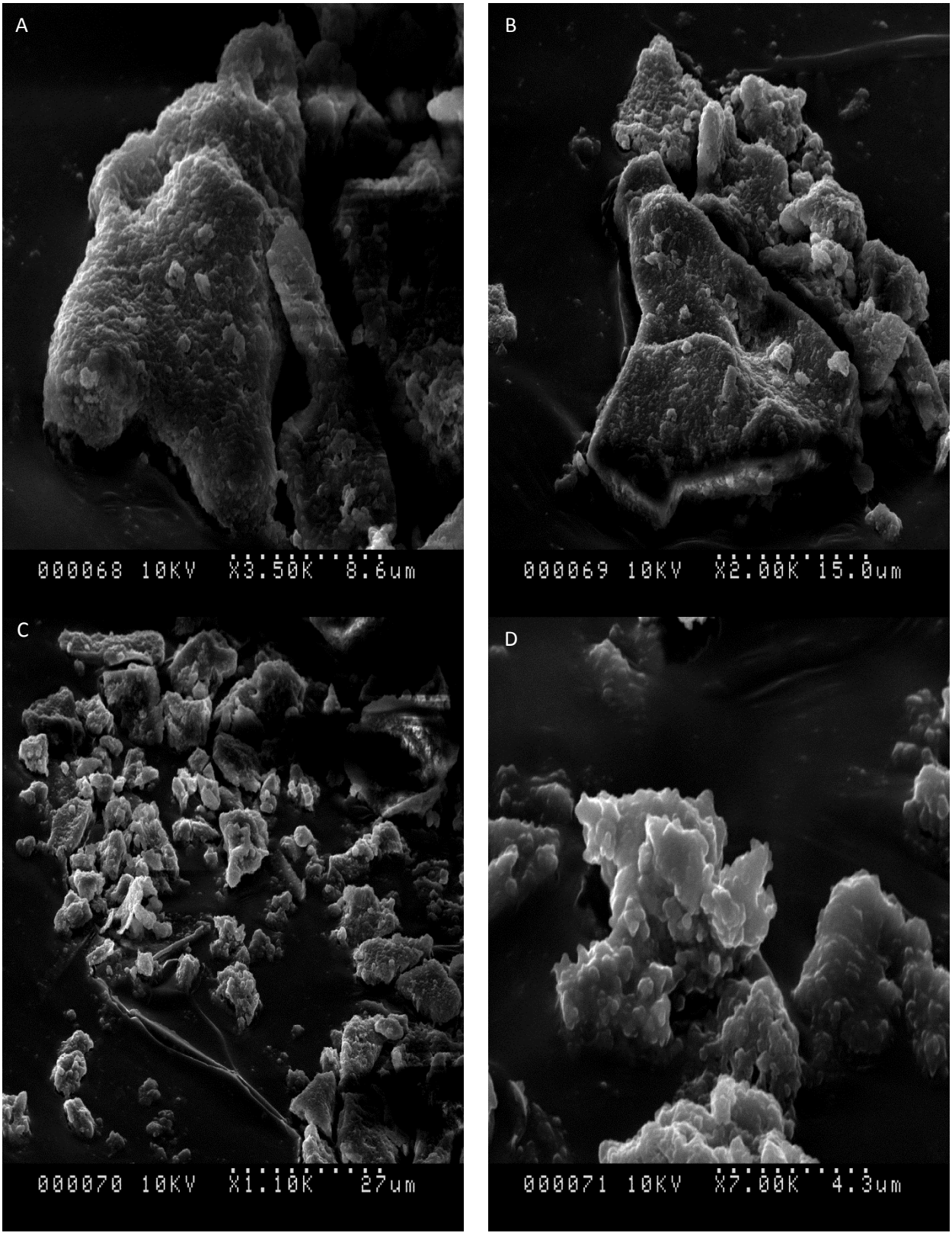

A-2. SEM images of phytoliths after dissolution for 70 days at T = 4˚C and pH = 4.

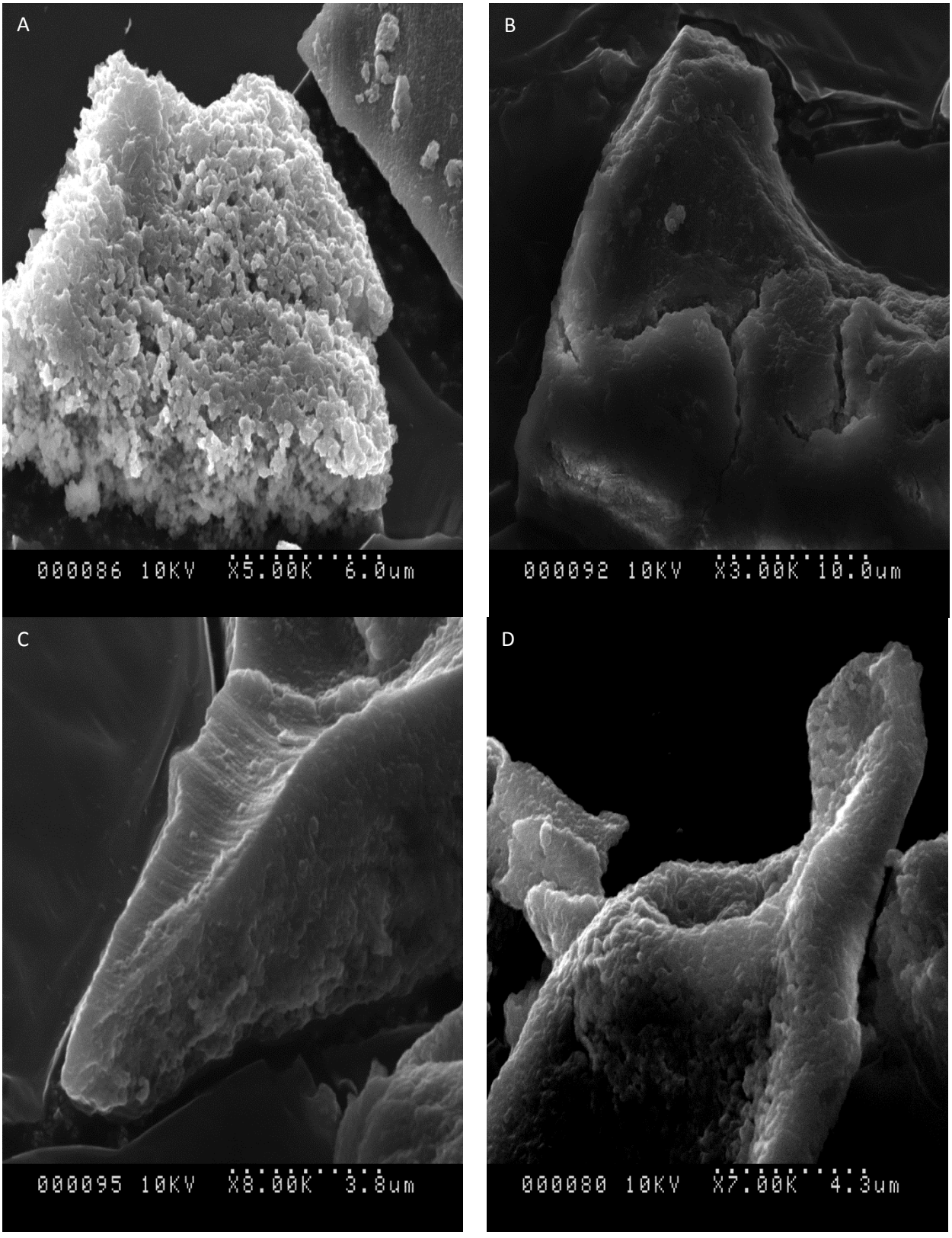

A-3. SEM images of phytoliths after dissolution for 10 days at T = 44˚C and pH = 10.

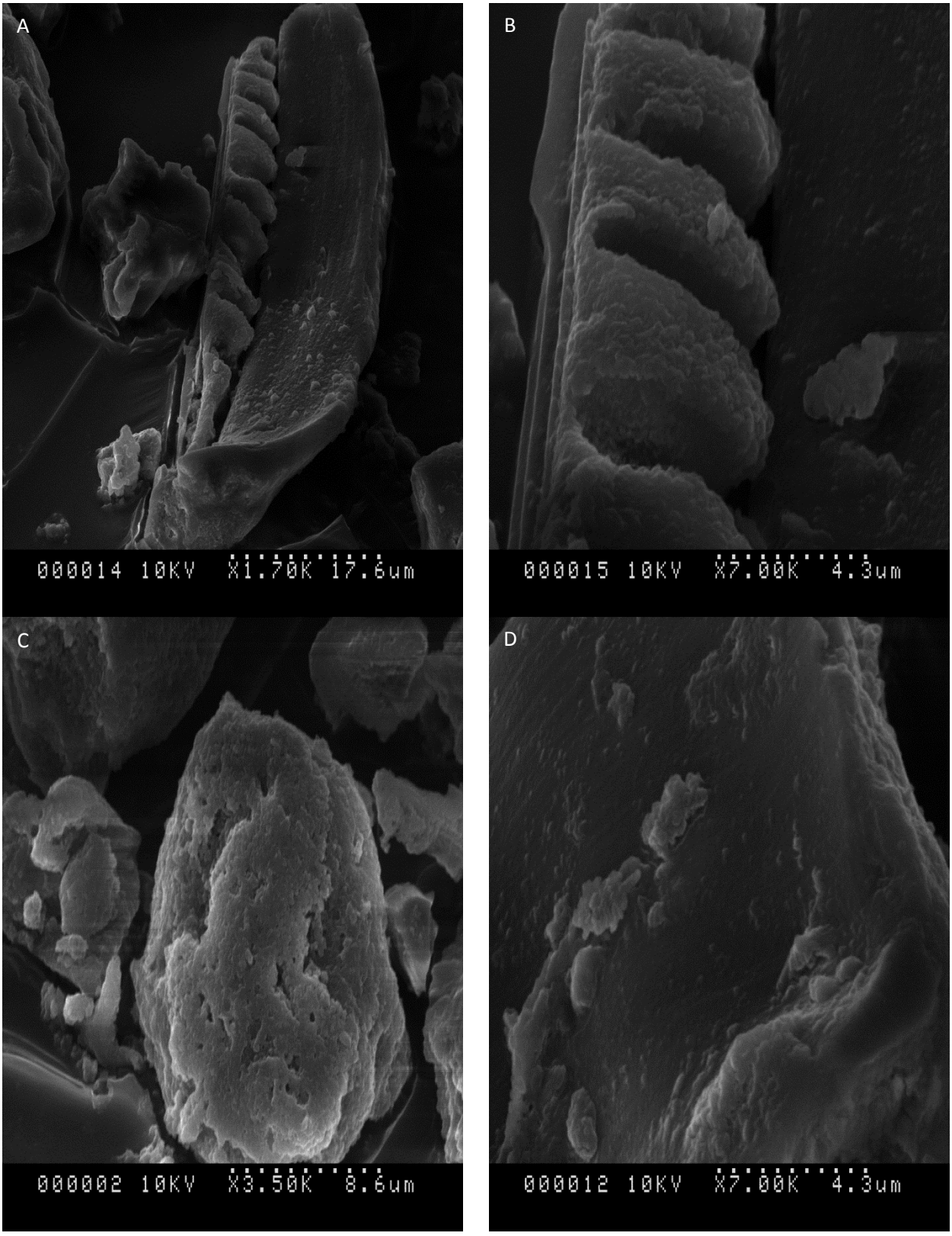

A-4. SEM images of phytoliths after dissolution for 28 days at T = 44˚C and pH = 4.

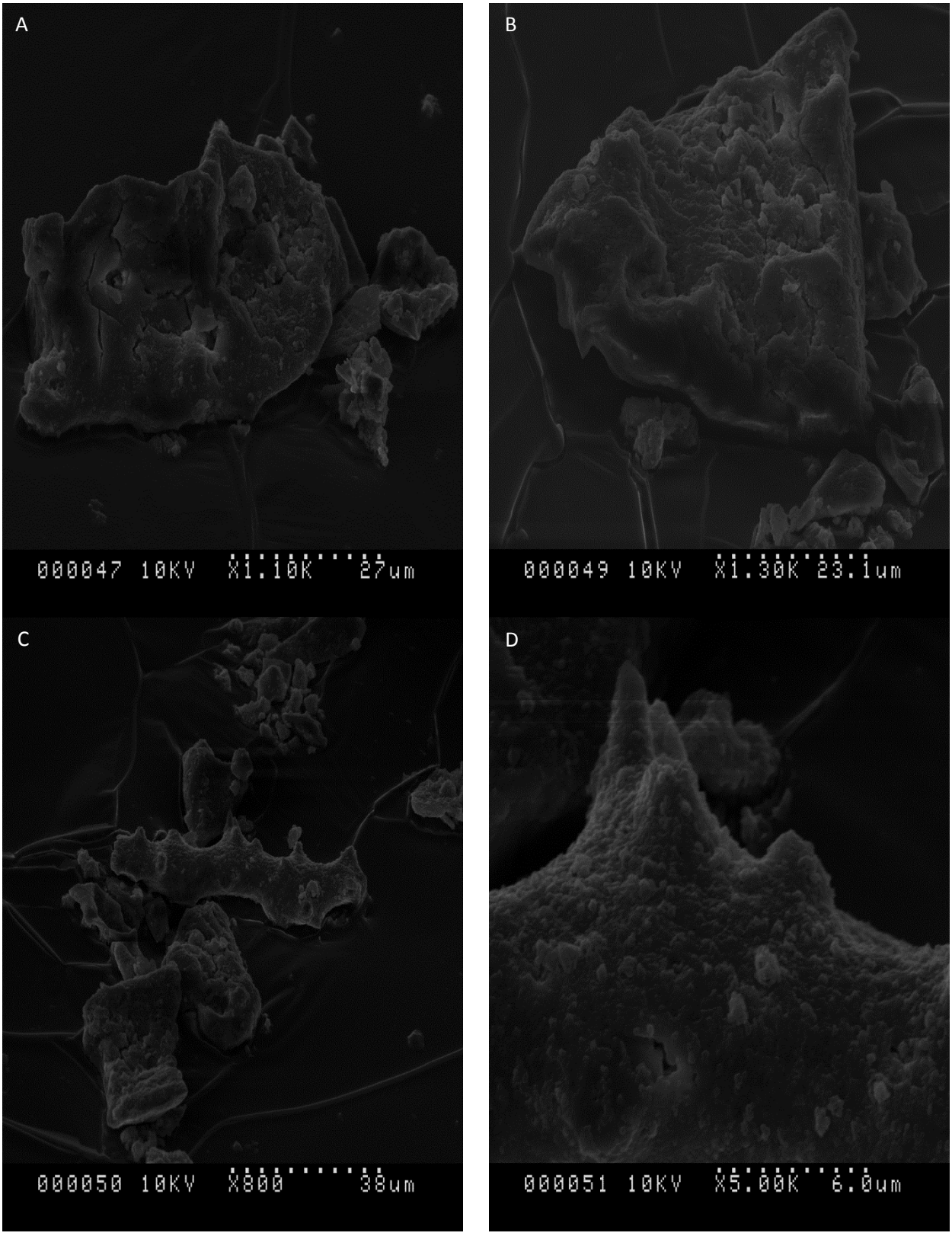

A-5. SEM images of phytoliths after dissolution for 70 days at T = 19˚C and pH = 6.

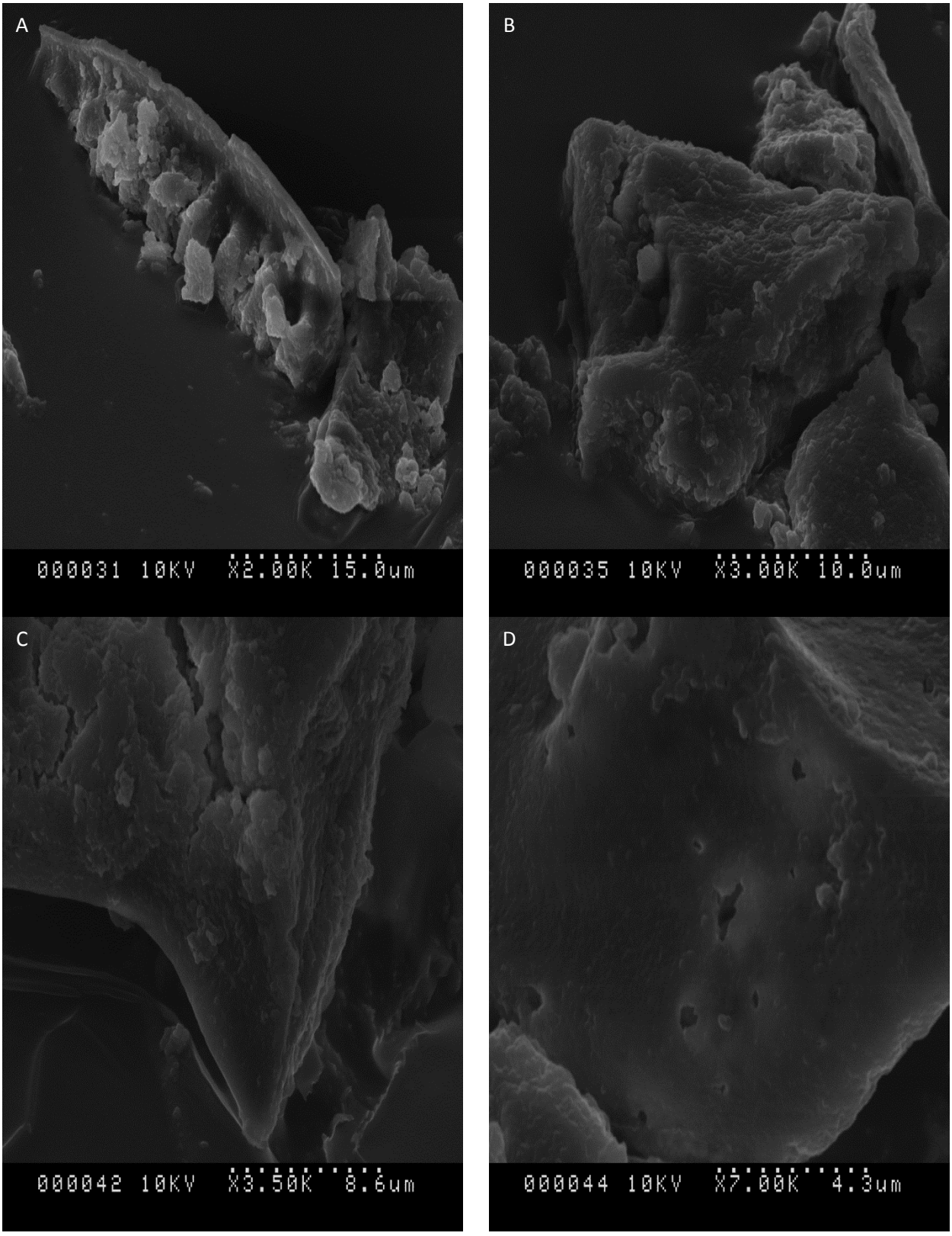

A-6. SEM images of phytoliths after dissolution for 10 days at T = 4˚C and pH = 10.

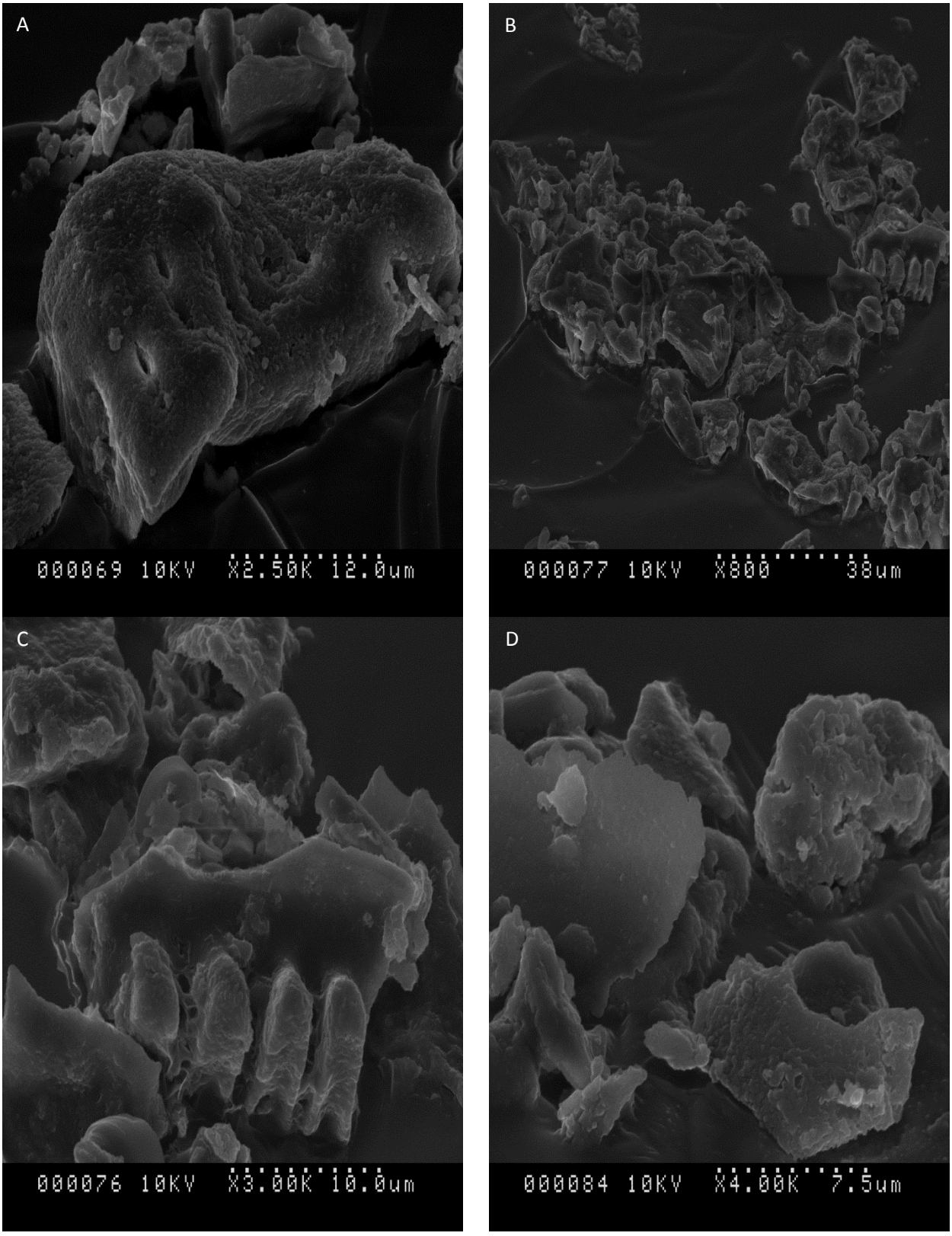

A-7. SEM images of phytoliths after dissolution for 10 days at T = 19˚C and pH = 10.

Appendix B. Summary of experimental conditions and results of dissolution experiments conducted on fresh phytoliths

Sample ID	# days	pH	T°C	µg/L	mg dissolved	% dissolved	modelled pH	% saturation	phytolith $\delta^{18}O_{VSMOW}$ (‰)	phytolith $\delta^{30}Si_{NBS-28}$ (‰)	dissolved $\delta^{30}Si_{NBS-28}$ (‰)	SSA (m^2/g)	mean particle size (µm)
HT-4-4-14	14	4	4	12.58	3.36	2.24	4.00	33.34					
HT-4-4-28	28	4	4	11.91	3.18	2.12	4.00	31.56	28.8	0.15	-3.03		
HT-4-4-42	42	4	4	14.93	3.99	2.66	4.00	39.57	30.4	0.33	-8.94		
HT-4-4-56	56	4	4	13.93	3.72	2.48	4.00	36.90	29.4	0.08	0.13		
HT-4-4-70	70	4	4	15.10	4.04	2.69	4.00	40.02		0.03	2.21		
HT-19-4-14	14	4	19	14.77	3.95	2.63	4.00	25.90					
HT-19-4-28	28	4	19	15.61	4.17	2.78	4.00	27.38	31.3	0.11	-0.84	209.03	36.20
HT-19-4-42	42	4	19	17.46	4.67	3.11	4.00	30.62	28.8	0.21	-3.83	226.62	32.69
HT-19-4-56	56	4	19	18.63	4.98	3.32	4.00	32.69	28.4	0.19	-2.98		
HT-19-4-70	70	4	19	20.65	5.52	3.68	4.00	36.23	26.4	-0.02	2.83	277.29	37.01
HT-35-4-14	14	4	35	10.84	2.90	1.93	4.00	14.00	32.1	0.22	-6.57		
HT-35-4-28	28	4	35	14.87	3.98	2.65	4.00	19.22	27.7	0.22	-4.93		
HT-35-4-42	42	4	35	18.01	4.82	3.21	4.00	23.28	27.1	0.12	-0.98		
HT-35-4-56	56	4	35	21.16	5.66	3.77	4.00	27.34	28.9	0.30	-5.40		
HT-35-4-70	70	4	35	23.57	6.30	4.20	4.00	30.46	30.2	0.20	-2.41		
HT-44-4-14	14	4	44	15.94	4.26	2.84	4.00	16.84					
HT-44-4-28	28	4	44	23.23	6.21	4.14	4.00	24.54	28.1	0.17	-1.88	273.78	37.39
HT-44-4-42	42	4	44	30.52	8.16	5.42	4.00	32.24	28.4	0.18	-1.47		
HT-44-4-56	56	4	44	35.85	9.59	6.38	4.00	37.87	28.0	0.41	-4.64	262.72	35.00
HT-44-4-70	70	4	44	41.63	11.13	7.42	4.00	43.98	30.7	0.13	-0.51	218.55	35.69
HT-4-6-14	14	6	4	16.11	4.31	2.87	5.93	42.69	30.7				
HT-4-6-28	28	6	4	13.93	3.72	2.48	5.94	36.90	31.8	0.71	-24.57		
HT-4-6-42	42	6	4	10.90	2.91	1.94	5.94	28.88	27.8	0.05	1.78		
HT-4-6-56	56	6	4	12.75	3.41	2.27	5.94	33.78	29.4	0.20	-4.72		
HT-4-6-70	70	6	4	15.44	4.13	2.75	5.93	40.91	25.2	0.08	0.35		
HT-19-6-14	14	6	19	13.10	3.50	2.34	5.92	22.98	31.9	0.35	-11.08		
HT-19-6-28	28	6	19	21.49	5.75	3.83	5.89	37.70	32.4	0.57	-12.08	200.79	38.73
HT-19-6-42	42	6	19	17.10	4.57	3.05	5.91	30.00	32.5				
HT-19-6-56	56	6	19	30.74	8.22	5.48	5.88	53.92	28.9	0.29	-3.40	246.22	39.09
HT-19-6-70	70	6	19	22.00	5.88	3.92	5.89	38.59	29.1	0.22	-3.13	225.54	37.37
HT-35-6-14	14	6	35	15.27	4.08	2.72	5.89	19.73	30.6	0.34	-8.95		
HT-35-6-28	28	6	35	24.02	6.42	4.28	5.86	31.04	28.1	0.49	-8.91		
HT-35-6-42	42	6	35	29.85	7.98	5.32	5.85	38.58	32.4	-0.02	1.90		
HT-35-6-56	56	6	35	34.56	9.24	6.16	5.84	44.67	30.2	0.17	-1.21		
HT-35-6-70	70	6	35	45.05	12.05	8.04	5.82	58.22	32.2	0.27	-1.98		
HT-44-6-14	14	6	44	26.71	7.14	4.76	5.84	28.21					
HT-44-6-28	28	6	44	43.76	11.70	7.80	5.80	46.22	28.9	0.42	-3.89	199.15	43.64

continued on next page

Sample ID	# days	pH	T˚C	µg/L	mg dissolved	% dissolved	modelled pH	% saturation	phytolith $\delta^{18}O_{VSMOW}$ (‰)	phytolith $\delta^{30}Si_{NBS-28}$ (‰)	dissolved $\delta^{30}Si_{NBS-28}$ (‰)	SSA (m^2/g)	mean particle size (µm)
HT-44-6-42	42	6	44	70.85	18.95	12.63	5.76	74.84	29.9	0.12	-0.12		
HT-44-6-56	56	6	44	89.36	23.90	15.91	5.74	94.39	30.9	-0.14	1.29		37.66
HT-44-6-70	70	6	44	93.85	25.10	16.71	5.74	99.13	30.2	0.00	0.51	336.62	38.14
HT-4-8-4	4	8	4	0	0	0	8.00	0	34.2	0.46			
HT-4-8-6	6	8	4	0	0	0	8.00	0	31.9	0.22			
HT-4-8-8	8	8	4	0	0	0	8.00	0	32.1	0.20			
HT-4-8-10	10	8	4	0	0	0	8.00	0	31.2	0.12			
HT-19-8-2	2	8	19	0	0	0	8.00	0	31.9	0.14			
HT-19-8-4	4	8	19	0	0	0	8.00	0	31.7	0.08			
HT-19-8-6	6	8	19	3.50	0.94	0.62	7.65	6.12	32.3	0.40	-50.24		
HT-19-8-8	8	8	19	4.51	1.21	0.80	7.59	7.89	32.6	0.13	-5.93		
HT-19-8-10	10	8	19	LOST					31.5	0.28			
HT-35-8-2	2	8	35	7.75	2.07	1.38	7.27	9.99		-0.01	6.64		
HT-35-8-4	4	8	35	10.11	2.70	1.80	7.17	13.03	31.5	0.27	-10.07	269.32	38.31
HT-35-8-6	6	8	35	12.74	3.41	2.27	7.09	16.44	31.8	-0.07	6.70	271.90	36.46
HT-35-8-8	8	8	35	11.56	3.09	2.06	7.12	14.92	32.7	0.07	0.71		
HT-35-8-10	10	8	35	16.16	4.32	2.88	6.99	20.86	32.4	0.32	-7.92		
HT-35-8-35	35	8	35	46.17	12.35	8.22	6.57	59.64	28.8	0.08	0.17	271.95	38.56
HT-44-8-2	2	8	44	12.63	3.38	2.25	6.98	13.32	31.1	0.12	-1.21		
HT-44-8-4	4	8	44	16.44	4.40	2.93	6.87	17.34	31.0	0.01	2.52		38.08
HT-44-8-6	6	8	44	23.23	6.21	4.14	6.73	24.51	29.1	0.10	-0.21		
HT-44-8-8	8	8	44	21.94	5.87	3.91	6.76	23.15	30.4	0.12	-0.80		
HT-44-8-10	10	8	44	26.65	7.12	4.75	6.68	28.12	28.5	0.18	-1.90	228.96	35.73
HT-44-8-35	35	8	44	82.07	21.95	14.61	6.20	86.67	29.6	0.25	-0.85	191.31	40.65
HT-4-10-2	2	10	4	11.24	3.00	2.00	9.56	25.06	29.9	0.29	-9.89		
HT-4-10-4	4	10	4	14.43	3.86	2.57	9.48	33.06	32.1	0.64	-20.97		36.86
HT-4-10-6	6	10	4	30.57	8.17	5.45	9.21	74.77	32.4	0.39	-5.23	249.12	36.89
HT-4-10-8	8	10	4	20.31	5.43	3.62	9.36	48.11	32.3	0.40	-8.28		
HT-4-10-10	10	10	4	14.26	3.81	2.54	9.49	32.64	30.6	0.24	-5.80	230.28	37.17
HT-19-10-2	2	10	19	23.00	6.15	4.10	9.09	36.30	30.3	0.19	-2.35		
HT-19-10-4	4	10	19	39.14	10.47	6.97	8.86	64.40	31.4	0.52	-5.69		
HT-19-10-6	6	10	19	43.35	11.59	7.73	8.82	71.75					
HT-19-10-8	8	10	19	55.28	14.78	9.85	8.71	92.62	33.3	0.45	-3.26		
HT-19-10-10	10	10	19	59.20	15.83	10.56	8.68	99.48	30.6	0.04	0.50		
HT-35-10-2	2	10	35	31.98	8.55	5.70	8.75	37.91	30.0	0.23	-2.35	245.52	37.89
HT-35-10-4	4	10	35	49.76	13.31	8.87	8.56	60.82	32.8				
HT-35-10-6	6	10	35	68.61	18.35	12.23	8.42	85.14	32.2	0.48	-2.75		36.65

continued on next page

Sample ID	# days	pH	T˚C	µg/L	mg dissolved	% dissolved	modelled pH	% saturation	phytolith $\delta^{18}O_{VSMOW}$ (‰)	phytolith $\delta^{30}Si_{NBS-28}$ (‰)	dissolved $\delta^{30}Si_{NBS-28}$ (‰)	SSA (m^2/g)	mean particle size (µm)
HT-35-10-8	8	10	35	59.47	15.90	10.60	8.48	73.34	31.7				
HT-35-10-10	10	10	35	81.51	21.80	14.52	8.34	101.80	32.2	0.39	-1.69		
HT-35-10-35	35	10	35	143.21	38.29	25.49	8.09	181.52	27.4	0.15	0.80	221.92	40.46
HT-44-10-2	2	10	44	83.13	22.23	14.81	8.21	84.90	29.9	0.05	0.28		
HT-44-10-4	4	10	44	129.03	34.50	23.00	8.02	133.37	29.3	-0.30	1.37		
HT-44-10-6	6	10	44	130.04	34.77	23.18	8.01	134.43	28.9	-0.13	0.80		
HT-44-10-8	8	10	44	141.78	37.91	25.29	7.97	146.83	30.1	-0.04	0.47		
HT-44-10-10	10	10	44	149.71	40.03	26.69	7.95	155.21	29.6	-0.11	0.63		
HT-44-10-35	35	10	44	160.60	42.94	28.60	7.92	166.71	29.8	-0.07	0.47		

Appendix C. Summary of experimental conditions and results of dissolution experiments conducted on burned phytoliths

Sample ID	# days	pH	T˚C	µg/L	mg dissolved	% dissolved	% saturation	phytolith $\delta^{18}O_{VSMOW}$ (‰)	phytolith $\delta^{30}Si_{NBS-28}$ (‰)	SSA (m^2/g)	mean particle size (µm)
HT2-4-4-14	14	4	4	6.68	1.79	1.19	17.70				
HT2-4-4-28	28	4	4	8.06	2.16	1.44	21.36	26.9	0.04		
HT2-4-4-42	42	4	4	9.43	2.52	1.68	25.00	27.0	0.13		
HT2-4-4-56	56	4	4	10.00	2.67	1.78	26.51	27.0	-0.02		
HT2-19-4-14	14	4	19	14.76	3.95	2.62	25.90	26.8	0.11	226.0	35.9
HT2-19-4-28	28	4	19	17.31	4.63	3.09	30.38	28.0	0.28	220.2	37.5
HT2-19-4-42	42	4	19	21.93	5.86	3.92	38.47	26.4	0.36	223.0	33.6
HT2-19-4-56	56	4	19	22.83	6.11	4.06	40.06	26.2			
HT2-4-6-14	14	6	4	9.52	2.55	1.70	25.23				
HT2-4-6-28	28	6	4	13.18	3.52	2.35	34.92	27.1	0.12		
HT2-4-6-42	42	6	4	16.10	4.30	2.87	42.66	27.2	0.23		
HT2-4-6-56	56	6	4	16.62	4.44	2.95	44.03	28.6	0.22		
HT2-19-6-14	14	6	19	29.87	7.99	5.33	52.39	28.0	0.38	254.1	36.3
HT2-19-6-28	28	6	19	39.55	10.58	7.05	69.38	27.8	0.24		
HT2-19-6-42	42	6	19	45.68	12.22	8.15	80.14	27.9	0.11		36.8
HT2-19-6-56	56	6	19	53.81	14.39	9.60	94.40	25.4			37.1
HT2-4-8-2	2	8	4	2.91	0.78	0.52	7.68	26.8	0.25	235.2	
HT2-4-8-4	4	8	4	4.08	1.09	0.73	10.76	28.6	0.17		
HT2-4-8-6	6	8	4	5.14	1.38	0.92	13.56	29.9	0.18	216.3	35.7
HT2-4-8-8	8	8	4	9.09	2.43	1.62	23.96	27.9	0.36		
HT2-4-8-10	10	8	4	9.51	2.54	1.69	25.06	28.2	0.42	235.1	39.0
HT2-19-8-2	2	8	19	13.08	3.50	2.33	22.72	25.6	0.23	202.2	36.9
HT2-19-8-4	4	8	19	17.90	4.79	3.19	31.10	26.7	0.25		
HT2-19-8-6	6	8	19	22.83	6.10	4.06	39.66	26.9	0.53	199.2	36.9
HT2-19-8-8	8	8	19	26.34	7.04	4.70	45.76	27.7	0.24		
HT2-19-8-10	10	8	19	28.37	7.59	5.07	49.29	26.7	0.19	189.0	37.2

Curriculum Vita

Name:	Andrea J. Prentice
Post-secondary Education and Degrees:	The University of Western Ontario London, Ontario, Canada 2003-2007 B.Sc. The University of Western Ontario London, Ontario, Canada 2003-2007 M.Sc.
Honors and Awards	Graduate Thesis Research Award 2008 Lumsden Fellowship in Earth Science 2010 Ontario Graduate Scholarship 2011-2012
Related Work Experience	Teaching Assistant The University of Western Ontario 2007-2013 Research Assistant The University of Western Ontario 2006-2007

Publications:

Prentice, A.J., Webb, E.A. (2010) A comparison of extraction techniques on the stable carbon isotope composition of soil humic substances. Geoderma 155, 1-9.